

Self-organization, structure and dynamics of liquid crystalline mesophases
composed by diols.

Dissertation

zur Erlangung des akademischen Grades

doctor rerum naturalium (Dr.rer.nat.)

vorgelegt der

Naturwissenschaftlichen Fakultät II-Chemie und Physik

der Martin-Luther-Universität Halle-Wittenberg

von Frau Diplom Chemikerin Jessie Lorenzo Chao

geb. am 16.Juni.1977 in Havanna, Kuba

Gutachter:

- 1) Prof. Dr. H. Kresse, Inst. für Chemie, Physikalische Chemie, Martin
Luther Universität Halle-Wittenberg
- 2) Prof. Dr. R. Stannarius, Dept. Nonlinear Phenomena, Otto von Guericke
Universität Magdeburg

Halle (Saale), den 5. 07. 2010

Index

1. Introduction	3
1.1 Liquid Crystals	3
1.2 Mesophase Structure of anisometric molecules	4
1.3 Dynamics of liquid crystalline mesophases.....	6
1.3.1 Dynamics of rod like molecules	6
1.3.2 Dynamics of achiral disc-like molecules	7
1.3.3 Study of the dynamics in chiral discotic mesogens	9
1.3.4 Dynamics in chiral switchable discotic mesogens	11
1.4 Structure and mesophase behavior of amphiphilic molecules	12
1.4.1 Simple diols molecules	15
1.4.2 Dynamics of the mesophases formed by diols	16
1.5 Motivation	17
2. Theoretical Introduction	19
2.1 Dielectric spectroscopy	19
2.1.1 Theory of dielectric spectroscopy	19
2.1.2 Dielectric spectroscopy of liquid crystals	25
2.2 Nuclear Magnetic Resonance	26
2.3 Infrared Spectroscopy	27
3. Experimental part	28
3.1 Synthesis of few substances	28
3.2 Equipment used	32
3.2.1 X-Ray investigations	32
3.2.2 Dielectric investigations	33
3.2.2.1 Low frequency dielectric investigations	33
3.2.2.2 High frequency dielectric investigations	34
3.2.3 Nuclear Magnetic Resonance measurements	34
3.2.4 Polarization microscopy	34
3.2.5 Differential Scanning calorimetry	35
4. Results	36
4.1 Extended investigation on a binary system	36
4.2 Investigation of the SmA phase	38
4.2.1 Dielectric behavior of the amide compound in the smectic phase	38
4.2.2 Mixture in the Smectic phase at $x_3=0.05$	40
4.2.3 Study of the SmA phase of the methyl substituted compound	43
4.2.4 DSC and microscopic study of the methyl urea compound in the SmA phase	44
4.2.4.1 X-Ray investigation of 1(2,3-dihydroxy-propyl)-3-(4-dodecyloxy-phenyl)-1-methylurea.....	45
4.2.4.2 Dielectric investigation of 1(2,3-dihydroxy-propyl)-3-(4-dodecyloxy-phenyl)-1-methylurea	46
4.2.5 Common behavior of the all SmA phases	48
4.3 Investigation of columnar mesophases	49
4.3.1 Columnar phase with hydrogen bonds of a mixture at $x_3=0.6$	49
4.3.2 Investigation of the columnar phase of methyl ureas	54
4.3.2.1 Characterization of the methyl ureas by DSC and polarization microscopy.	54
4.3.2.2 X-Ray investigation of methyl urea compounds	55
4.3.2.3 Dielectric investigation of the methyl urea compounds	60

4.3.2.4 IR investigation at the isotropic/columnar phase transition	63
4.3.3 Study of the columnar mesophase of the nethylated amide compound.....	65
4.3.3.1 X-Ray investigation of the methylated amide compound	65
4.3.3.2 Dielectric behavior of the methylated amide compound	66
4.3.4 Investigation of the sulfone compound	69
4.3.4.1 X-Ray investigation of the sulfone compound	69
4.3.4.2 Dielectric investigation of the sulfone compound	71
4.3.5 Investigation of a methylene compound	72
4.3.5.1 X-Ray investigation of the methylene compound	73
4.3.5.2 Dielectric investigation of the methylene compound	74
4.3.5.3 Nuclear Magnetic investigation of the methylene compound	76
4.3.6 Assignment of the different relaxation processes in the columnar phase.....	78
4.4 Investigation of the cubic phase	84
4.4.1 The formation of the micellar cubic phase	84
4.4.2 Dilectric investigations	84
4.4.3 Specific behavior of the micellar cubic phase	86
4.5 Study of the cubic/columnar phase transition of the methyl-amide compound with three chains	86
4.5.1 X-Ray investigations	87
4.5.2 Dielectric investigations	87
4.5.3 Study at the cubic/columnar phase transition by infrared spectroscopy	89
5. Discussion of the results on the binary mixture	91
6. Summary	93
7. References	96
Appendix 1. NMR-HSQC measurements of compound 10 in the liquid state.....	102
Acknowledgments	103
Publications	105
Curriculum Vitae	106
Eidestattliche Erklärung	107

Abbreviations

θ	Bragg angle
Br ₂	Dibromo
CH ₂ Cl ₂	Dichlormethane
CHCl ₃	Trichloromethane
Col _H	Columnar Hexagonal phase
CP-MAS	Cross Polarization Magic Angle Spinning
Cub _v	Cubic phase formed by micelles
d	duplett
<i>d</i>	layer distance
dd	duplett-duplett
DSC	Differential Scanning Calorimetry
E _A	Activation Energy
Et ₂ O	Diethylether
f _R	Relaxation frequency
HBC	Hexabenzacoronene
HSQC	Heteronuclear Simple Quantum Correlation
IR	Infrared
K ₂ CO ₃	Kalium Carbonate
KSCN	Kalium Thiocyanate
LiAlH ₄	Lithium aluminium hydrid
m	multipllett
MeCN	Acetonitril
MeOH	Methanol
N	Nematic
NaHCO ₃	Sodium Bicarbonate
NaOH	Sodium Hydroxide
N _D	Nematic Discotic phase
NMMNO	N-methylmorpholine-N-oxide monohydrate
NMR	Nuclear Magnetic Resonance
OsO ₄	Osmium Tetroxide
RT	Room temperature
S	Order Parameter

SmA,C,E...	Smectic phases type A, C, E....
SOCl ₂	Thionylchloride
THF	Tetrahydrofurane
UV	Ultra Violet
Zn	Zinc
ϵ	Dielectric Permittivity
τ	Relaxation time

1. Introduction

1.1 Liquid Crystals

The first description of the liquid crystalline state was given by Reinitzer and Lehmann in 1888 [1]. Since then, because of the fact that the properties of the liquid crystalline state are combinations of that of the crystalline and liquid states, this special aggregation form of matter became an object of investigation [2].

The crystalline state is characterized by the three dimensional periodic arrangements in certain places within the network. Particles are bonded in a way that only vibrations around the equilibrium position and limited rotation are possible. Therefore, crystalline networks exhibit positional and orientation long-range orders on which their physical properties depend on direction of observation, that is, the so-called anisotropy.

An increasing crystal temperature intensifies particle mobility. Then, at a characteristic temperature (melting temperature) phase transition to an isotropic liquid state, in which the network structure is lost, occurs. In the isotropic state, particles have neither long-range order, because of the high mobility, nor preferred orientation. Therefore the physical properties of the liquid state are the same in all directions.

Some compounds show one or more mesophases between the crystalline and the isotropic state. If one regards the plastic crystals as solid modification the term “mesophase” has the same meaning as “liquid crystal”. The additional phase transition from the mesophase existing at the highest temperature into the liquid state is called clearing process. Transition temperatures between different mesophases and the clearing temperature are typical. The molecules forming liquid crystalline phases are anisotropic and have a certain degree of orientation and position long-range order, depending on the complexity of the phase, and some mobility. Thus, the resulting mesophases can show anisotropy of the physical properties. This in combination with (Due to this anisotropy of the physical properties associated with the positional long-range order and) the fluidity (-related mobility), results in an extraordinary behavior interesting for technical application. (Liquid crystals are remarkable substances concerning the way they react to external forces.) Thus, for example,

the orientation (structure and properties) of the mesophases can be manipulated by applying an external electric field.

According to the classic concept, there are two kinds of liquid crystalline mesophases due to two different kind of phase formation. If mesophase formation is only temperature-dependent, the mesophase is called thermotropic. In addition to temperature dependence, if formation is due to the solution of an amphiphilic molecule in a solvent, it depends also on the amphiphilic molecule concentration, and the term lyotropic mesophase is used. Moreover, although chemical structure affects the physical and morphologic characteristics of mesophases, therefore the molecules are also classified according to the classic concept in such with an anisometric shape or with an amphiphilic character of mesomorphic molecules. Between these borderline cases a lot of intermediated states are observed. Thus, in thermotropic liquid crystals phase separation can play an important role as clearly shown in liquid crystalline side group polymers [3,4]. It has to be pointed out that in the first example main chain and side group are chemically incompatible whereas in the second case both parts are miscible. This example illustrates that structure formation is very sensitive on small changes on the molecular level. This is also well illustrated in the investigations by Tschierske [5].

1.2 Mesophase structure of anisometric molecules.

Anisotropic molecules are those which exhibit rigid structure elements, a defined geometric shape and direction-dependent molecular elongation. Consequence of the anisometric molecular form is the anisotropic steric interactions and steric repulsion forces that are the driving forces of the formation of liquid crystalline mesophases of this kind of molecules.

There is a very close interrelation between the form of the mesogene and the structure of the formed liquid crystalline mesophase [6]. Anisometric molecules form mostly thermotropic mesophases. As example, the calamitic mesophase structure of rod-like molecules and the discotic phases of disc-like molecules should be mentioned. Recently a lot of molecules with unconventional form were synthesized for example: banana-shaped, ring form and pyramidal shape molecules [7].

Calamitic molecules are the most important class of anisometric molecules and the most investigated. They built preferably nematic and smectic mesophases. In nematic phases the molecules don't have any positional long range order but have a preferential orientation of the molecule long axis described by the director n so called orientational long range order. In the smectic phases the molecules have as well orientational long range order as a certain degree of positional long range order in one or two dimensions. Furthermore, the molecules are sorted parallel to each others in layers. The molecular long axis can be oriented perpendicular to the layer plane (SmA) or can also have an inclination (SmC). Inside of the layers the molecules don't have any positional long range order in the case of the SmA and the SmC phases. There exist another kind of smectic phases that are formed at lower temperatures were the molecules exhibit certain degree of positional order inside the layers (SmB, SmF, SmI) were the restriction of the movements are strong [8-19]. This measurement demonstrates the step by step transition into the solid state where this dynamics is frozen in.

The ability of disc like molecules to form liquid crystalline mesophases was discussed in 1923 by Vorländer [20] but was proven by Shandrasekhar and coworker in 1977 [21]. The easiest mesophase formed by disc-like molecules is the Nematic discotic (N_D) which is very similar to that formed by the rod like molecules. In this phase the discotic molecules have again orientations parallel to each other were the sheets normal is oriented in direction of the director of the phase. Disc like molecules can also form columnar mesophases, were the molecules are organized in columns. Along the columns the molecules can have more or less order. The molecule plane can be perpendicular oriented or shows an inclination with respect to the axis of the column.

There are also other types of molecules forming discotic mesophases which are not limited to the above discussed disc-shape. Depending on the molecular structure and the intermolecular interactions involved, they can be side-chain polymers without mesogenic moiety, dendrimers, pseudo polymeric chains of metal soaps, polycatenar molecules, or other systems driven by specific interactions such us hydrogen bonding or dipolar interactions [22,23]. Examples of the general types of thermotropic liquid crystalline phases are presented in Figure 1.1.

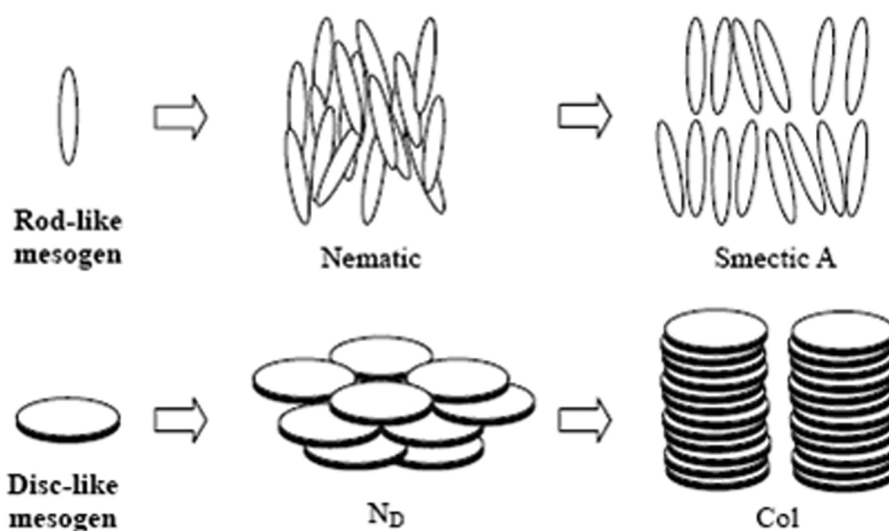


Figure 1.1 Mesophases formed by rod-like molecules and discotic molecules.

1.3. Dynamics of liquid crystalline mesophases

1.3.1 Dynamics of rod like molecules.

Rod-like molecules are compounds with two or more rigidly bonded aromatic or aliphatic rings also attached to two alkyl chains. Usually, these compounds exhibit nematic or smectic arrangements with dielectric behavior dominated by two processes: hindered rotations around the short axis of the molecule, and faster rotation around the long axis. Based on the synthetic work of Weissflog et al. [24-28], several dielectric measurements on samples with special steric interactions were performed in the Halle group. Dielectric investigations in 4-n-pentyliminomethylphenyl-4-n-hexyloxybenzoate compound exhibiting an N-SmA polymorphism [28] show that the stronger dipole-dipole interaction in the SmA phase results in a decrease of the dielectric permittivity at the phase transition N-SmA. This was also found by another compounds and another authors [29-32]. Neither the relaxation times nor the activation energies change strongly at this phase transition.

Similar investigations on compounds with the SmC phase show that the dielectric permittivity decreases at the phase transition N-SmC [33]. This effect results from the stronger dipole-dipole correlation as well as from the tilt of the molecules within the

layers. The step is bigger than at the phase transition N-SmA [34-36] and the relaxation times don't change too much.

The smectic low temperature phases SmB, SmG, SmH, SmE are characterized by a very strong restriction of the rotation of the molecules around their short axis and partially also by stronger hindrance of the dynamics around the molecular long axis. Investigations of 4-n-alkyloxybenzylideneamino-4'-cyanobiphenyls [37,38] show that the transition into the SmE phase is accompanied with a decrease of the relaxation frequencies of more than one decade. This process is a Debye relaxation with activation energies between 80 ± 10 and 130 ± 15 kJmol⁻¹. The dielectric permittivity increases at this phase transition indicating that the dipole-dipole correlation doesn't change too much. The dynamics around the long axis is a little bit reduced at phase transitions if the low temperature smectic phases exhibit a herring bone structure [39]. Generally a slower dynamics is observed if the liquid crystalline phases approach the solid state.

Investigations of 4-n-hexyloxybenzylidene-4-n-hexylaniline [40] that exhibit a SmE mesophase show a small increase in the dipole-dipole correlation with respect to the SmA and SmC phase seen by a small decrease in the permittivity and an increase of the relaxation times at the phase transition. The big decrease of relaxation frequency of a factor 13 corresponds well with the step in the degree of order if the model by Martin, Meier and Saupe is extended to smectic phases [41].

The results show that the dielectric method is suitable to study the hindrance of the dynamics due the formation of the different liquid crystalline phases and the interactions of molecules in the short range.

1.3.2 Dynamics of achiral disc-like molecules

Large disc-like molecules were designed to increase the phase stability of columnar mesophases. Molecules that contain rigid disc-like central units radially surrounded by a sufficient large number of flexible chains are mostly stacked into columns and have π - π overlap of the aromatic cores [42]. This is in favor of high conductive properties in direction of the column axis. Such compounds can be regarded as "molecular wires". In

HBCs for example the high charge carrier mobility is above $1 \text{ cm}^2\text{V}^{-1}\text{s}^{-1}$ [43-44] and some triphenylene derivatives the value of $10^{-2} \text{ cm}^2\text{V}^{-1}\text{s}^{-1}$ was measured [45].

Many studies indicate that the conductivity of these compounds is greater in the crystalline phase [46]. This behavior was attributed to the disorganized peripheral chains inducing a less efficient face to face ordering and also to the molecular rotation around the columnar axis. That's way knowledge about the intrinsic rotational dynamics of the disc is of interest. As example of large disc-like cores are coronenes [47-48] that can exhibit columnar columnar phases within a temperature range of about 300°C [49], hexa-peri-hexabenzocoronenes [50-51], perylenes [52-55], tricycloquinazolines [56] and triphenylene porphirazines [57].

Studies about the dynamic and stability of columnar mesophases composed by achiral molecules for example, benzacoronenes [58], triphenylene and benzene [59] derivatives were carried out.

A dielectric investigation on triphenylene and benzene derivatives reveals the presence of two relaxation processes in their columnar mesophases. The low frequency α -process is related with the rotation of the discs around the columnar axis and is often influenced by the glass transition. At higher frequencies a β -process, with an Arrhenius behavior of the relaxation times, ascribe to a local librational motion of the side chains involving the carbonyl group of the ester linkage of the side chains. This process has activation energies between 37 and 40 kJ/mol [59]. In this case many authors have taken the language of the dynamics in polymers in order to point to the difference between more collective and local processes.

Benzacoronenes present an absorption dielectric spectrum due to the rotation of the molecules in the plane perpendicular to the long axis of the molecule and librational movements. These two processes, which could be well separated in some functionalized HBC compounds, occur at Kilohertz range. Usually, they cannot be separated in the frequency scale, and that separation is observed only in the case of molecules with very strong dipole moments rigidly attached to the aromatic ring. The assignation of different bands was possible by investigating the dipole-dipole coupling constant via pressure-dependent dielectric spectroscopy and Nuclear Magnetic Resonance (NMR). The process

with more necessity of volume, out of plane rotation, relaxes at lower frequencies than the axial rotation of the molecules. This a very important result contributing to the understanding of the dynamics, specifically the dielectric behavior, of the columnar phases composed by diol molecules investigated in this work.

The determination of the local order parameter $S = 0.42$ of the aromatic core was possible at intermediate temperatures were the disc dynamics interfere with the Kilohertz range pertinent with NMR experiments. A very strong reduction of the local coupling constant $^1\text{H}-^{13}\text{C}$ in CP-MAS confirmed the movement intensification and, in particular, at an angle of about 38° founded for the out-of-plain motion [60] Fig 1.2.

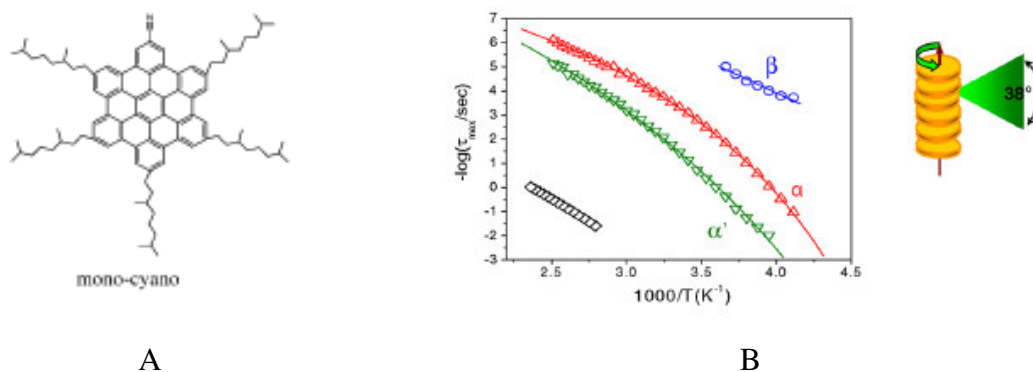


Figure 1.2 A) Structure of the mono-cyano substituted benzacoronene B) Graphic of relaxation time measured with dielectric spectroscopy versus temperature of the mono-cyano compound already published [60], α' process is related to the out of plain motion of the molecules, α process is caused by the rotation of the molecules around the columnar axis, the slow process (rhombus) due to ionic mobility and β process is connected with the motion of the side chains.

1.3.3 Study of the dynamics in chiral discotic mesogens

The introduction of chirality into liquid crystals composed of discotic molecules with a triphenylene core generates a spiral column with a pitch extending several discs within the column. This is the case of 2S,3S-2-chloro-3-methyl-penta-noyloxypentakis(pentyloxy) triphenylene which exhibit a hexagonal ordered phase and a helical super-structure with a pitch of 3,0 nm which corresponds to a stack of 8 molecules. The interlinking of the discs hinders the rotation of the discs around the columnar axis, even in the liquid crystalline state. The dynamics of this system was investigated by dielectric spectroscopy and NMR techniques.

The dielectric spectrum shows the existence of two relaxation process, α and β . The β relaxation corresponds to the motion of the side chain and is dominated by the rotation of the ester group around the linkage to the discotic core. This process shows an Arrhenius behavior with activation energy of 37 ± 3 kJ/mol. The α process is related with the axial motion of the molecules, the rotation around the main axis of the columns and is related also with the glass transition, characteristic of this kind of compounds. This process doesn't have Arrhenius behavior and occurs between 10^1 Hz and 10^5 Hz. The assignment of this process was corroborated for this compound by the use of NMR techniques. ^2H -NMR spectrums show a reduction in width by a factor of 2 indicating that the molecules rotate around the column axis with rates between 10 kHz and 10 MHz [61].

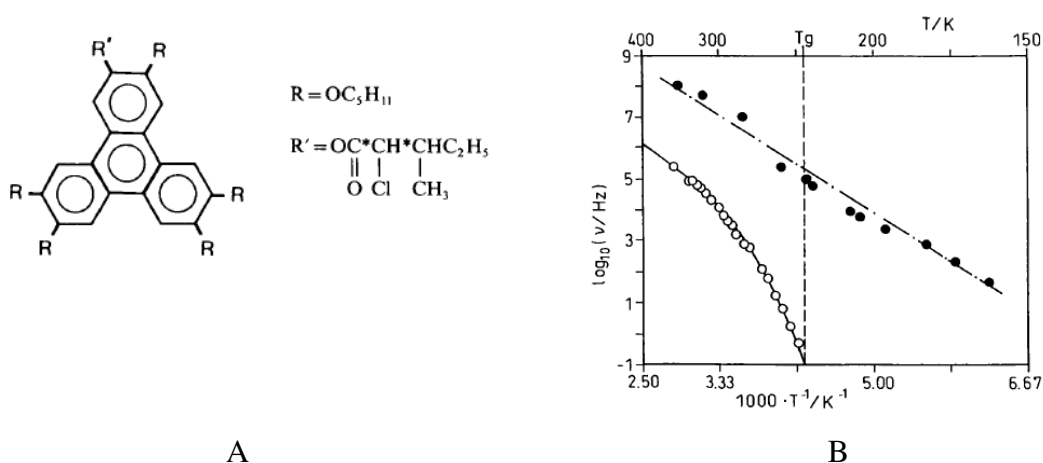


Figure 1.3 A) Structure of the 2S,3S-2-chloro-3-methyl-penta-noyloxy-pentakis(pentyloxy)triphenylene

B) Graphic of the time versus temperature of the triphenylene derivative [61]. (○) represent the α process related to the rotation of the molecules around the columnar axis (●) represent the motion of the side chains.

Investigations of the dynamics of these compounds were used to investigate more in detail the nature of some process of the columnar phases, like the glass transition which is an anisotropic phenomenon in liquid crystals and manifest itself very strong along the columnar axis [62-63]. During this process the movements are frozen without crystallization and are not depending of the substitution of the triphenylene [64].

The π - π overlap of the aromatic cores makes possible the one dimensional charge carrier properties of these compounds. The mixed with donator or acceptor molecules forming

charge transfer complexes can enhanced this properties. Even in these complexes the correlated rotational motion of discotic molecules around the columnar axis seems to be a general feature of columnar phases and was corroborated by dielectric spectroscopy [65-67].

1.3.4 Dynamics in chiral switchable discotic mesogens

Some compounds forming also columnar mesophases are penta-substituted 1,3 diphenylpropanedione ligands complexes to either vanadium(IV), copper (II), or palladium(II). This gives rise to a disc-like core surrounded by ten flexible chiral tails derived from L-(-)-lactic acid [68a]. These mesophases formed exhibits also electro-optic switchable properties and helical order within the columns.

The dielectric spectrum of this mesophase shows the contribution of 3 motions, see Fig. 1.4. Two of them were also observed in columnar phases composed by chiral and achiral discotic mesogenes discussed before. The fastest relaxation process is related to the reorientation of the side groups and has a non Arrhenius behavior in the liquid crystalline phase. This process is involved in the glass transition because of the proximity of the chains to the rigid part of the molecule.

The second process is related to the motion of the discs around the columnar axis. It follows the Arrhenius law with activation energy of 56 kJ/mol. Both processes are also present in the isotropic phase as a consequence of the existence of a local order. The appearance of the second process in the isotropic phase too, indicates a local order where the discs are still packed to columns. The situation may be comparable with that of the “cybotactic groups” in few classic nematic compounds.

The third mechanism appears below the phase transition I-Col_r* at lower frequencies, around 10³ Hz. This is a columnar mode related to the chiral and tilted character of the Col_r* phase similar to the Goldstone mode observed in the SmC* phases [69]. This is a collective mode related to the azimuthal fluctuations of the director around the helical axis. This mode presents a larger strength than the others dominating the dielectric spectrum [68b].

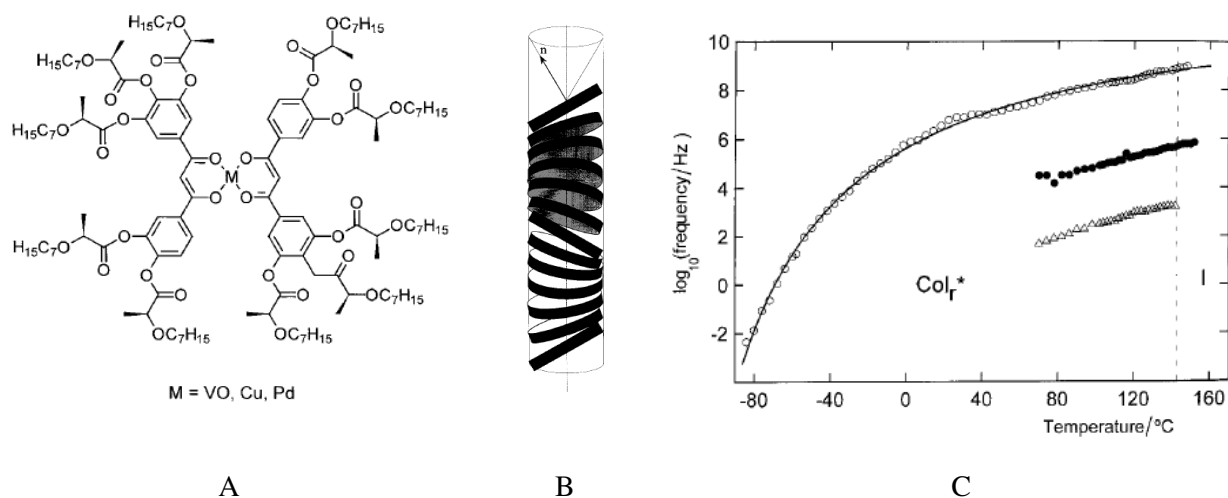


Figure 1.4 A) Structure of the penta-substituted 1,3-diphenylpropanedione ligands complexes B) Structure of the columnar mesophase Col_r^* C) Graphic of the relaxation times versus the temperature [68 B] (○) Motion of the side groups (●) Rotation of the molecules around the columnar axis (◇) columnar relaxation process.

Dielectric spectroscopy provides information on the dynamics and structure of some mesophases. The evidence of low-frequency absorption in some liquid crystals with columnar arrangement confirms the presence of helical structures. On the other hand, distinctive dielectric behaviors exhibited by some molecules arise from chirality. Dielectric investigations in chiral dibenzopyrene derivatives that exhibit switching columnar mesophase shows a single absorption process at 10 Hz [70].

1.4 Structure and mesophase behavior of amphiphilic molecules

Segregation of incompatible molecules segments is the driving force for the formation of liquid crystalline mesophases composed by amphiphilic molecules [71-74]. Classic amphiphilic molecules are built by a hydrophilic and hydrophobic part attached each other covalently. The combination of polar/nonpolar, hydrocarbon/fluorocarbon, hydrocarbon/siloxane or flexible/rigid molecular units can also form molecules with amphiphilic character. This kind of molecules show thermotropic as well as lyotropic character that means they have the ability to form both types of liquid crystalline mesophases, thermotropic and lyotropic. Amphiphilic molecules show amphotropic behavior [75-77].

The formation of mesophases formed by this kind of molecules can be understood as follows. The different segments of the molecule try to separate each other. A macroscopic separation is not possible because of the covalent interconnection. These results in the formation of macrodomains where the segments are allocated. The macrodomains can be building units of liquid crystalline mesophases. The kind of mesophases formed in this way depends mainly on the degree of chemical and structural differences, the size and geometry of the incompatible building blocks. Thus, the microsegregation gives rise to the formation of lamellar, columnar or spheroidal aggregates which organize to smectic, columnar and cubic mesophases like in lyotropic liquid crystalline mesophases [78]. Examples of such molecules are alkyl-diols, diols[79] and polyols. Some of them are illustrated in Figure 1.5. Like is shown the morphology is conditioned by the size of the hydrophobic with respect to the hydrophilic part and can be tailored by the variation of the number of alkyl chains attached to the aromatic ring or the number of the polar groups [80-86] as illustrated in the figure. The formation of mesophases composed by these polyols implies other attractive interactions like the formation of hydrogen bonds or, in other molecules, ionic interactions that gives rise to high intramolecular polarity contrast between the molecular segments. This kind of mesophases exhibits a high conductivity. For that reason perfluor-, carboxisiloxan fragments are more used than hydrogen bonds interactions to increase the stability of the mesophases.

Also the number of hydroxyl groups present in the molecules, their position with respect to each other and their position in respect to the lipophilic-hydrophobic interface influence the structure of the mesophase illustrated in Fig 1.6. As can be seen, the more compact and larger the polar part, the bigger is the probability to form columnar mesophases. This is an important factor governing the hydrophilic-lipophilic interface curvature and thus the type of the mesophase [83].

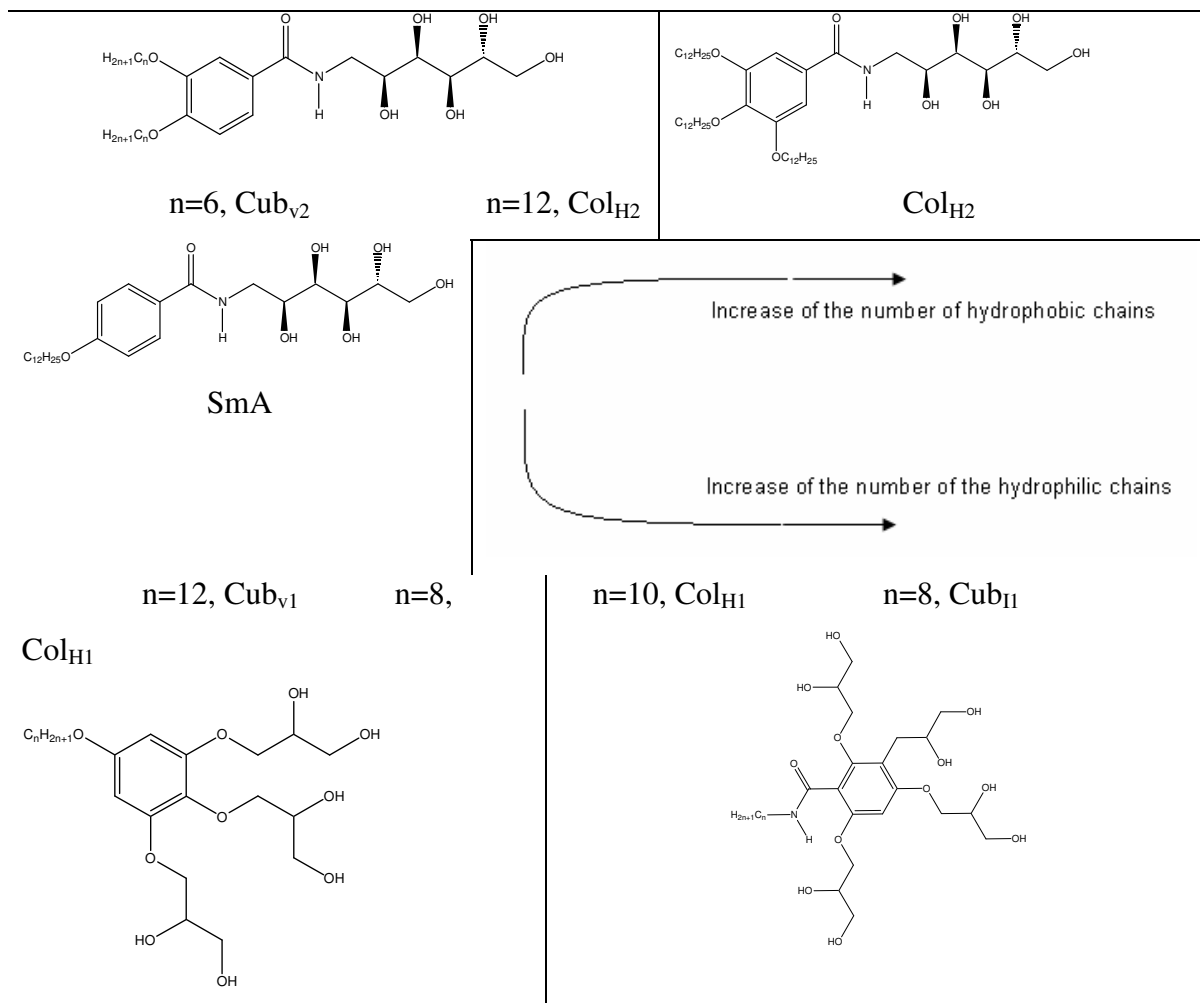


Figure 1.5 Mesophase behavior depends on the structure of the molecules.

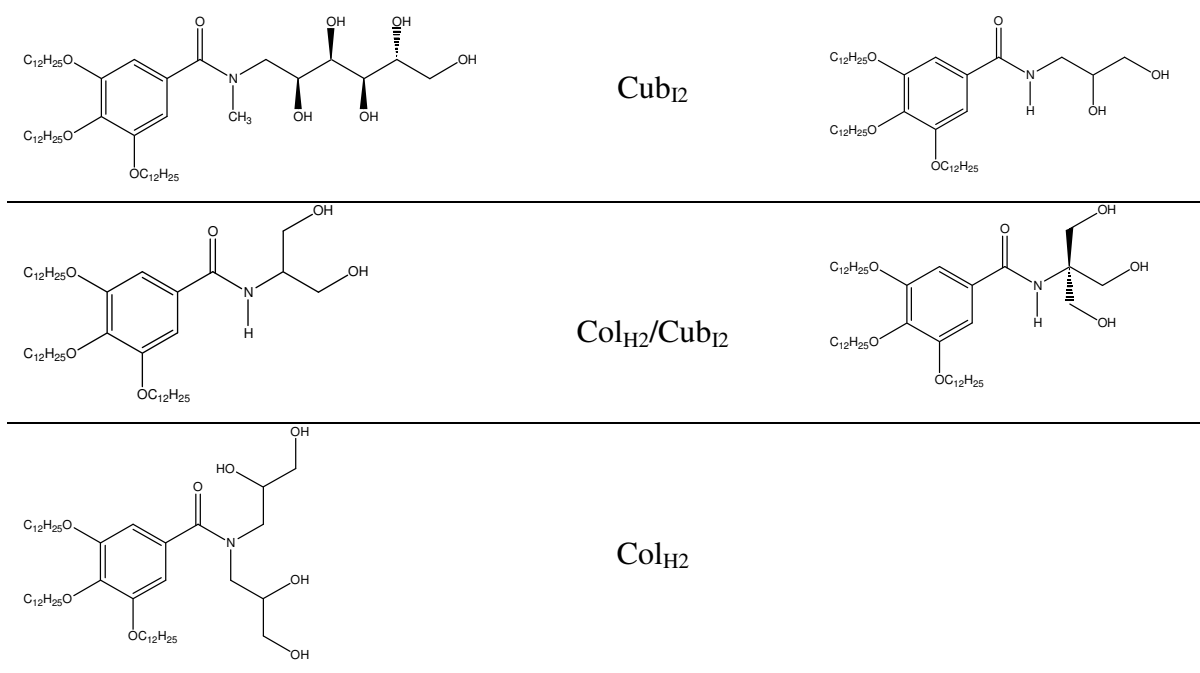


Figure 1.6 Mesophase behavior of 3,4,5-tridodecyloxybenzamides with different hydrophilic groups.

1.4.1 Simple diols molecules

The reduction of the number of hydroxy groups reduces the clearing temperatures of the liquid crystalline mesophases by reducing the possibilities of the intermolecular interaction by hydrogen bonds making possible the better investigation of those compounds. The mesophase behavior and the structure of the liquid crystalline mesophases composed by amphiphilic diols molecules were already investigated [82]. In dependence of the number of alkyl chains different mesophases were found. A SmA phase in the case of the compound with only one carbon chain attached to the aromatic ring, a columnar hexagonal mesophase for the compound with two alkyl chains and a cubic mesophase for the compound with three alkyl chains.

Cubic phases can be formed by spherical micells. In the case where the nonpolar segments are in bigger number and size than the polar one the network of hydrogen bond is the center of the sphere. Therefore these phases are called inverse cubic phases (Cub_{I2}) with even more localized hydrogen bonds network (see structure in Fig 1.6). There are also some diols forming polymorphism Cub_{I2}/Col_{H2} . The existence of polymorphic phases shows that one cannot regard the molecules and their interaction as a static situation. A higher kinetic energy of the system is able to change the shape of the aggregates on the molecular level and produce in this way a complete new organization of the aggregates. At such a phase transition often a hysteresis of the phase transition temperature is observed.

In the case of the columnar phase the molecules are arranged into a disc-like plate, the discs are stapled forming columns that are arranged in columnar hexagonal mesophases like those formed by disc-like molecules Fig 1.7

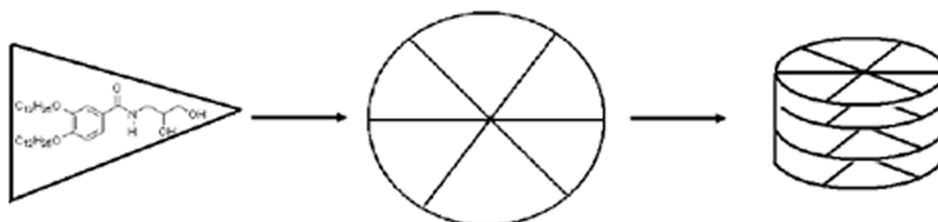


Figure 1.7 Process of self-organization of wedge shape molecules into columnar arrangement.

The polar groups of the molecules are forming a network of hydrogen bonds like a wire along the columnar main axis. This gives these mesophases a high electrical conductivity. The aromatic rings are stapled face to face to each other like in the disc-like shaped molecules.

1.4.2 Dynamics of the mesophases formed by diols.

The dynamics of the mesophases composed by diol compounds was partially investigated by the dielectric method to understand some aspects about the formation and the structure of the mesophases because of the formation of hydrogen bonds. Some easier diol molecules consisting of a alkyl chain and a polar diol segment at the end of the molecule forming Lamellar α and Lamellar β phases. A 2D hydrogen bond network exists in both cases. The alkyldiols were mainly dielectric investigated above 10 MHz because at low frequencies, very high electrical conductivity and similar disturbs the measurements of the dielectric permittivity. The compounds discussed show a very interesting dielectric behavior as long only observed in water that has a 3D hydrogen bond network. In the frequency range of about 1 GHz the orientation of the hydroxyl groups [87] and that of additional dipoles [88] could be detected.

Wedge shape diols were also preliminary investigated in our group [89]. In the columnar phase a complex dielectric behavior was found at low frequency range. Two processes could be observed, one of them at very low frequencies very difficult to separate from the conductivity, very similar to the columnar process observed in columnar mesophases composed by disc-like molecules with helical arrangement. The second mechanism occurs at MHz frequencies but the nature of this mechanism remains unclear.

In samples showing the polymorphism Cub_{I2}/Col_{H2} a strong increase in the dielectric absorption intensity at this phase transition could be observed. A decrease of the conductivity at this phase transition corroborate that the hydrogen bond network of the micelles in the cubic phase are centered in the middle of the micelles. Some compounds exhibiting this polymorphism are interesting to investigate the change of the properties at this phase transition.

A problem, not so often discussed in the literature, is the tendency of some multifunctional alcohols to absorb water from the air. Preliminary dielectric investigations on a selected strongly hygroscopic compound show an increase of the clearing temperature as well as of the dielectric permittivity, but practically no change in the time constant of the relaxation process [90]. The samples investigated here were tested by polarization microscopy. Furthermore they were heated to more than 120°C and measurements were performed directly after a waiting time of about 20 minutes. In most of the cases different experimental runs were done. Significant changes of the clearing temperature were not observed.

1.5 Motivation

Diols are amphotropic molecules that exhibit thermotropic mesophases with the same structure like lyotropic mesophases. The driving forces for the formation of mesophases are the formation of hydrogen bonds of the polar part of the molecules and the separation of the aliphatic/aromatic part on microscopic level which takes place in a first step of the process of self-organization. In a second step the aggregates form liquid crystalline mesophases. This very interesting process of two-fold self-assembly can be investigated by different methods like X-ray scattering and dielectric spectroscopy. In that way the aims of this work are to investigate the change of the physical properties with the change of chemical structure and with temperature on selected samples. This helps to understand also the complex processes of self-assembly in the nature. Our investigations were part of the “Graduierkolleg 894“ in which scientists of different branches worked together.

The compounds investigated form different mesophases in dependence of the size of the nonpolar part with respect to the polar part. That gives rise to the formation of cubic, columnar and smectic mesophases where the hydrogen bonds networks are located in different matter, in form of points, wires and planes. In that way one of the objectives is the investigation of the change of the properties with the change of the dimension of the network.

The dynamics of some liquid crystalline mesophases were preliminary and separately investigated but some aspects related with the nature of it remain unclear. A very important

aspect is the dynamics of super-structure caused by intermolecular hydrogen bonds. Especially the columnar mesophases reveals a very complex dynamical process which is related with a complicated arrangement of the molecules inside of the columnar lattice. The elucidation of the dynamics of those mesophases can help to understand a little bit more about the structure of the mesophases and also the role of intermolecular hydrogen bonds for the formation and stabilization of such complex systems.

For that purpose some homologues compounds exhibiting structures like Smectic A, columnar hexagonal and cubic mesophases, like molecules with different intermolecular interactions have to be synthesized and to investigate with the above mentioned techniques and in some cases also by Infrared and NMR spectroscopy as additional methods. Furthermore, a binary system consisting of two compounds with a network of hydrogen bonds in form of points and of a plane should be systematically characterized. In this way small changes of the different super-structure should be seen which can not be observed by measuring discrete compounds.

2. Theoretical introduction

2.1 Dielectric Spectroscopy

The dielectric permittivity is a property which quantifies the orientation of the dipole moments in an electric field. Substances without resultant dielectric moment exhibit a dielectric permittivity between 2 and 3 which is also detected in the solid state where the dynamics is frozen in. The dielectric permittivity can be separated in contributions when the frequency of the applied electric field is increased. In that way, one can see which parts of the molecules are moving, and which type of collective movements as phase-related response takes place.

2.1.1 Theory of dielectric spectroscopy

Dipolar molecules under an electric field show a torque which tends to align the dipoles in the direction of the field. In contrast, the thermal energy tries to orient the molecules and the dipoles statistically. Explicitly, the energy of a molecule with dipole moment μ in an electric field E is $-\mu E \cos \theta$, where θ is the angle between the dipole moment and the electric field. The molecule is in thermal contact with its surroundings, for which the thermal energy is $k_B T$ can be assumed. For low electric fields, the ratio between thermal and electrical energy is very small and, therefore, the change of order induced in the sample by the electric field can be neglected. Especially in our case where the measuring voltage is 1 V no induction of additional structures appears. The orientation-related part of the polarization P_{or} is composed by the contributions of all polar particles.

$$P_{or} = N \langle \mu \rangle \quad \text{Eq. 1}$$

Where N is the number density of the particles and $\langle \mu \rangle$ is the molecular dipole vector averaged over all possible orientations of the molecules. In absence of the electric field, $\langle \mu \rangle$ vanishes and statistical order would exist. For small values of $\mu E / k_B T$, the angle of the molecules with the electrical field direction will deviate only slightly from the situation in field-free conditions. Under these conditions, it is possible to investigate the molecules and the environment in thermal equilibrium [91].

When a constant external electric field $E(t)$ is applied to a system in thermal equilibrium, the equilibrium is disturbed and the polarization (P) reaches a new equilibrium with a characteristic time τ (Figure 2.1) [92]. Such measurements are called time-domain spectroscopy. An alternative approach is to apply a constant ac electrical voltage and change the frequency (frequency-domain measurements). When the frequency of the applied electric field increases, the time needed to attain equilibrium is smaller, and P decreases (Figure 2.2). The frequency at which P_{or} decreases to 50% is called relaxation frequency f_R and is related to the relaxation time by $f_R=1/2\pi\tau$. The polarization has the contributions of the orientation processes P_{or} , atomic and electronic processes that relax at higher frequencies [93]. With the increase of the frequency the reorientation of different dipoles cannot follow the external field. Thus, different rotational movements can be detected characterized by different relaxation frequencies f_R . Only the induced polarization due to atomic and electronic contributions remain $P_{ind}=P_E+P_A$ (P_{ind} is related to deformation of bond electrons and of electron distribution of the different atoms). In that way, relaxation experiments are very useful to determine the macroscopic relaxation times and frequencies of systems. As mentioned above, the reorientation of the molecules or of parts of complicated molecules is influenced by the surroundings. In this way, it reflects changes in the short-range order and partially also the formation of aggregates.

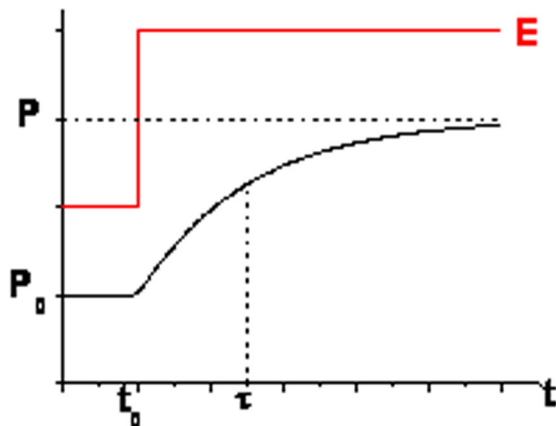


Figure 2.1 Polarization versus time. The polarization reaches a constant value P after the application of a constant field E .

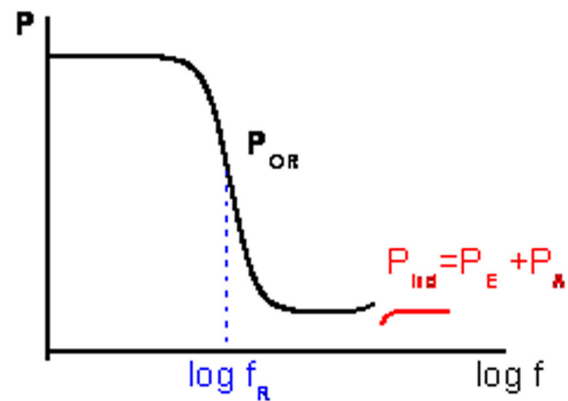


Figure 2.2 Polarization versus $\log f$. With the increase of the frequency the molecules stop to orient, the polarization decays and remains only the polarization due to electronic and atomic contributions $P_{ind}=P_E+P_A$.

A more detailed consideration of the dielectric response starts with the phenomenological description of the polarization: Orientation and induced polarization are responsible for the

polarization of the sample (Eq. 2) which is also related to the dielectric permittivity and the dielectric susceptibility.

$$P = P_{ind} + P_{or} = \epsilon_0 \chi E = \epsilon_0 (\epsilon - 1) E \quad \text{Eq. 2}$$

P_{ind} is the induced polarization, P_{or} is the dipolar polarization due to the orientation of the dipoles, ϵ_0 is the dielectric permittivity of the free space, χ the dielectric susceptibility and ϵ the dielectric permittivity. ϵ is a complex function, $\epsilon^* = \epsilon' - i\epsilon''$, where the real and imaginary parts ϵ' and ϵ'' , are also called dispersion and absorption components, respectively.

The induced polarization occurs in the time scale of $\sim 10^{-16}$ s, whereas the dipolar reorientation between 10 s and $\sim 10^{-12}$ s. Atomic (A) and electronic (E) processes occur at higher frequencies in the Infrared (IR) and Ultraviolet (UV) regions, respectively.

The time-dependent polarization $P(t)$ of the sample, being induced by a weak measuring electric field $E(t)$, is proportional to the field:

$$P(t) = \epsilon_0 (\epsilon^* - 1) E(t) \quad \text{Eq. 3}$$

where

$$E(t) = E_0 \exp(i\omega t) \quad \text{Eq. 4}$$

is a sinusoidal electric field applied to the sample, ω is the angular frequency $2\pi f$, and f is the frequency of external measuring electric field. The amplitude of the electric field E should be small enough so, the structure of sample under investigation remains unchanged. In order to satisfy the condition $\mu E/kT \ll 1$, the potential energy of a dipole moment μ due to the presence of the electric field E should be much smaller than the potential energy due to the thermal effect. Under this condition, the dependence of the polarization on the electric field is linear. This is very important for the investigation of liquid crystals where some helical structures can produce ferroelectricity [94].

For a real sample, a phase shift between $P(t)$ and $E(t)$, which results in a complex dielectric permittivity, must be considered. Furthermore, the electric conductivity has to be included in the imaginary part.

$$\epsilon^*(\omega) = \epsilon'(\omega) - i\epsilon''(\omega) - i\frac{\sigma}{\epsilon_0\omega} \quad \text{Eq. 5}$$

where σ is conductivity related to Ohmic resistance of the sample.

There are two limiting values of the dielectric permittivity (Figure 2.3): $\epsilon'(f \rightarrow 0) = \epsilon_{LF}$ is the traditionally dielectric permittivity of the sample, and $\epsilon'(f \rightarrow \infty) = \epsilon(\infty) = \epsilon_{HF}$ is the limit of the dielectric permittivity at high frequencies. For both limiting cases, the imaginary part is zero. Nonpolar materials have constant dielectric permittivity in the frequency range below 10 GHz $\epsilon_{LF} = \epsilon_{HF}$. For polar materials, the process of reorientation of the dipoles leads to absorption of energy when the frequency is close to the relaxation frequency. At this frequency, the curve of the imaginary part of the dielectric permittivity attains a maximum which is utilized to obtain f_R experimentally. The imaginary part of the dielectric constant ϵ'' is related directly with the energy absorbed per unit volume during this process. During this process the polarization is becoming out of phase with respect to the applied electric field. If the frequency of the external electric field is lower or equal than the characteristic rotational frequency of the dipoles, the rotating dipoles will be perturbed by the electric field, so producing a decreasing real part of the dielectric constant and a maximum in the imaginary part. Conversely, field frequencies higher than the relaxation frequency of dipoles have no influence on the dielectric constant.

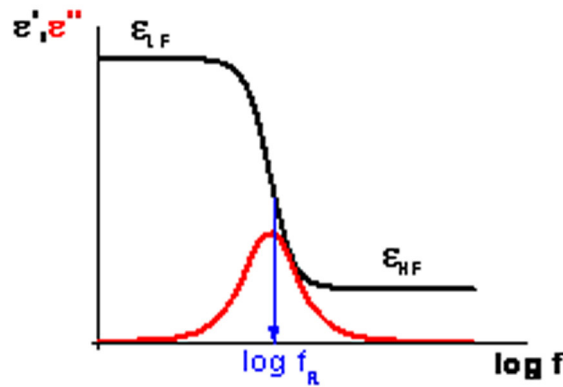


Figure 2.3 Representation of the complex dielectric permittivity versus $\log f$

Debye was the first to identify the contribution of molecular dipoles to the dielectric constant of isolating fluids [92]. He also gave the mathematical description of a simple relaxation behavior (see eqs. 8 and 9) and a phenomenological explanation of the relaxation time via the rotation viscosity of the molecules. However, the behavior of dipolar liquids cannot be accurately described by his dielectric theory. A better starting

point for a microscopic theory of the dielectric properties of liquids is given by Onsager [95a], which includes the Debye relation as special case.

Onsager introduced the fact that the reorienting field experienced by dipoles and the internal field caused by reaction are different.

$$(\epsilon - 1) = \frac{N_0 F h}{\epsilon_0} \left[\frac{\mu^2 F}{3k_B T} \right] \quad \text{Eq.6}$$

N_0 is the number density, ϵ_0 is the permittivity of empty space, μ is the molecular dipole moment, α is the mean polarizability, T is the absolute temperature, and the internal field factors for the reaction field (F) and the cavity field (h) are defined as:

$$F = \frac{(2\epsilon + 1)(n^2 + 2)}{3(2\epsilon + n^2)} \quad \text{Eq.7}$$

$$h = \frac{3\epsilon}{(2\epsilon + 1)} \quad \text{Eq.8}$$

Onsager's interpretation of the static dielectric permittivity is limited to isotropic non-associated dipolar liquids. The reduction of the effective molecular dipole moment due to the association of the molecular dipoles is described by introducing the correlation factor g which takes into account the short-range dipole-dipole interactions [95b]. This can be written as a function of the position of the molecular dipoles. This factor gives an idea of the local dipole organization in fluids. If $g > 1$, dipoles are locally ordered in parallel, while for $g < 1$ there is a local antiparallel organization of the dipoles. Until this point, the dipolar molecules are assumed to be rigid, or that there is only a single dipole contributing to the dielectric properties.

In order to understand the dielectric properties of dipolar molecules and the frequency-dependent properties of flexible molecules, it is important to consider that when the dipolar groups, μ_j are not rigidly connected, they contribute separately to the dielectric constant and then, the dielectric increment can be written as a sum of these contributions:

$$\epsilon(0) - \epsilon(\infty) = \frac{F^2 h}{3\epsilon_0 k_B T} \sum_j N_j \mu_j^2 \quad \text{Eq.9}$$

For a single relaxation (DEBYE relaxation), the real and imaginary parts of the complex permittivity are given by :

$$\epsilon'(\omega) - \epsilon'(\infty) = \frac{[\epsilon'(0) - \epsilon'(\infty)]}{[1 + \omega^2 \tau^2]} \quad \text{Eq.10}$$

$$\varepsilon''(\omega) = \frac{\omega\tau[\varepsilon'(0) - \varepsilon'(\infty)]}{[1 + \omega^2\tau^2]} \quad \text{Eq.11}$$

A convenient way to represent the dependence of the dielectric permittivity with the frequency is the Cole-Cole plot and described by the equation 12:

$$\varepsilon^*(\omega) - \varepsilon(\infty) = \frac{(\varepsilon'(0) - \varepsilon'(\infty))}{1 + (i\omega\tau_0)^{1-\alpha}} \quad \text{Eq.12}$$

This empirical equation represents a relaxation process having a symmetrical distribution of relaxation times on a logarithmic scale about a critical time τ_0 . The parameter α is a measure of the width of the distribution. This equation is used in this work to fit all the data. This function is appropriate for a single dipolar relaxation experiencing fluctuations in its local environment. Another equation describing the dielectric behavior is the Cole-Davidson equation:

$$\varepsilon^*(\omega) - \varepsilon(\infty) = \frac{(\varepsilon'(0) - \varepsilon'(\infty))}{(1 + i\omega\tau_0)^\beta} \quad \text{Eq.13}$$

This equation can be used to fit an asymmetric Cole-Cole plot and the parameter β is a measure of the width of an asymmetric distribution of relaxation times. The election of one of them depends on the characteristic of the process itself and requires experience and knowledge about the structure and the dynamics of the sample. A useful generalization is the Havriliak-Negami equation which contains the Cole-Cole and Cole-Davidson cases. More detailed information about the meaning of α and β as well as about the calculation are given in [96].

$$\varepsilon^*(\omega) - \varepsilon(\infty) = \frac{(\varepsilon'(0) - \varepsilon'(\infty))}{[1 + (i\omega\tau_0)^{1-\alpha}]^\beta} \quad \text{Eq.14}$$

The disadvantage of the dielectric method is that the half-width of the absorption curves is more than one decade (see Figure 2.3). Therefore the resolution of dielectric measurements is wronger than that of other spectroscopic methods. But due to the broad frequency range used in the resent time many authors use the term dielectric spectroscopy [96].

Another parameter that characterizes a relaxation process is the activation energy $E_A = R(\partial \ln \tau / \partial T^{-1})_p$ [97]. The change in the activation energy can be interpreted as a change in the barrier.

2.1.2 Dielectric spectroscopy of liquid crystals

In the case of liquid crystals, the dielectric investigations are interesting because the dielectric permittivity is a tensor quantity. Thus, the data obtained on oriented samples can be better related to the molecular dipoles. When the dielectric tensor is defined with respect to a set of principal axes, the number of independent components is reduced to three diagonal components. The dielectric tensor for uniaxial liquid crystals has only two independent components, the parallel and the perpendicular to the single axis of symmetry and is defined as follows:

$$\bar{\epsilon} = \begin{pmatrix} \epsilon_{\perp}^* & 0 & 0 \\ 0 & \epsilon_{\perp}^* & 0 \\ 0 & 0 & \epsilon_{\parallel}^* \end{pmatrix} \quad \text{Eq.15}$$

The dielectric permittivity tensor may also be specified by its average value $\bar{\epsilon}$ and the anisotropy $\Delta\epsilon$, defined as:

$$\bar{\epsilon} = \frac{1}{3}(\epsilon_{\parallel} + 2\epsilon_{\perp}) \quad \text{Eq.16}$$

$$\Delta\epsilon = (\epsilon_{\parallel} - \epsilon_{\perp}) \quad \text{Eq.17}$$

For isotropic materials, the anisotropy is zero and the permittivity can be represented by the scalar quantity ϵ . For anisotropic materials, the measured permittivity depends on the direction of measurement. For example, with the help of a magnetic field, nematic liquid crystals can be aligned perpendicular or parallel to the electric measuring field.

The different components of the tensor show different frequency- and temperature-dependences for uniaxial liquid crystals. First theoretical description based on the Onsager model was given by Meier and Meier. Using the model of nematic potential, the retardation of relaxation times could be explained by Meier and Saupe [98]. An example where the stepwise retardation of the reorientation time for the dynamics about the short

axes is related to the structure of different LC phases is given by Kresse [39]. In the case of biaxial liquid crystals phases (for example the Smectic C phase), there are two directors and, in order to obtain a monodomain sample, both must be aligned. This is difficult, therefore such kind of measurements are rare for liquid crystals.

New developments in the field of liquid crystals are bent-shaped molecules, which also show certain opposition to reorientation about the long axes of the molecules [99]. In dependence of the bent angle a order of the perpendicular dipoles can be build up. This results in interesting physical behaviors, particularly the dielectric one. For this reason, measurements for colleagues of the “Graduierertenkolleg” were performed and published together [100,101]. These investigations will not be discussed in this thesis.

2.2 Nuclear Magnetic Resonance (NMR)

Nuclear Magnetic Resonance is an important method to study the dynamics of molecules and is very useful for the interpretation of complicated dielectric spectra. Molecular-level information facilitates assigning the different dielectric absorption processes via some parameter relations such as the one between the coupling constant and the angle of movement of the part of the molecule in study.

The NMR investigations can help to understand how the molecules moves and how big this movements are. The dipole-dipole coupling constant D_{CH} and the local order parameter S , contain information about of the molecular motion. The averaging of the coupling constant needs motions on a time scale faster than 10^5 Hz. Cualitative Cross Polarization experiments are a useful tool to determinate the 1H - ^{13}C dipol-dipol coupling constant D . In this experiments the magnetization in transferred from the 1H atoms to the ^{13}C during a contact time and after that is acquired in the ^{13}C atom. This process is modulated by the coupling constant [102].

S is the order parameter and can be calculated by $S=D_{sol}/2D_{LQ}$ given in the form of the second order Legendre polynomial and is obtained as the ratio of the measured effective dipole –dipole coupling constant to that of a static pair. In that way the geometry of motions in this time scale can be obtained. It is known that the rotation of the molecules in the plane perpendicular to the main axis of the column reduces the coupling constant in a

factor of 2 and additional librational movements are responsible for the rest of the reduction in di-like molecules [103].

2.3 IR Spectroscopy

Infrared spectroscopy exploits the fact that molecules have specific frequencies at which they rotate or vibrate corresponding to discrete energy levels (vibrational modes). These resonant frequencies are determined by the shape of the molecular potential energy surfaces, the masses of the atoms and the associated vibronic coupling. In order for a vibrational mode to be IR active, it must be associated with the changes in the permanent dipole. The resonant frequencies can be related to the strength of the bond and the mass of the atoms at either end of it. Thus, the frequency of the vibration can be associated with a particular bond type. The infrared spectrum of a sample is collected by passing a beam of infrared light ($10 - 14\,000\text{ cm}^{-1}$) through the sample. Examination of the transmitted light reveals how much energy was absorbed at each wave length. The wave number of absorbance measured and is connected in the simplest way with molecular data by:

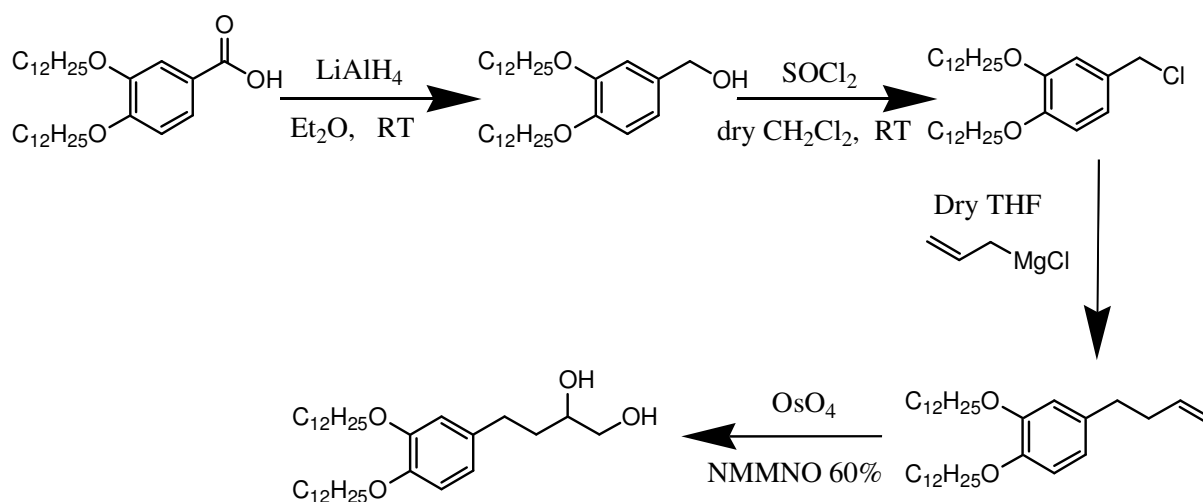
$$\nu = \frac{1}{2\pi} \sqrt{\frac{k}{\mu}} \quad \begin{array}{l} k = \text{spring constant for the bond} \\ \mu = \text{reduced mass of the A-B} \\ \text{system} \end{array} \quad \text{Eq. 18}$$

In that way every interaction that changes the spring constant or the reduced mass can change the wave number of the absorption band. Hydrogen bonds formation can be followed by IR Spectroscopy, since they reduce the force constant and shift the absorption bands to lower wavenumbers.

3. Experimental Part

3.1 Synthesis of few substances.

Synthesis of 4-(3,4-didodecyloxyphenyl)butane-1,2-diol



3,4-Didodecyloxybenzylalcohol.

3,4-Didodecyloxybenzoic acid (5g, 10.3 mmol) was reduced with LiAlH_4 (2g, 5.26 mmol) in dry THF (200 ml). After 24 hours reaction time water (4ml) were added dropwise to the reaction mixture stirring, followed by NaOH (15%, 4 ml) and water (12 ml). The granular salts were filtered and extracted 3 times with THF (50 ml) by refluxing for 1 hour. The THF was evaporated under vacuum and after crystallization from acetone a white solid (3.23g, 66%) was obtained.

4-Chloromethyl-1,2-didodecyloxybenzene.

To a solution of 3,4-didodecyloxybenzylalcohol (2g; 4.20 mmol) in dry CH_2Cl_2 (20ml) in a 3neck flask equipped with a magnetic stirrer thionylchloride (1ml) was added slowly. After 3 hours reaction by reflux the solvent and the excess of SOCl_2 was removed under high vacuum and collected. The freshly prepared compound was used immediately without any other purification in the next reaction step.

4-But-3-enyl-1,2-didodecyloxybenzene.

4-Chloromethyl-1,2-didodecyloxybenzene was dissolved in dry THF (20 ml) and allylmagnesium chloride (10 ml) in dry THF was added during 15 minutes at room temperature under argon atmosphere. The mixture was refluxed for 12 hours, was allowed to cool and then hydrolyzed by carefully adding a saturated ammonium chloride solution. Organic materials were extracted with ethyl ether (100 ml, 3 times) and the combined extracts were washed with saturated aqueous sodium bicarbonate and brine (100 ml). After drying over sodium sulphate the solvent was evaporated to give an oily residue which was purified by filtration through silica gel (60 Korn, 0.040-0.063 μm , Merck) with CHCl_3 to give 4-but-3-enyl-1,2-didodecyloxybenzene (1.95g, 93 % yield).

^1H NMR (400 MHz, CDCl_3 , ppm): 6,77 (d, $J = 8$ Hz, 1H, H-Ar), 6,70 (d, $J = 2$ Hz, 1H, H-Ar), 6,69(dd, $J = 8$ Hz, $J = 2$ Hz, 1H, H-Ar), 5,88-5,78 (m, 1H, $\text{CH}=\text{CH}_2$), 5,05-4,93 (m, 2H, $\text{CH}=\text{CH}_2$), 3,97-3,45 (m, 4H, O- CH_2), 2,63-2,59 (m, 2H, CH_2 -Ar), 2,35-2,29 (m, 2H, CH_2 - CH_2 -Ar), 1,82-1,73 (m, 4H, - CH_2 -), 1,48-1,4 (m, 4H, - CH_2 -), 1,248 (m, 32H, - CH_2 -), 0,86(t, $J=6,6$ Hz).

4-(3,4-Didodecyloxyphenyl)butane-1,2-diol

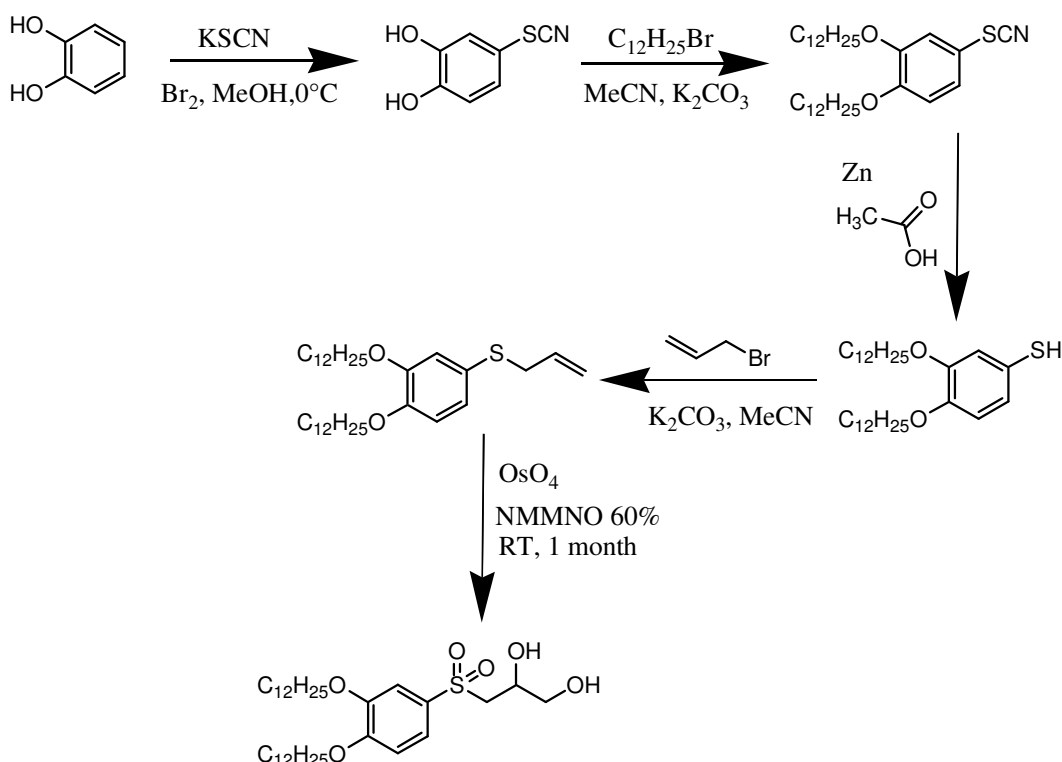
4-But-3-enyl-1,2-didodecyloxybenzene (1.72g, 3,4 mmol) dissolved in acetone (150 ml) was placed in a 500 ml flask equipped with a magnet stirrer . A solution of *N*-methylmorpholine-*N*-oxide monohydrate (60 % solution in water 2.9ml, 17.2 mmol) was added and after a solution of osmium tetroxide in tert.-butanol (0.004 M, 3ml, 17.2 mmol) was added. After 1 month reaction time saturated aqueous sodium sulphite solution (5 ml) was added and the mixture was stirred for 30 minutes at room temperature. The mixture was filtered over a silica bed and washed three times with acetone (50 ml). The solvent was evaporated in vacuum. The residue was dissolved in ethyl acetate (100 ml). The solution was washed with dilute sulfuric acid (10 %, 30 ml), saturated NaHCO_3 (30 ml) and water (30 ml). The organic layer was dried over sodium sulphate and the solvent was evaporated in vacuum. Purification was done by filtration over silica. First, elution with chloroform removed the nonreacted starting material (0,32 g, 0,64 mmol) and afterwards the product was eluted with methanol. After evaporation of the solvent the product was crystallized from EE/PE 1:1 (yield: 1.09 g, 60 %).

^1H NMR (400 MHz, CDCl_3 , ppm): 6,77 (d, $J = 8$ Hz, 1H, H-Ar), 6,71-6,67 (m, 2H, H-Ar), 3,96- 3,92 (m, 4H, O- CH_2), 3,72-3,70 (m, 1H, CH-OH), 3,66-3,61 (m, 1H, CH_2 -OH), 3,48-

3,42 (m, 1H, CH₂-OH), 2,75-2,57 (m, 2H, CH₂-Ar) 1,99-1,67 (m, 6H, -CH₂-CH-O, -CH₂-CH₂-O), 1,49-1,39 (m, 4H, -CH₂-) 1,246 (m, 32H, -CH₂-), 0,86 (t, J = 6,6 Hz, 6H, CH₃).

¹³C NMR (400 MHz, CDCl₃, ppm):

Synthesis of 3-(3,4-didodecyloxybenzenesulfonyl)propane-1,2-diol



4-Thiocyanatobenzene-1,2-diol

A solution of Br₂ (7ml, 0.13 mol) in a saturated solution of NaBr in methanol (70ml) was added during 5 minutes at 0°C to a solution of 1,2-dihydroxybenzene (10g, 0,1 mol) and potassium thiocyanate (30.8 g, 0.35 mol) in a saturated solution of NaBr in methanol (150 ml).

The reaction mixture was stirred at 0°C for 1 hour. Water (150 ml) was added. The aqueous phase was extracted with ethylacetate (3 times, 150 ml). The organic solution was washed with water, neutralized with a solution of NaHCO₃, dried over sodium sulphate and evaporated on a rotary evaporator under vacuum. The product (18.81 g, 112%) was used in the next step without further purification.

¹H NMR (400 MHz, Acetone-d₆, ppm): 8,61(2H, OH), 7,10 (d, J=2,28 Hz, 1H, H-Ar) 7,05 (dd, J₁=8,3, J₂=2,28 Hz, 1H, H-Ar), 6,93 (d, J=8,1 Hz, 1H, H-Ar).

1,2-Didodecyloxy-4-thiocyanatobenzene

To a solution of 4-thiocyanatobenzene-1,2-diol (5.1g, 30.5 mmol) in acetonitril (150 ml) and K₂CO₃ (8.5g, 61.1 mmol) was added dodecylbromide (16 ml, 61.1 mmol). The mixture was heated at reflux during 16 hours until the reaction was finished. Water was added and the organic components were extracted with Dichloromethan, washed three times with solution of sodium bicarbonate neutralized and dried over sodium sulphate. After evaporation of the solvent the product was purified by chromatography (silica gel, eluent CHCl₃:n-pentan 2:1) (6.24g, 43%).

¹H NMR (400 MHz, CDCl₃, ppm): 7,07 (dd, J₁=8,3, J₂=2,28 Hz, 1H, H-Ar), 7,01 (d, J=2,28 Hz, 1H, H-Ar), 6,84 (d, J=8,1 Hz, 1H, H-Ar), 3,98 (t, J=6,6 Hz, 4H, CH₂-O-), 1,83-1,76 (m, 4H, -CH₂-), 1,47-1,40 (m, 4H, -CH₂-), 1,248 (m, 4H, -CH₂-), 0,88-0,84 (m, 6H, -CH₃).

¹³C NMR (400 MHz, CDCl₃, ppm): 151,1 (C-O), 150,2 (C-O), 125,1 (CH-Ar), 116,8 (CH-Ar), 114,3 (CH-Ar), 113,7 (-C-S), 111,5 (S-C-N), 69,6 (C-O), 69,4 (C-O), 14,1(-CH₃)

3,4-Didodecyloxybenzenethiol

1,2-Didodecyloxy-4-thiocyanatobenzene (4.24g, 9 mmol) was heated in acetic acid (100 ml) and zinc powder was added until the reaction was finished. Water was added and the zinc was filtered and washed with dichlormethane. The acetic acid was neutralized with NaOH and NaHCO₃ until *p*_H =7 and washed three times with water (100 ml). The organic solution was dried over sodium sulphate und evaporated. The product (4g, 99%) was used in the next step without purification.

¹H NMR (400 MHz, CDCl₃, ppm): 6,84-6,82 (m, 2H, H-Ar), 6,74-6,72 (m, 2H, H-Ar), 3,95-3,91 (m, 4H, -CH₂-O-), 1,81-1,72 (m, 4H, -CH₂-), 1,66-1,39 (m, 4H, -CH₂-), 1,244 (m, 4H, -CH₂-), 0,87-0,84 (m, 6H, -CH₃).

4-Allylsulfanyl-1,2-didodecyloxybenzene

3,4-Didodecyloxybenzenethiol (1.82g, 3.8 mmol) in acetonitril (40 ml) was heated under argon atmosphere. Sodium hydroxide (0.18g, 4.5 mmol) was added to the solution and after 10 min allyl bromide (0.38 ml, 4.5 mmol) was added and refluxed for 12 hours. The solvent was evaporated. The solid was dissolved in chloroform. The solution was washed

until $p_{\text{H}}=7$ and dried over sodium sulphate. The solvent was evaporated and the product (1.13g, 58%) was used for the next reaction without purification.

^1H NMR (400 MHz, CDCl_3 , ppm): 6,93-6,90 (m, 2H, H-Ar), 6,78-6,75 (m, 1H, H-Ar), 5,88-5,80 (m, 1H, $\text{CH}=\text{CH}_2$), 5,78-5,01 (m, 1H, $\text{CH}_2=\text{CH}$), 4,98 (s, 1H, $\text{CH}_2=\text{CH}$), 3,96-3,92 (m, 4H, O- CH_2), 3,43-3,41 (m, 2H, S- CH_2), 1,81-1,73 (m, 4H, - CH_2 -), 1,50-1,39 (m, 4H, - CH_2 -), 1,283 (m, 32H, - CH_2 -), 0,86(t, $J=7,05$ Hz, 6H, CH_3).

3-(3,4-didodecyloxybenzenesulfonyl)propane-1,2diol

The dihydroxylation was done with the same procedure as described before. 4-Allylsulfanyl-1,2-didodecyloxybenzene (1.13g, 1.9mmol), *N*-methylmorpholine-*N*-oxide monohydrate (1.62ml, 9.6 mmol) and a solution of 0,004 M of osmium tetroxide in tert-butanol (1.7m, 9.6 mmol) in acetone (100 ml). Purification was done by filtration over silica, first with chloroform to remove the 1,2-didodecyloxy-4-(prop-2ene-1-sulfonyl)benzene (0.44 g, 0.8 mmol, 42 %) and afterwards with methanol to collect the product which was crystallized from EE/PE 1:1 and washed with cold methanol (0.18g, 0,31mmol, 16 % yield).

3.2 Equipments used

3.2.1 X-ray investigations

X-ray investigations on powder-like samples were carried out with a Guinier film camera (Huber). The samples were kept in glass capillaries (\varnothing 1 mm) in a temperature-controlled heating stage, quartz-monochromatized $\text{CuK}\alpha$ radiation was used. The film patterns were calibrated with the powder pattern of $\text{Pb}(\text{NO}_3)_2$. The diffraction of the same samples in the small-angle region was recorded by a modified Kratky camera with a position-sensitive linear detector (MBraun) using Ni-filtered $\text{CuK}\alpha$ radiation. 2D patterns for surface-aligned samples on a glass plate on a temperature-controlled heating stage were recorded with a 2D detector (HI-STAR, Siemens) using Ni-filtered $\text{CuK}\alpha$ radiation. The alignment takes place at the sample – glass or at the sample – air interface on slow cooling, usually giving domains, which are fiber-like disordered around an axis perpendicular to the interface).

3.2.2 Dielectric investigations

3.2.2.1 Low frequency dielectric investigations

Dielectric measurements in the frequency range between 1Hz and 10 MHz were done using the Solartron-Schlumberger Impedance Analyzer Si 1260. Due to the high electrical conductivity of all diols investigated measurements at lower frequencies makes no sense.

The components and the mixtures were heated to about 15 K above the clearing point in order to evaporate additional water and filled after a waiting time of about 20 min in the calibrated measuring capacitor (brass cell coated with gold, $d = 0.05$ mm). The samples could not be oriented using a magnetic field. Dielectric measurements were made during slow cooling. The temperature was stabilized by a Eurotherm equipment to 0.1 °C.

The experimental data were fitted to two Cole-Cole mechanisms consisting of:

$$\epsilon^* = \epsilon_2 + \frac{\epsilon_0 - \epsilon_1}{1 + (j\omega\tau_1)^{1-\alpha_1}} + \frac{\epsilon_1 - \epsilon_2}{1 + (j\omega\tau_2)^{1-\alpha_2}} - \frac{jA}{f^M} + \frac{B}{f^N} \quad \text{Eq. 19}$$

the limiting values ϵ_i of the dielectric permittivity and the corresponding relaxation times τ_i with $\omega=2\pi f$ (f - frequency), α_i - Cole-Cole distribution parameters, the conductivity term A as well as M , B and N as further fit parameters responsible for the slope of conductivity and capacity of the double layer were calculated. The imaginary and real part of the dielectric permittivity, the contributions of conductivity and double layer were fitted together (complex fit). Only in this way all measured data could be analyzed in the best way. This way of data processing is important to get the right information for higher conducting materials like diols.

For calculation of the specific conductivity the dielectric loss ϵ'' measured in the frequency range between 100 and 1000 Hz was fitted to the fourth term in Eq. 19 under the condition $M=1$. This limitation was necessary in order to exclude saturation effects seen at very high dielectric losses and on the other side the influence of dielectric relaxation. The condition $M=1$ was practically also fulfilled with M as open parameter because the M parameter obtained in this way are between $0.985 < M < 1,000$. From the fitted A -parameter the specific conductivity κ was calculated according to

$$\kappa = A \cdot 2 \cdot \pi \cdot 8.85 \cdot 10^{-12} \text{ Sm}^{-1}. \quad \text{Eq. 20}$$

3.2.2.2 High frequency dielectric measurements

Impedance Analyzer Agilent 4291 B with frequency range $10^6 - 1.8 \times 10^9$ Hz with temperature control by a Nitrogen-jet stream Quatro Cryosystem by Novocontrol was used. A parallel plate capacitor of about 5 mm diameter and 1 mm thickness is formed with the sample by using two gold-plated electrodes. The capacitor is located inside the RF cell located at the end of the RF extension line. The measurements were done at the Material Physics department of the 'Universidad del país Vasco'. For details see <http://www.sc.ehu.es/sqwpolim/PSMG/dielab.html>

3.2.3 NMR measurements

NMR measurements were done with Bruker Avance-II Spectrometer with frequency of ^1H channel of 400 MHz and ^{13}C channel 100 MHz, equipped with a 4mm-Bruker MAS double resonance probe head. Cross Polarization Magic Angle spinning under 10 kHz rotation with nutation frequencies of 60 kHz was used. Heteronuclear ^1H - ^{13}C decoupling during acquisition was achieved using TPPM decoupling sequences. All measurements in the liquid crystalline phase were performed by cooling down the sample. The measurements were done at the NMR Group of Halle. For details see: <http://www.physik.uni-halle.de/fachgruppen/nmr/>

3.2.4 Polarization microscopy

The optic textures were observed with polarization microscope Leitz Laborlux. This is equipped with Linkam Heatable Mettler FP80 with temperature regulation of ± 0.1 K. For the documentation of the textures a Nikon camera was used. The samples were situated between two glasses covers, and observed under crossed polarizers. In this way first information about the polymorphism of the liquid crystals could be obtained. This method was also very useful to see the possible influence of water in the air on the transition temperatures and to study single concentrations of the phase diagram. Thus, we could develop a measuring procedure which practically excludes the influence of water on the transition temperature. The transition temperatures between the liquid crystalline phases and the clearing temperature were taken from runs by slow cooling.

3.2.5 Differential scanning calorimetry (DSC)

The calorimetric measurements were done with a Pyris 1 DSC from the Perkin-Elmer company. The standard program was a measurement during heating, a second run during cooling and a third one heating again. In this way the melting temperature could be obtained from the first run and the transition temperatures between liquid crystalline phases and the clearing temperature from the second run. The cooling run gives also the possibility to investigate the metastable liquid crystalline or isotropic phase range due to supercooling effects. The phase transition temperatures were measured during slow cooling because only in this way the data could be compared with that of the other methods due to hysteresis effects. The known weight of the samples did allow calculating the transition enthalpies using a standard program of the Perkin-Elmer software.

4. Results

4.1 Extended investigations on a binary system

With the purpose of researching the dynamics and the change of the properties with the change of the super-structure of mesophases composed by diols, a binary system was investigated. This is composed by two components that form two different kinds of mesophases. One of the components exhibits a smectic phase and the other shows a cubic phase. The difference in the number of the alkyl chains attached to the aromatic ring decides the type of organization of the molecules. That changes the size ratio between the hydrophobic and hydrophilic parts and determines the type of mesophase.

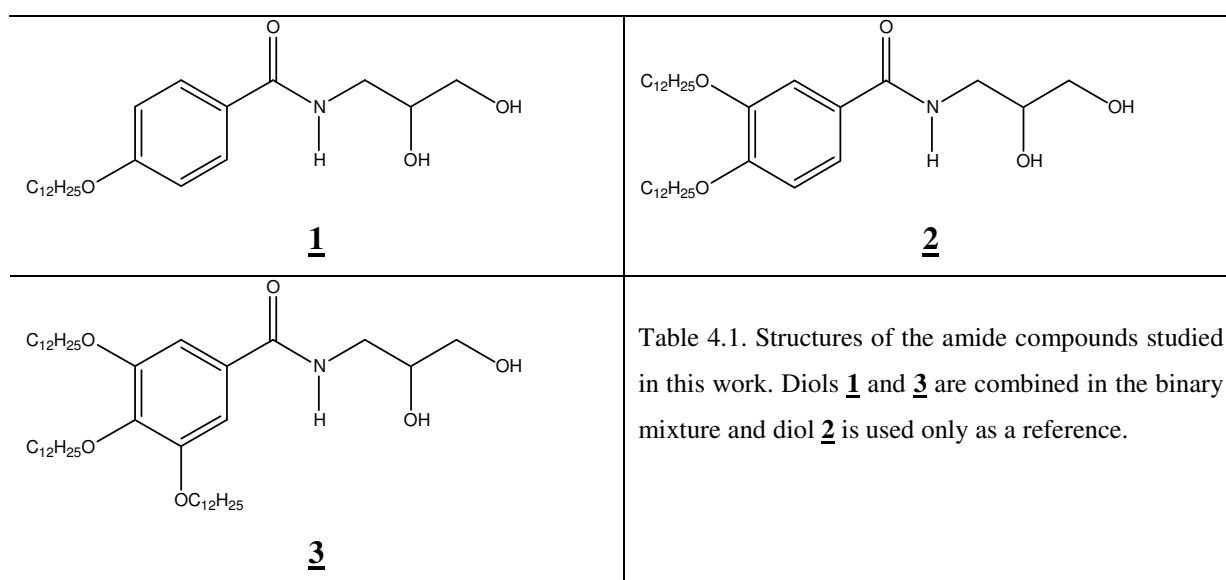
The compound with two alkyl chains in the hydrophobic part forms a columnar phase and the dynamics was already investigated by the dielectric method [89]. The dynamics of this compound is dominated by the orientation of the dipole moments of the middle part of the molecule. Furthermore, the strong intermolecular interactions connected with the hydrogen bonds between the amide-group produce a high clearing temperature. For this reason measurements in the isotropic phase are restricted due to the thermal instability of the substance. For example, the columnar phase of this compound exists between 110 and 150 °C (see structure of compound **2** in the Table 4.1).

A very strong absorption band at 1 MHz frequency is observed in the whole mesophase temperature range [89]. Up to now, the model in which the molecules form discs packed into columns could not be corroborated. Only X-ray investigations can help to elucidate the hexagonal packing of the columns inside the mesophase.

In the middle concentration range of this binary mixture, a columnar mesophase is induced. Despite the very high clearing points of the mesophases, the phases are thermally stable, and the presence of the columnar phase in a broad concentration range allows the elucidation of the slow dynamics of this phase.

With the investigation of a binary system, the concentration of the components can be systematically varied and, in that way, the phase behavior can be changed. This gives now the possibility to relate changes in the dielectric behavior to differences in the super-structure more clearly.

The substances were re-synthesized [83] and characterized by DSC and polarization microscopy. Substance **1**, p-n-dodecyloxy-N-(2,3-dihydroxypropyl)benzamide, shows the polymorphism Cr 358 K SmA 403 K I (phase transition temperatures from the first heating run). For the third compound, 3,4,5-tris-dodecyloxy-N-(2,3-dihydroxypropyl)-benzamide (**3**), the polymorphism Cr 344 K Cub₁₂ 399 K I was confirmed [83]. The compound **2** with 2 chains shows a columnar phase between 110°C and 150°C and was already measured and reported by Kresse et al, 1997 [89]. Some experimental data will be used to compare the results of the columnar phase of the single component **2** with that of the columnar phases of the binary mixture investigated. The reason for this procedure is that the 1 to 1 mixture of the compounds **1** and **3** exhibit the same number of alkyl chains than substance **2**.



The phase diagram shown in Figure 4.1 was obtained by microscopic investigations and published at first by Borisch and coworker [83]. We have extended the diagram to lower temperatures by results of dielectric measurements.

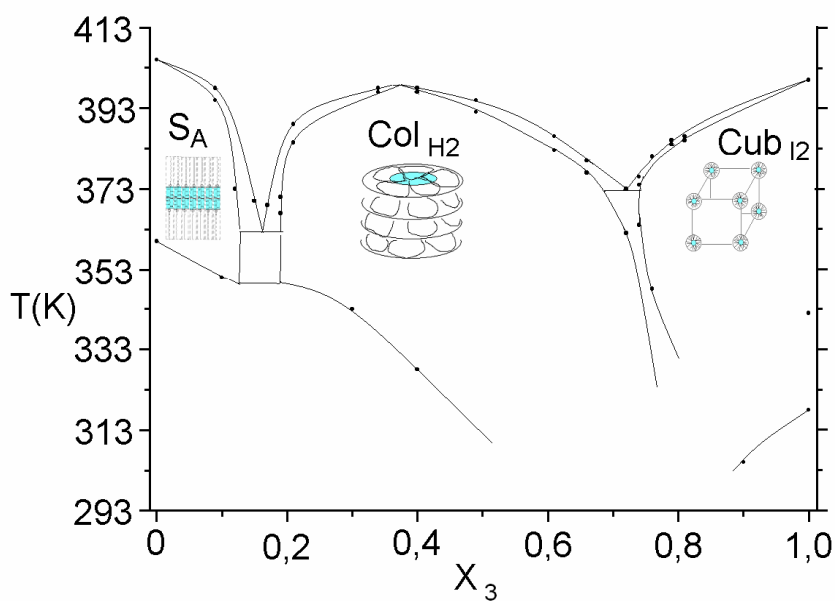


Figure 4.1 Phase diagram of the binary system depending on the concentration of compound **3** with inserted structural models. The blue elements indicate the hydrogen bonds networks in the mesophases.

4.2 Investigation of the SmA phase

In the following part pure samples and mixtures showing SmA polymorphism are investigated and discussed together. The mixture of the binary system with $x_3=0.05$ is included in this consideration because the phases were chosen as main order principle. The results of the phase diagram will be discussed later.

4.2.1 Dielectric behavior of the amide compound in the smectic phase

After the general description of the dielectric method in the experimental part we will discuss here the errors and results of the fit critical and more in detail. The high conducting compound **1** with the 2D network of hydrogen bonds seems to be an extreme and suitable example. At low frequencies and high temperatures, the contribution of the conductivity to ϵ'' and that of the formation of an electrical double layer to ϵ' dominate the spectrum. As seen in Figure 4.2, the real part of measured dielectric functions ϵ' approaches the “static” dielectric permittivity ϵ_0 of about 20 at frequencies above 30 kHz. A dielectric absorption range starts at frequencies above 0.5 MHz.

The errors of the static dielectric constant ϵ_0 measured in the SmA phases are about 1% at low and 2% at high temperatures. The fitted parameters ϵ_1 and τ_1 show an uncertainty at low temperatures of about 5% and 20% respectively, and the specific conductivity of 1%. It has to be noted that, additionally, all data measured in anisotropic phases contain a much higher error arising from the unknown orientation of the samples.

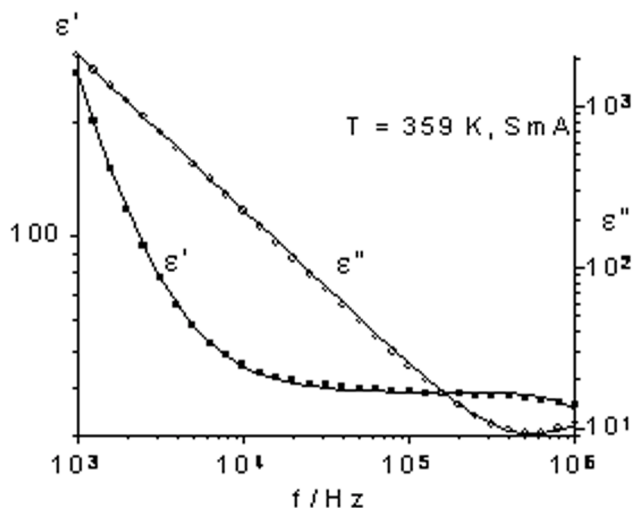


Figure 4.2 Complex dielectric function of substance 1 and the fitted curve.

The experimental curves reveal the presence of an absorption range at frequencies higher than 1 MHz. This process could not be really measured at higher temperatures as demonstrated in figure 4.2 because it is in the limit of the frequency range of the low frequency equipment. Therefore, measurements at higher frequencies are required to investigate this process.

Measurements at different temperatures did allow extracting dielectric parameters from the fit. The static dielectric constant of compound 1 increases in a stepwise fashion at the phase transition and, after that, continuously with decreasing temperature to about 40 (Figure 4.3). The formation of the 2D hydrogen bonds network of the SmA phase occurs with a reorganization of the structure, so a positive correlation of the dipole moments during the formation of the layers at the phase transition is responsible for the increase of the dielectric permittivity. Other systems like water with a 3D network of hydrogen bonds show a dielectric permittivity of 80.

In the isotropic state, the dielectric permittivity increases linearly with falling temperature. This relative strong change can arise from the dielectric response of the isotropic distribution of single molecules or cybotactic groups. The temperature of the clearing point is high and therefore, the dielectric absorption band is at too high frequencies that it cannot be detected with the low frequency equipment (see also figure 4.2).

The conductivity increases at the I/SmA transition (Fig 4.4), which indicates that the smectic A layers are oriented preferably parallel to the measuring electric field. The 2D structure of the hydrogen bonds network allows the conduction of charge carriers in the direction of the electric field when the layers are parallel to the applied electric field (see also figure 4.5). In this configuration, the contribution of the hydrogen bonds to ϵ_0 is also higher than when the layers are perpendicular to the applied electric field see Fig. 4.3.

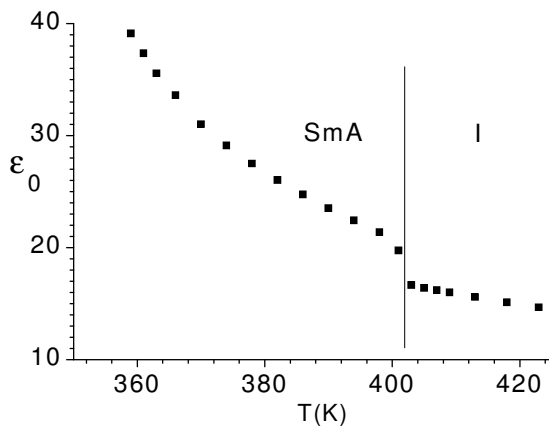


Figure 4.3 Static dielectric permittivity versus the temperature in K of substance 1.

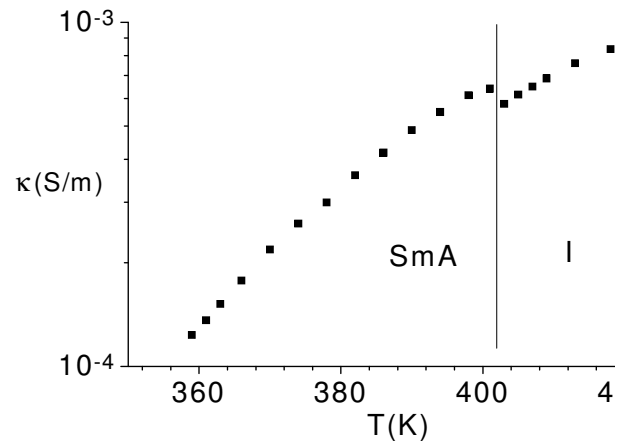


Figure 4.4 Specific conductivity versus temperature in K of substance 1.

4.2.2 Mixture in the SmA phase at $x_3=0.05$

The dielectric behavior of the mixture is similar to that of the pure compound discussed before. Like in the previous investigations, the relaxation process could not be found, but some interesting phenomena, depending of the orientation of the sample, were observed in the values of the dielectric permittivity measured at different runs.

The orientation of the layers with respect to the electric field plays a role in the value of the dielectric permittivity because it is defined as a tensor (see the introduction Eq. 15). In order to demonstrate this influence, two measurements of the same sample with $x_3 = 0.05$

were carried out. In both cases the same sample was heated into the isotropic state and after that cooled down. The orientation of the layers with respect to the electric measuring field was not influenced by a magnetic field. We assume that the actual orientation of the sample depends on surface interaction with the gold layer of the measuring capacitor, on the cooling rate and may be also on statistical effects. In order to understand the experimental results a more detailed consideration of the electrical conductivity and the change of conductivity at the clearing temperature are necessary.

The conductivity is the result of the transport of charge carriers in the direction of the electric field. Protons or ions as impurities can act as charge carriers. The SmA phases of the diols exhibits channels for the transport of charge carriers along the 2D network of hydrogen bonds as demonstrated in figure 4.5. If the layers are perpendicular to the electric field, the charge diffusion through the channel of hydrogen bonds is favorable and the conductivity is higher than that when the dielectric field is perpendicular to this channel. In the isotropic phase molecules as well small aggregates (cybotactic groups) are statistically distributed. Therefore, a mean value $\kappa = 1/3 (2 \kappa_{\perp} + \kappa_{\parallel})$ will be measured. The subscripts “perpendicular” and “parallel” are related to the layer normal.

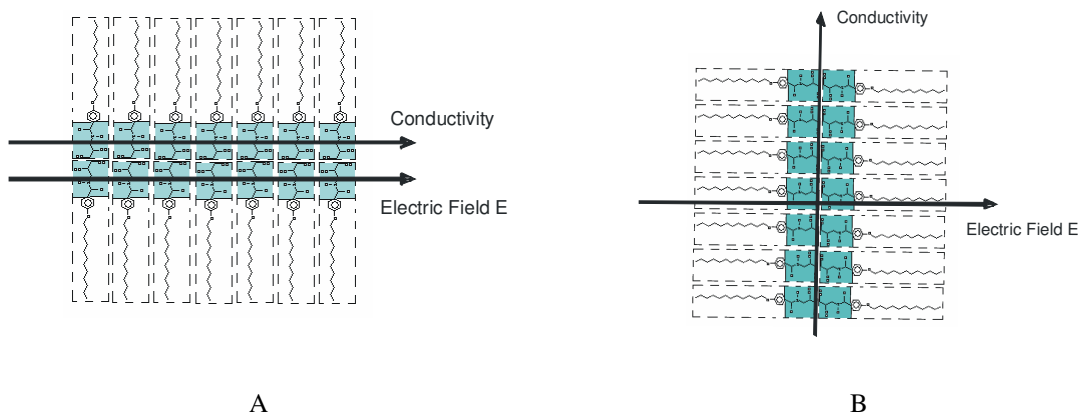


Figure 4.5 Influence of the conductivity of the orientation of the smectic phase in the electric field A) Electric field is parallel to the hydrogen bonds network B) Electric field is perpendicular to the hydrogen bonds network in the smectic phase. The axis of highest conductivity is also indicated by an arrow.

For the first measurement (Figure 4.6, first run), the layers of the SmA phase are preferably oriented perpendicular to the measuring field. Therefore, the static dielectric permittivity

and the conductivity (Figure 4.7, first run), increase at the transition into the isotropic phase.

For the second run, which was performed two days later, practically no step in both quantities is observed. This strange behavior, obtained by chance, indicates a more statistical orientation of the layers with respect to the measuring electric field. A comparison between the two runs is represented in the Figures 4.6 and 4.7. The increase of the conductivity in the isotropic phase for the second run is not connected with a remarkable shift of the clearing temperature (see figure 4.6). We assume that it is mainly caused by slight decomposition of the sample.

The three possible situations in which the 2D network of hydrogen bonds is preferably parallel to the electrical field (figure 4.4), perpendicular to the measuring field (figure 4.7, first run) and statistically distributed (figure 4.7, second run) could be realized. Thus, using the model sketched in figure 4.5 one is able to say something about the relation of the dielectric tensors with respect to the layer normal. The related data of the dielectric permittivity clearly show that the measured permittivity in direction of the network (fig 4.3) show higher values at the transition into the SmA phase. In the case of statistical distribution no step of the permittivity at the I/SmA transition is seen, only the slope changes (figure 4.6, second run). In the other case a stepwise decrease (figure 4.6, first run) is seen indicating that the dielectric permittivity parallel to the layer normal much lower than that in direction perpendicular to it.

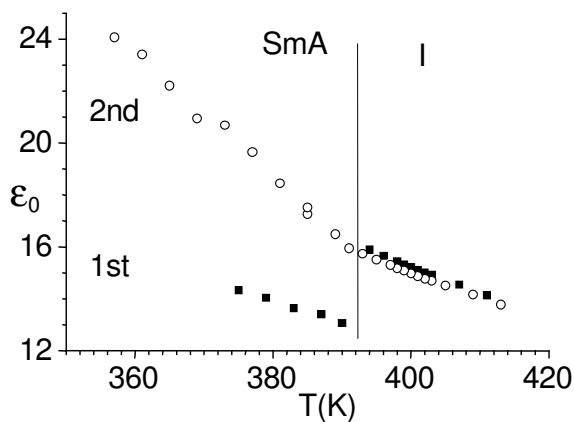


Figure 4.6: Static dielectric constants vs T(K) of the sample with $x_3=0.05$ for two runs.

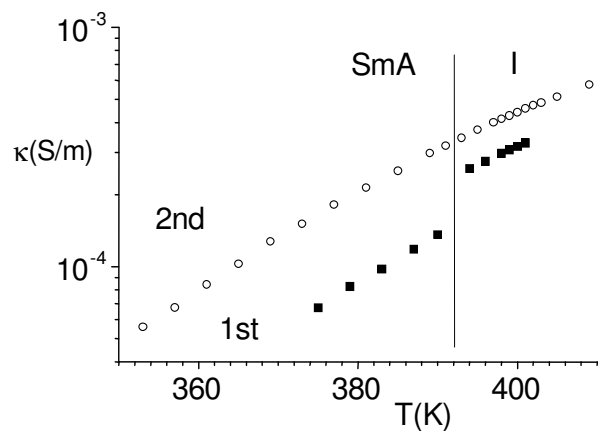
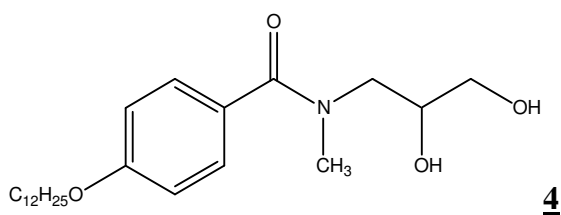


Figure 4.7: Specific conductivity of the sample with $x_3=0.05$ for two runs.

4.2.3 Study of the SmA phase of methyl-substituted compound.

As expected, the substance with only one alkyl chain at para position of the substituted benzamide and methylated at the nitrogen exhibits a SmA mesophase. The substitution of the -H of the amide group by -CH₃ reduces the possibility to form hydrogen bonds. The concept to synthesize this substance was to reduce the electrical conductivity by reduction of the possibility to form an extended network of hydrogen bonds and to reduce eventually the clearing temperature. Furthermore, the change of the properties of the mesophase with the change of the structure of the molecule can be investigated. The structure of the methylated amide compound is the following:



Structure of N-(2,3-Dihydroxypropyl)-N-methyl-4-dodecyloxybenzamide **4**

The mesophase behavior and the temperature of the compound is:

4	Cr	←	SmA	←	I
		295 K		353 K	

Table 4.2. Mesophase behavior of compound **4**

The Guinier powder patterns show a single Bragg reflection in the small angle region with d values ranging from 3.6 nm at 353 K to 3.9 nm at 313 K.

The dielectric spectrum, at 313 K, of the SmA phase (Figure 4.8) shows only one relaxation process at frequencies of 1 MHz which could be only well separated at low temperatures. This is a very intense process. The dielectric behavior measured with decreasing temperatures suggests no considerable changes in the correlation of the dipole moments in the SmA phase (Figure 4.9). According to our considerations in chapter 4.2.2 the sample was nearly statistically oriented (see figure 4.10). There is only an increase of conductivity of about 5% at the I/SmA transition. This one is accompanied by a small step in the dielectric conductivity. A strong deviation of the conductivity from the Arrhenius law is observed in the isotropic state. At the given temperature of about 370 K we are not

expecting strong decomposition of the compound. Therefore, we assume that clusters with liquid crystalline order exist in the isotropic state, too.

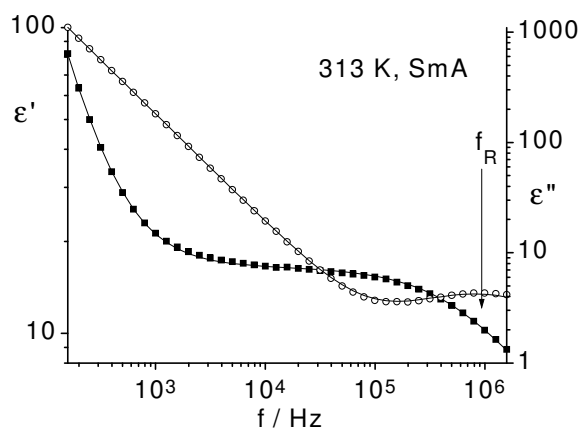


Figure 4.8: Row data and fit curve of compound **4** in SmA phase.

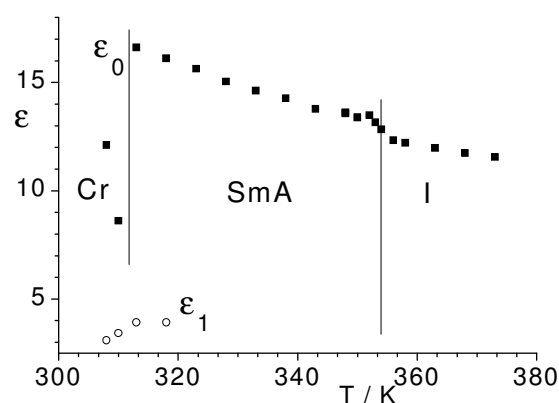


Figure 4.9: Limits of the dielectric permittivity of compound **4** in different phases.

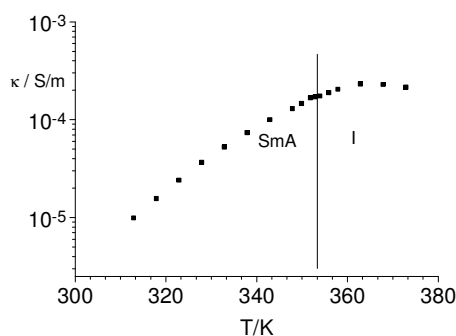
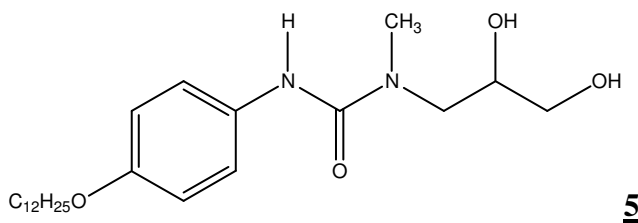


Figure 4.10: Conductivity versus temperature of the compound **4**.

4.2.4 DSC and microscopic study of the methyl urea compound in the SmA phase.

The urea compounds are a new synthetic variant which are forming a network of hydrogen bonds. Therefore, few substances were synthesized by I. Grebenchtchikov [105]. That gives the possibility to investigate another system with a more extended middle part and also with the possibility of the formation of intermolecular hydrogen bonds. Other compounds with a urea group in the middle part of the molecule were also synthesized but their thermally instability makes them not interesting for physical investigations. That's way they were not investigated. The substitution of one hydrogen attached to the urea group brings thermally stability and also lower clearing temperatures.

The compound with a methyl urea group in the middle part of the molecule and one alkyl chain attached to the aromatic ring exhibits also a SmA mesophase as proven by X-ray measurements. The phase behavior is shown in Table 4.3.



Structure of the 1(2,3-Dihydroxypropyl)-3-(4-dodecyloxy-phenyl)-1-methyl-urea

Compound	Phase behavior and Temperatures (K)		
5	Cr	323	387
		←→	←→
		SmA	I
		282	383

Table 4.3 Mesophase behavior the 1(2,3-Dihydroxypropyl)-3-(4-dodecyloxy-phenyl)-1-methyl-urea

4.2.4.1 X-Ray investigation of 1(2,3-Dihydroxypropyl)-3-(4-dodecyloxy-phenyl)-1-methylurea

The mesophases of compound **5** show layer reflections in the small angle region and a diffuse scattering in the wide angle region of the X-ray patterns (Figure 4.11), the latter having maxima on the equator of the 2D patterns indicating an on-average orthogonal arrangement of the long axes of the molecules or molecular associates within the layers as typical for SmA phases ($d = 3.8 \text{ \AA}$ at 353 K).

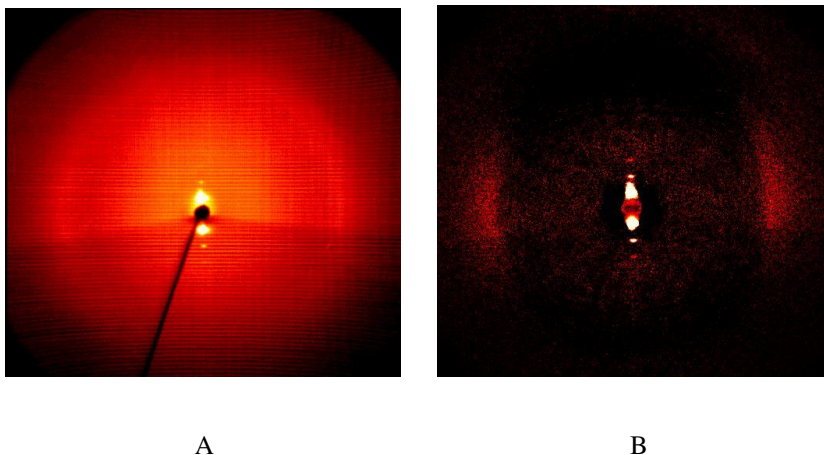
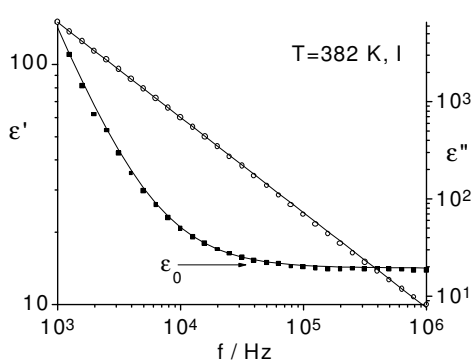


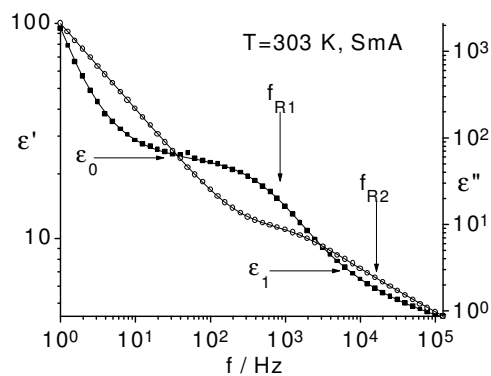
Figure 4.11 X-ray patterns of surface-aligned samples: A) SmA phase of 5 at 347 K (original pattern), B) pattern A minus the scattering of the isotropic liquid to improve the visibility of the maxima of the diffuse outer scattering on the equator of the pattern.

4.2.4.2 Dielectric investigation of 1(2,3-Dihydroxypropyl)-3-(4-dodecyloxy-phenyl)-1-methyl-urea

The error of the static dielectric constant ϵ_0 measured in the SmA phase is about 1% at low and 2% at high temperatures. The fitted parameters ϵ_1 and τ_1 show an uncertainty of about 2% and 20%, respectively. Raw data and the fitted curves according to Eq. 19 of the complex dielectric function $\epsilon^* = \epsilon' - j\epsilon''$ of compound 5 in the isotropic and SmA phase are presented in the Figure 4.12 A and B respectively. There is no contribution of any relaxation mechanism for the isotropic phase in the frequency range investigated. In the SmA phase a very broad relaxation range appears which could be separated into two Cole-Cole relaxation processes at very low temperatures with $\alpha=0,21$ for the mechanism of lower frequencies and $\alpha=0,47$ for the second. At higher temperatures only a part of that could be fitted and the $\alpha=0,27$.



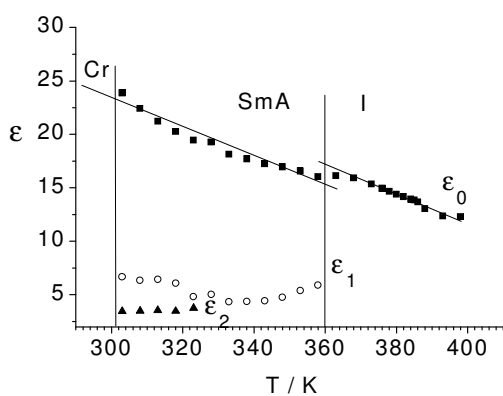
A



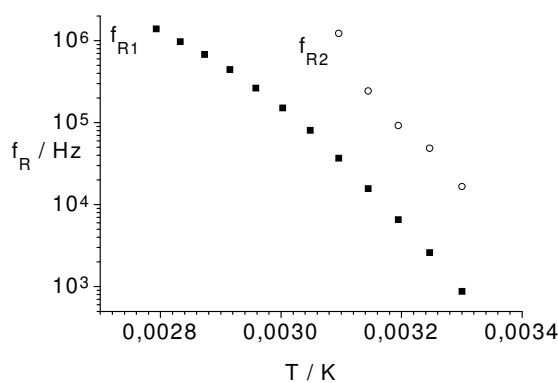
B

Figure 4.12. Raw data and the fitted curves according to equation 1 of sample 5 in the isotropic (A) and SmA phases (B).

The dielectric behavior of the compound in the whole temperature range doesn't change to much. See Figure 4.13 A. Only a decrease in the dielectric permittivity from 23 to 17 occurs at the phase transition I-SmA, probably as result of a more perpendicular orientation of the plane net of hydrogen bonds to the electrical measuring field. This statement is supported by the decrease of electrical conductivity at the transition from the isotropic into the SmA phase. The high frequency relaxation processes shows probably an Arrhenius behavior, whereas the low frequency one exhibits a slight tendency to glass behavior (see Fig 4.13 B). The first mechanism f_{R1} has activation energy of 52 ± 3 kJ/mol.



A



B

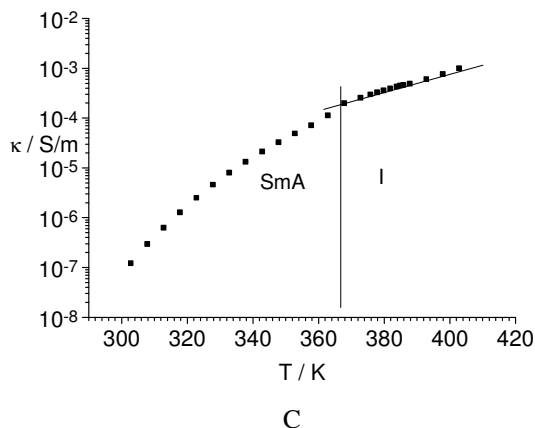


Figure 4.13 Dielectric behavior of compound **5**

- A) Dielectric permittivity versus the temperature.
 - B) Relaxation frequencies versus the inverse of the absolute temperature, f_{R1} for the slower mechanism and f_{R2} for the faster one.
 - C) Conductivity versus the temperature.
- The lines are only guides for the eyes.

4.2.5 Common behavior of the all SmA phases

A preliminary assignment of the mechanisms can be done based on the results given in figure 4.13 A. Dielectric data at higher frequencies and results on other methods are necessary for a more detailed discussion of the mechanisms. This will be made in chapter 4.3. If we assume that the dynamics within the network of hydrogen bonds is a very fast process which cannot be detected till frequencies up to 1 MHz we have to explain the relaxation ranges detected by the dipoles in the middle part of the molecules. Thus, for compound **5** two mechanisms can be assumed. At 300K the low frequency mechanism at 1 kHz reduces the dielectric permittivity from 22.5 to 7.5. Probably, this high value of the dielectric increment can be related to dynamics of the dipole moments of the --CONH- group which is influenced by the network of hydrogen bonds. This mechanism shows a glassy behavior as demonstrated in figure 4.13B. The reorientation of the alkyloxy groups as assumed in [69] and shown in figure 1.4 can be not responsible for this process because of the high dielectric increment. The -N(CH₃)- groups in the middle part of the molecules are not hindered by hydrogen bridges and reorient at 300 K within 10 kHz. This motion reduces the dielectric permittivity to about 3.7.

Substance **4** shows a high frequency limit of $\epsilon_1 = 4$ in the temperature range where no crystallization can be expected. In both cases a high frequency process is possible which reduces the dielectric permittivity to about 2. If we use this argument also for the other compounds investigated with a SmA phase we can conclude that the dielectric absorption

seen at about 1MHz is related to the dynamics of the middle part of the molecules which is partially influenced by the network of hydrogen bonds.

The conductivity change at the clearing temperature did us allow to say that the dielectric permittivity measured in the plane of the network is much higher than that measured in direction of the layer normal. All of these are common features of the SmA phase, whereby the chemical nature of the compounds plays only a secondary role.

4.3 Investigation of columnar mesophases

The reason to form a discotic phase is based on the wedge-shaped geometry of the molecules in which the hydrophobic part is much bigger than the hydrophilic one. Thus, the organization as a disc in which the hydrophilic part is in the center gives the best possibility to reduce the free volume on one side and to make a separation of the phases on microscopic level on the other side. The discs form a columnar phase like the classical disc-like molecules. The formation of an “inverse” structure with the hydrophobic part inside of the column is characterized by the subscript 2 in the short name of the phase Col_{H2}. Furthermore, the columnar mesophases are characterized by the face-to-face packing of the aromatic rings, which stabilizes the discotic character of the packing of the discs. The investigation of several compounds which are capable of forming hydrogen bonds can help to understand the change of the dynamics of these mesophases and the change of the properties with the change of the structure of the molecule.

4.3.1 Columnar phase with hydrogen bonds of a mixture at $x_3=0.6$

The Col_{H2} phase appears in the middle concentration range of the binary system presented in figure 4.1. To point to a peculiarity in the dielectric behavior of the Col_{H2} phase the real part of the dielectric permittivity of the isotropic and the Col_{H2} phase are compared with each other in figure 4.14. In both cases the experimental data can be described at low and high frequencies by a straight line. The first is representing the influence of double layer and the second a limiting dielectric permittivity. If we are looking more carefully we can see that in the curve of the isotropic phase at 387 K, the dielectric constant decreases abruptly till 3 kHz to a constant value of 6. This behavior can be well described only by the

double layer term and the static dielectric permittivity according to Eq. 18. In contradiction to that the data obtained at the columnar phase decreases more softly to reach the constant value of 10 at about 1 MHz. Using the same procedure of data analysis as for the isotropic phase a good description of the data was not possible. The deviation of this curve between the frequencies of 3 kHz and 0.1 MHz from the experimental data is the consequence of an additional low frequency absorption process that is the only observed in the columnar arrangement. A classical maximum in the absorption curve can not be seen because of the strong absorption due to the conductivity at these low frequencies. Therefore these data are not represented. Mainly based on the real part of dielectric permittivity a broad Cole-Cole mechanism with a distribution parameter of $\alpha=0.45$ was obtained from the complex fit. The exponent M in the last term of Eq.18 responsible for the conductivity is, in this case, 0.73 and not between 0.98 and 1.00, as usually, when the absorption is smaller. We assume that the change in the slope of the high conductivity results mainly from saturation effects because a even bigger part of ions is fixed in the double layer and cannot take part in the conductivity.

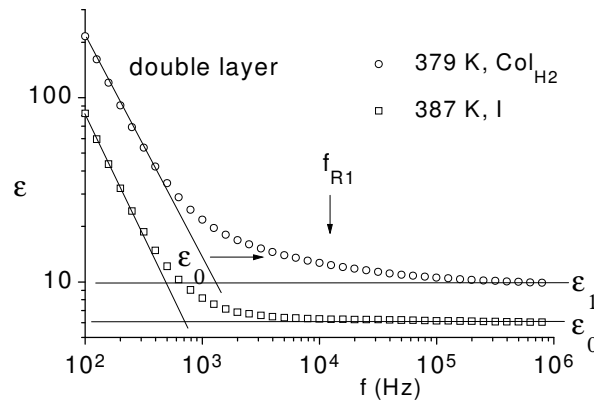


Figure 4.14 Dielectric permittivity vs frequency before and the phase transition I/ CoI_{H_2} . The static dielectric constant and the relaxation frequency are indicated by arrows.

When temperature decreases, the process discussed before disappears. The additional relaxation process observed only in the CoI_{H_2} phase can be better observed and separated at higher temperatures. This indicates that the activation energy of the low frequency absorption is higher than that of the electric conductivity which disturbs the separation of this mechanism. The same effect is known also for the main relaxation process at higher frequencies. As demonstrated in figure 4.15 for the dielectric loss overlapping of the low frequency side of absorption range and the conductivity becomes stronger at lower

temperatures. This figure shows also the change of the slope in the dielectric loss at low frequencies and high temperatures discussed before if the loss is higher than 1000.

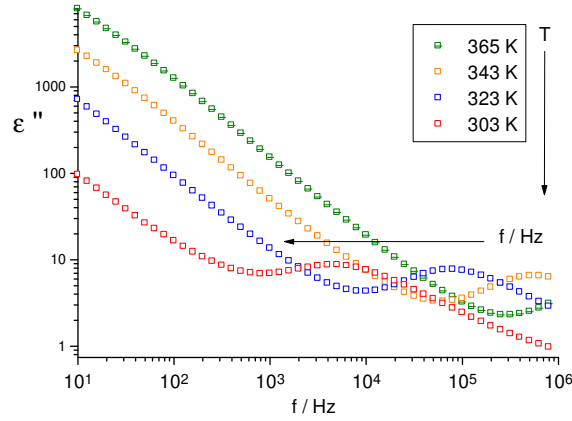


Figure 4.15 Imaginary part of the dielectric permittivity versus the frequency at different temperatures of the mixture $x_3=0,6$.

In Figure 4.16, the real and the imaginary part of the dielectric permittivity of the columnar phase at 303 K are represented. For the fit of the low frequency Cole-Cole mechanism data down to 10 Hz were used. The main relaxation range shown in Fig. 4.16 could not be well fitted by only one Cole-Cole process. A quite better fit was obtained using two further Cole-Cole mechanisms. The high frequency limit of the third Cole-Cole process is 3.71. That means that this process actually ends at higher frequencies not measurable by our equipment. Thus, the data in the columnar phase were described by three relaxation processes and the term of the conductivity. Due to the dominating term of the double layer, the error of ϵ_0 and of the related relaxation time is large.

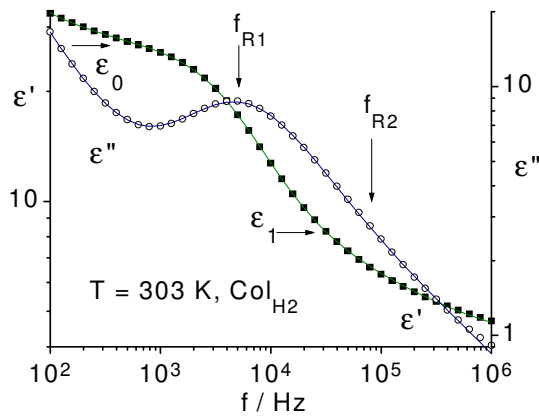


Figure 4.16 Dielectric function vs f (Hz) and fitted curves for the mixture with $x_3 = 0.6$.

The dielectric permittivity in the isotropic phase of the mixture with $x_3 = 0.6$ decreases only very slightly with increasing temperature (Figure 4.17). This may indicate equilibrium between a small concentration of columnar micells and isolated molecules. The strong increase of ϵ_1 and the appearance of an additional low-frequency absorption range with the limit ϵ_0 in the Col_{H_2} phase demonstrate the formation of the columns, the organization to a hexagonal lattice and the dynamics within the columns. The relaxation frequencies show a nearly linear dependence on the temperature for all processes at temperatures as shown in Figure 4.18. That suggests an Arrhenius behavior and the activation energies are $41 \pm 0,55$ kJ/mol and $42 \pm 0,57$ kJ/mol for f_{R2} and f_{R3} respectively.

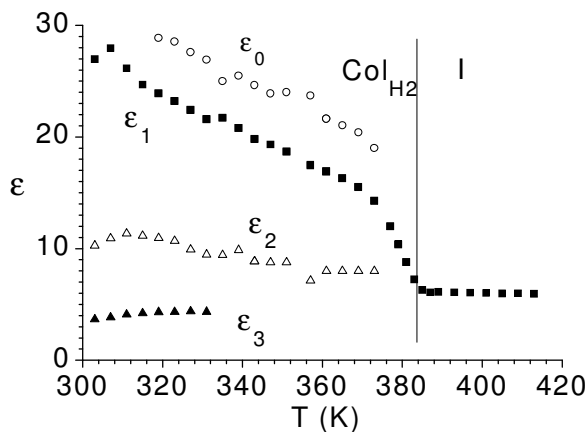


Figure 4.17 Limits ϵ_i versus temperature (K) of the mixture with $x_3=0.6$.

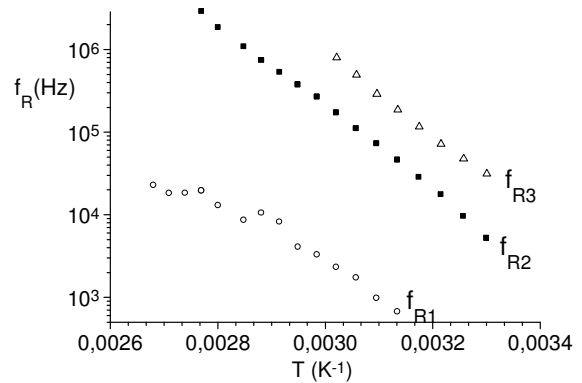


Figure 4.18 Relaxation frequency versus inverse of the temperature (K^{-1}) of the mixture with $x_3=0.6$.

As demonstrated in chapter 4.2.2, the investigation of the conductivity at the phase transition helps to know the orientation of the columns with respect to the electric field (Figure 4.19). If columns are ordered preferably in direction of the measuring field, the

current passes the network of the hydrogen bonds in the center of the columns as in a wire. The blue region in the middle part of the columns represents the hydrogen bonds network. In that way, when the columns are oriented parallel to the direction of the hydrogen bonds, charge transport is favorable and the conductivity is high. The formation of the columnar lattice can increase the conductivity if the columns grow with an orientation parallel to the current (A) and should also decrease if the columns are perpendicular to that (C).

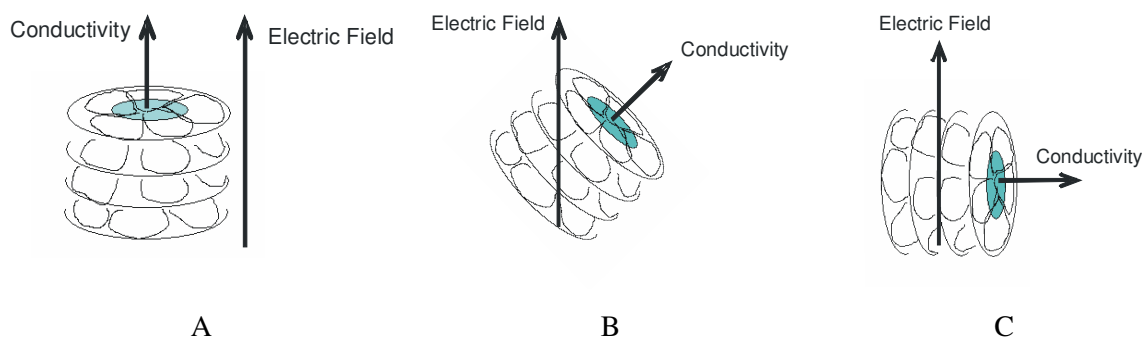


Fig 4.19 Influence of the relative orientation between the columnar phase and the electric field in the conductivity. A higher electrical conductivity, C lower conductivity than in the isotropic state. B small change of conductivity at the phase transition.

The specific conductivity increases at the phase transition I/Col_{H_2} (Figure 4.20). That means that columns formed by the mixture of two different kinds of molecules are preferably oriented in direction of the electric field. The formation of the columnar phase in the mixture occurs through a two-phase range between 386 and 376 K as usually observed in mixtures (see also fig 4.1). This one is also observable in the change of the conductivity and is indicated between the lines parallel to the y-axis of the Figure 4.20. The lines are only guides for the eyes. The formation of the columnar lattice occurs gradually with the decrease of the temperature.

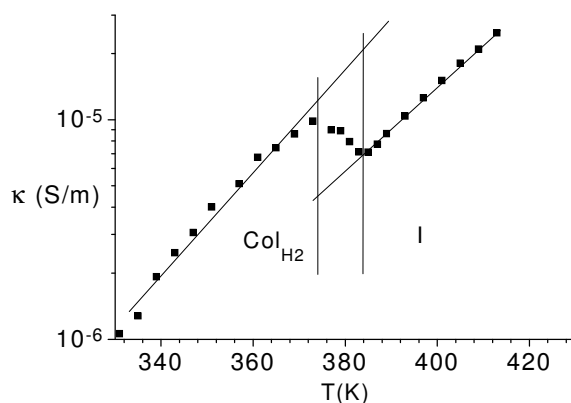
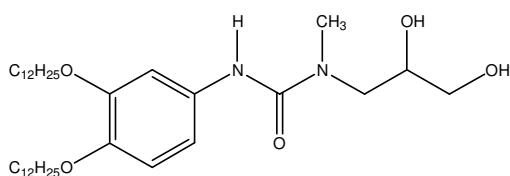


Figure 4.20 Specific conductivity versus Temperature (K) of the mixture with $x_3=0.6$.

4.3.2 Investigation of the columnar phase of methyl ureas

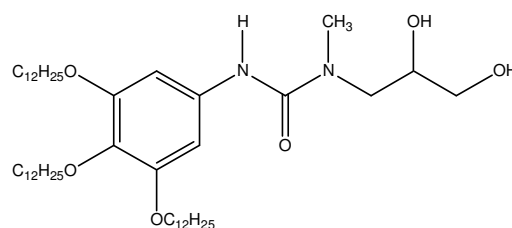
Like in the case of mono-alkylated urea compounds also the di-alkylated substances with a urea group in the middle part of the molecule form intermolecular hydrogen bonds and a columnar phase but they are thermally unstable. Thus, only rough microscopic investigations were made. It was impossible to determinate the structure and to the study the dynamics. But the at the nitrogen atom mono-methylated urea compounds give this chance. The relatively low clearing temperatures make it possible to characterize these mesophases in a very broad range of temperature and in the isotropic phase, too.

The structures of two methylated urea compounds are the following:



6

Structure of 3-(3,4-Bis-dodecyloxyphenyl)-1-(2,3-dihydroxy-propyl)-1-methyl-urea



7

Structure of 1-(2,3-dihydroxy-propyl)-1-methyl-3-(3,4,5-tris-dodecyloxyphenyl)-urea

4.3.2.1 Characterization of the substances by DSC and polarization microscopy

The transition temperatures of compounds **6** and **7** were obtained from the first and second heating run with a rate of 3 Kmin⁻¹.

Compound	Phase behavior and Temperatures (K)				
6	Cr	← 315 → 306	Col _{H2}	← 356 → 355	I
7	Cr	← 287 →	Col _{H2}	← 328 → 325	I

Table 4.4. Mesophase behavior of the methyl-urea compounds

For the three-fold alkylated compound **7** we did expect a cubic mesophase, but the lateral methyl group and the more extended middle part in relation to the amides (see substance **3**) seems changes the shape of the molecule so strongly that the cubic phase in compound **7** is destabilized. This is the reason why two of the three substituted methylurea compounds exhibit a columnar phase. This fact is very useful for our purpose because we can discuss the influence of phase versus that of chemical structure. As example Figure 4.21 shows the spherulites formed by compound **7** as a typical texture of a columnar phase under crossed polarizers of the heating stage microscope.

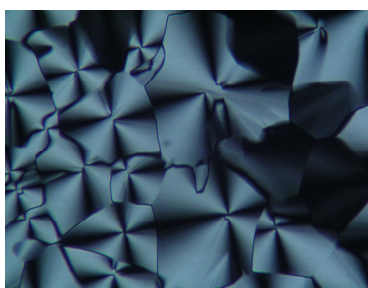


Figure 4.21: Texture of compound **7** at 356 K by cooling.

4.3.2.2 X-ray investigations of the methyl urea compounds

The 2D X-ray patterns from aligned samples of the mesophases of compounds **6** and **7** confirm their hexagonal columnar structure (Figure 4.22 for **6**, Figure 4.25C for **7**). The lattice parameters are summarized in Table 4.5.

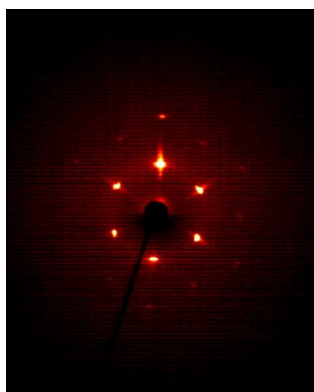


Figure 4.22 X-ray patterns of surface-aligned samples: Col_{H2} phase of **6** at 347 K. The hexagonal order can clearly be seen.

Table 4.5 Layer spacing d , hexagonal lattice parameter a , and average number n_U of molecules in the cross section of the columns in the Col_{H2} phase

Compound	Parameter / nm (T / K)	V_U^a (nm ³)	V_M^b (nm ³)	n_U^c
<u>6</u>	$a = 4.1$ (353)	7.5	1.16	6.5
<u>7</u>	$a = 3.8$ (313)	5.8	1.55	3.7

^a V_U = volume of a unit cell with a height of $h = 0.47$ nm (corresponding to the average distance of the molecules along the columnar axis derived from the maximum of the outer diffuse scattering in the 2D X-ray patterns, see Figure 4.25D); ^b V_M = crystal volume for a single molecule as calculated using the volume increments reported by Immirzi and Perini [106] corrected for an assumed average packing coefficient in the liquid crystalline phase of ~ 0.55 (~ 0.7 in the crystal) [107]; ^c n_U = number of molecules in the unit cell, calculated according to $n_U = V_U/V_M$.

The models shown in Fig 4.23 and 4.24 are based on data of X-ray investigations.

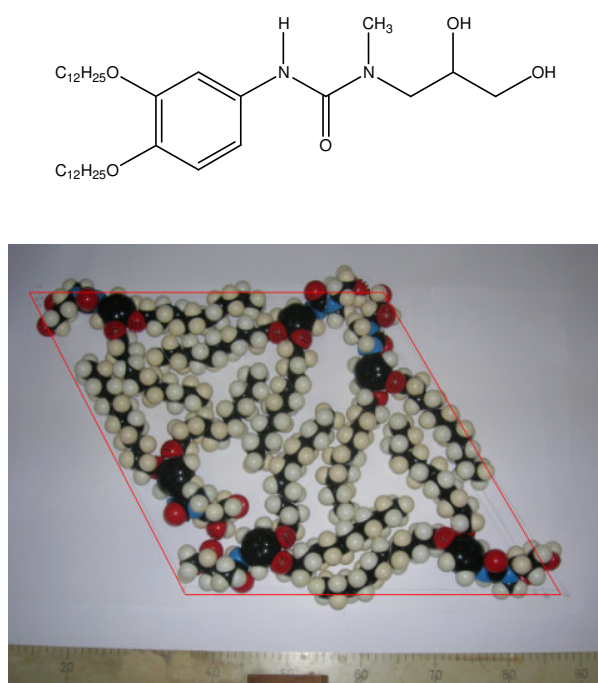


Figure 4.23 . Model for the unit cell in the columnar phase for the compound 6.

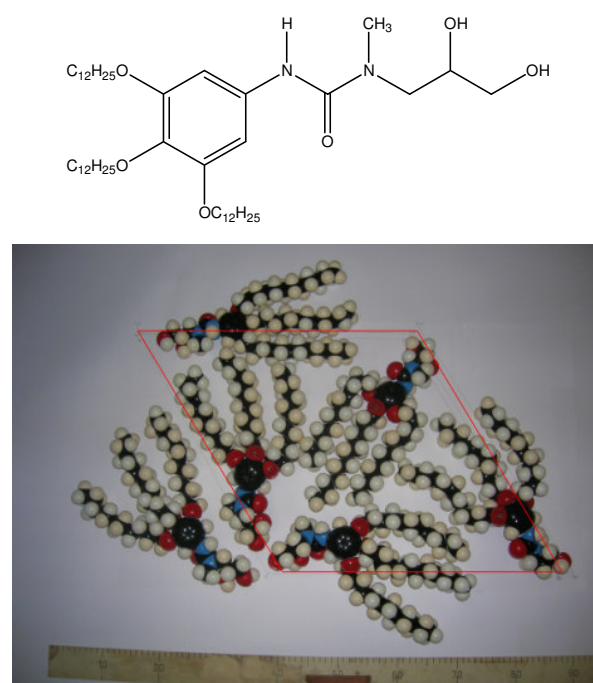


Figure 4.24 Model for the unit cell in the columnar phase for the compound 7.

The two-dimensional X-ray pattern in the isotropic liquid of compound **7** at 403 K shows the typical diffuse ring in the wide angle region corresponding to the short-range ordered lateral distances of the molecules. Additionally, a comparatively intensive diffuse scattering is found in the small angle region (Figure 4.25A) which becomes much more intensive with decreasing temperature (Figure 4.25B). Below the phase transition, the X-ray pattern shows the formation of the columnar 2D lattice (Figure 4.25C). A more detailed study of the outer diffuse scattering in this phase shows that it has a maximum on the equator of the pattern which corresponds to the average intra-columnar distance of the molecules, hence the molecules are not considerably tilted with respect to the long axes of the columns (Figure 4.25D,E).

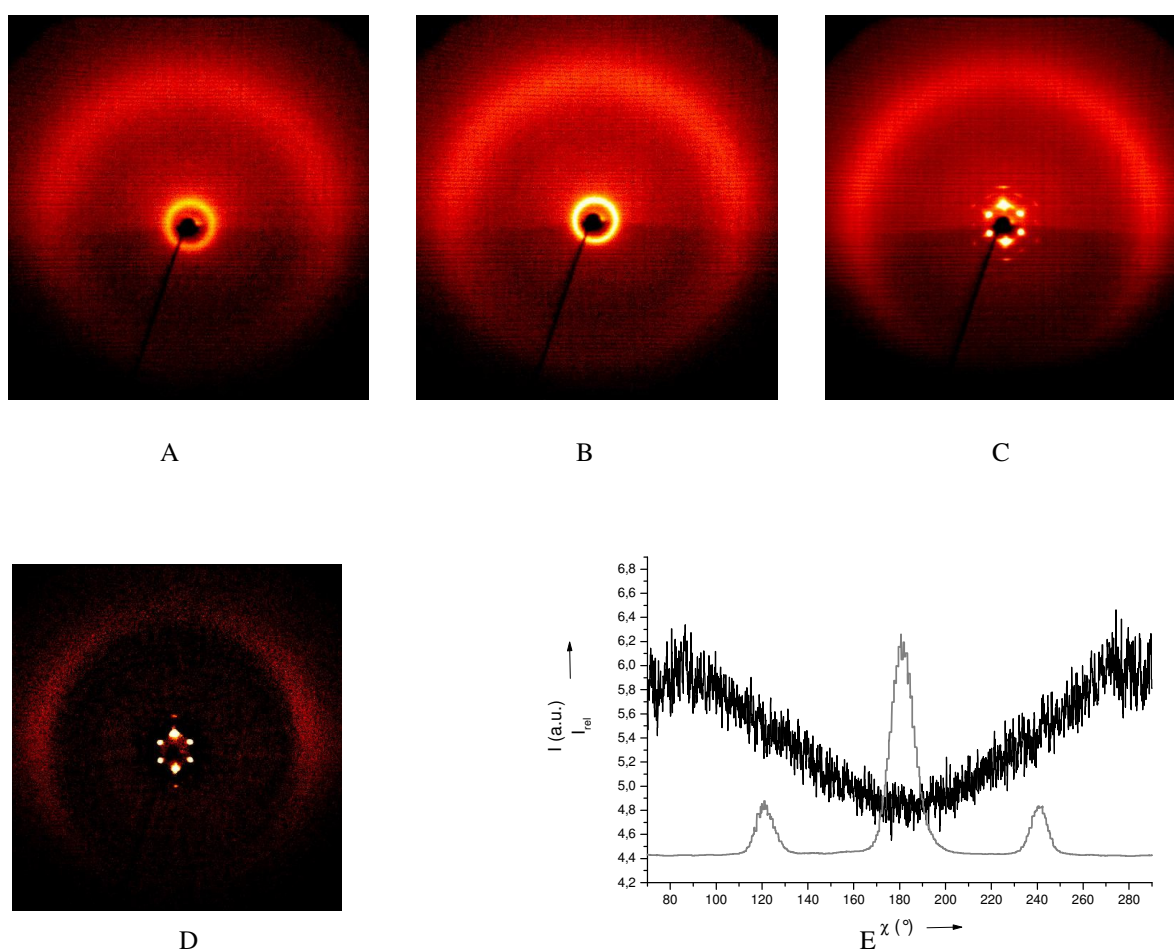


Figure 4.25 2D X-ray patterns of a surface-aligned sample of **7** (on cooling): (A) isotropic liquid of **7** at 403 K, (B) isotropic liquid at 343 K, (C) Col_{H2} phase at 298 K, (D) Col_{H2} phase at 323 K on cooling (The long axes of the columns lie parallel to the surface and are fiber-like disordered around an axis perpendicular to it): intensity of the scattering at 323 K minus that of the isotropic liquid to show the maxima of the diffuse outer scattering at the equator of the image, (E) Col_{H2} phase at 323 K: intensity distribution of the outer diffuse scattering at $\theta \approx 9.5^{\circ}$ along χ (black line, $I_{\text{rel}} = I(323 \text{ K})/I(403 \text{ K})$) in comparison to that of the 10 (inner) reflection of the hexagonal lattice (gray line, I in a.u.).

The unusually high intensity of the inner scattering in the isotropic phase indicates the existence of short-range correlations with a characteristic spacing corresponding to the long axes of the molecules or clusters of molecules. Furthermore, the interesting dielectric behavior of the isotropic liquid with practically no slope (see figure 4.30) motivated us to measure the temperature dependence of the scattering using the small angle camera on heating. During the phase transition from the columnar liquid crystalline phase to the isotropic liquid, the intensity distribution changes from a sharp Bragg-like reflection (as typical for the long-range or quasi-long range order of the lateral correlations between the columns in a columnar phase) to a diffuse one (typical for short-range order), but the maximum of the inner reflection shows only a small change in the corresponding d values with $d_{\text{hex}} = 3.20$ nm at 327 K and $d_{\text{diffuse}} = 3.26$ nm at 361 K (see temperature dependence of the small angle diffraction in Figure 4.26A, phase transition at 329K, black curve, and step in the θ values in Figure 4.26B). Extending the measurements to higher temperatures leads to a continuous decrease in the intensity of the scattering, but because of a simultaneous thermal decomposition of the compound this effect cannot be uniquely assigned to a reduction of the number of clusters in the sample (see SAXS-curves for temperatures between 333 and 443 K in Figure 4.27). For the same reason we can give only a qualitative interpretation of the increase of the FWHM (Full-Width at Half Maximum) values with increasing temperature within the isotropic liquid (Figure 4.26B) which may be attributed to a reduction of the correlation length of the clusters. The mesophase behavior is shown in Figure 4.28. After the clearing temperature the columns exist but reduced in shape and isotropically distributed.

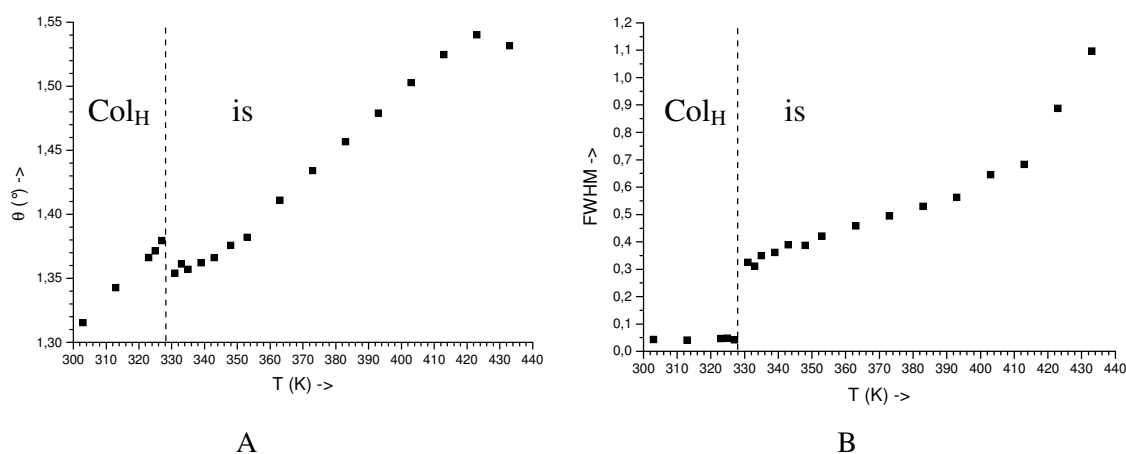


Figure 4.26 Temperature depending small-angle X-ray diffraction from a powder-like sample of **7** (on heating): (A) scattering curves between 303 and 353 K, (B) θ values for the maxima in the Col_{H2} phase (10 reflection) and in the isotropic liquid.

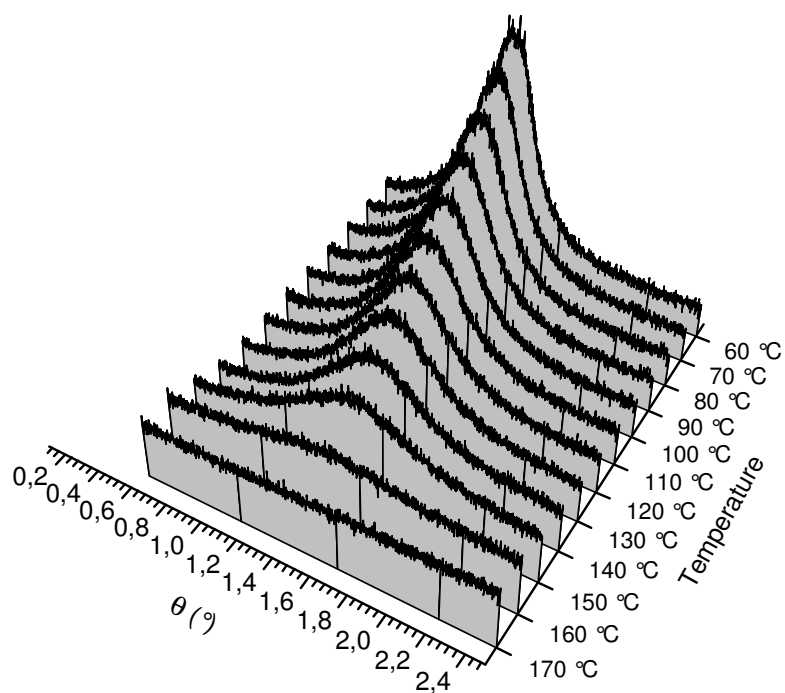


Figure 4.27 X-ray diffraction curves for the diffuse scattering in the small angle region of a powder-like sample of **7** in the isotropic liquid. Between 150 and 160 °C rapid thermal decomposition starts.

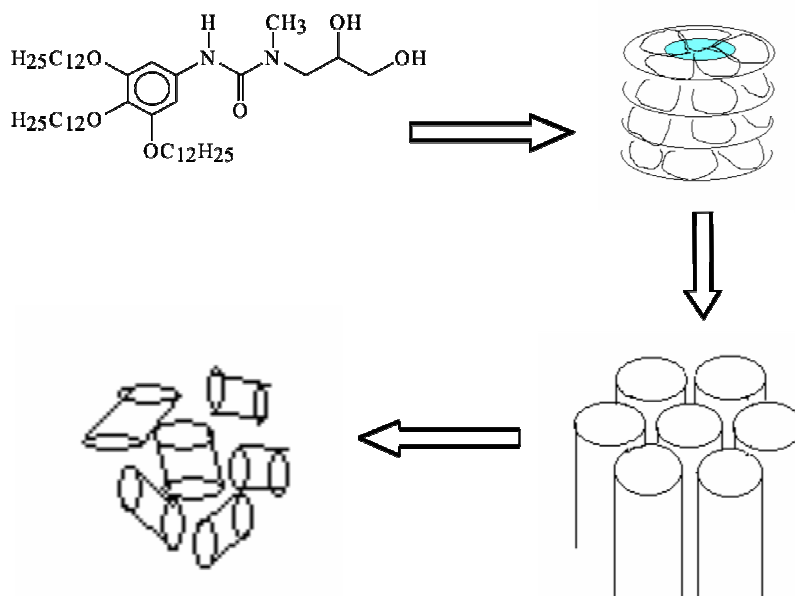


Figure 4.28 Schema of the mesophase behavior. Existence of clusters in the isotropic phase.

4.3.2.3. Dielectric investigations of methyl urea compounds

Compound **7** has a relatively low clearing temperature and the isotropic phase could be investigated in a very broad temperature range. Figure 4.29A shows the experimental data of **7** at 327 K in the isotropic phase. The experimental data of the isotropic phase can be well described with the static dielectric permittivity ϵ_0 , the conductivity and the dominating double layer terms of Eq. 19 (Figure 4.29A). A relaxation range is observed which is separated in two mechanisms f_{R2} and f_{R3} . The data are only well described with two relaxation mechanisms $\alpha_1 = 0,20$ and $\alpha_2 = 0,34$ at 327 K as well as the conductivity and the double layer terms of Equation 18.

For the description of the data in the columnar phase additionally low frequency absorption has to be introduced which reduces the dielectric permittivity from ϵ_0 to ϵ_1 . The static dielectric permittivity ϵ_0 in the Col_{H2} state reaches an error of 10%. This big error results from the superposition of double layer and conductivity with the dispersion range. The related process is not active in the isotropic phase. Therefore the molecular mechanisms, seen in the isotropic and the columnar phase, are now characterized as the second and third process. The separation of the collective mechanism from the contribution of the conductivity is difficult and becomes even more difficult with decreasing temperature. In order to prevent problems with the fitting procedure of the first from the second relaxation range the frequency range was limited to about 10 kHz and the high frequency range was fitted as one relaxation process (see figure 4.29B). On the other hand for the above discussed splitting of the second relaxation range into the second and third mechanism the low frequency side was limited to 100 Hz and the first mechanism was described as “conductivity” (figure 4.29C). Only in this way the experimental data could be well described. To resume the dielectric spectrum of the columnar phase was described with three Cole-Cole processes f_{R1} , f_{R2} and f_{R3} with $\alpha_1 = 0,20$, $\alpha_2 = 0.16$ and $\alpha_3=0.71$ respectively at 317 K.

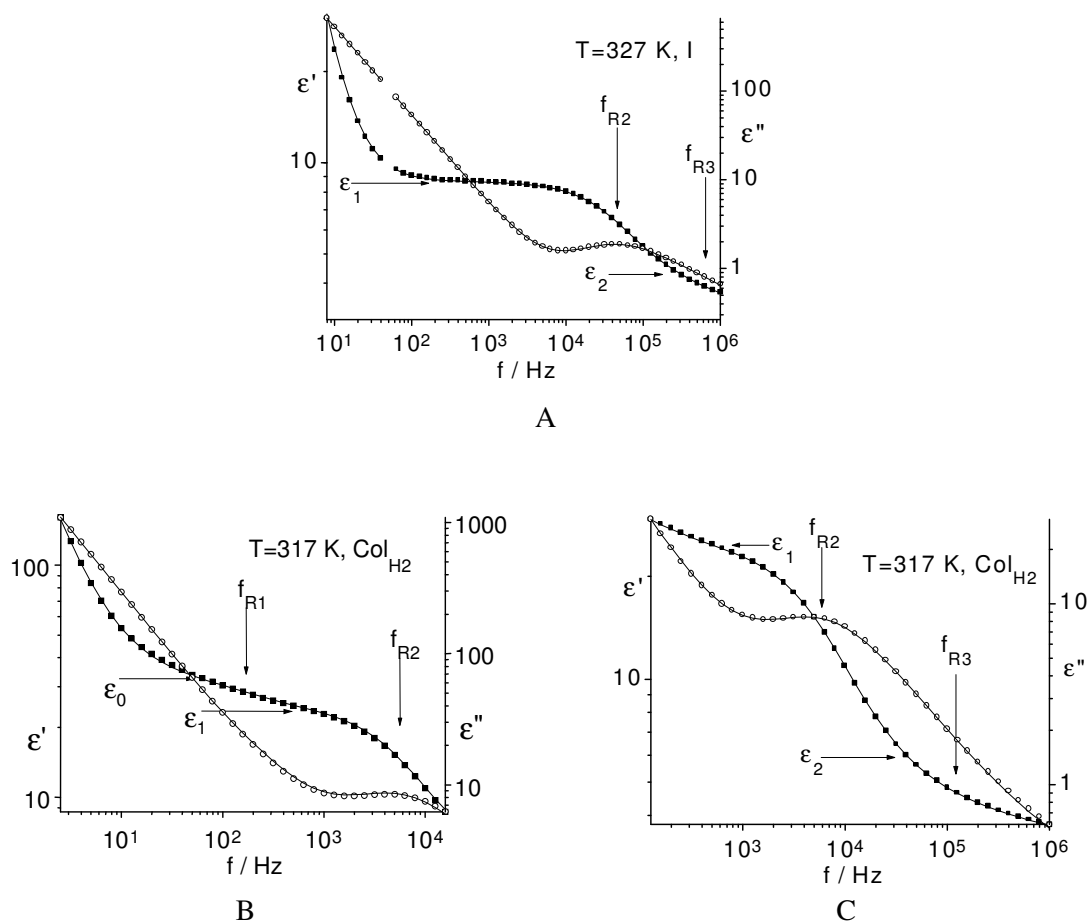


Figure 4.29 The complex dielectric permittivity and the fitted curves of sample 7 in the isotropic (A) and columnar phase at 317 K (B, C), (B) representation of the low frequency range. Two relaxation ranges are present, f_{R1} and a broad one, the second mechanism was separated in another two f_{R2} and f_{R3} .

The dielectric permittivity increases at the phase transition from the isotropic into the columnar phase because of the formation of the columnar arrangement in which the 1D network of hydrogen bonds is mainly parallel to the electrical measuring field (Figure 4.30). The mechanism f_{R1} and f_{R2} make the most important contribution to the dielectric strength. f_{R1} reduces the dielectric permittivity from $32(\epsilon_0)$ to $24(\epsilon_1)$, f_{R2} reduces again to 6 (ϵ_2) and f_{R3} reduces until 3 (ϵ_3) at 317 K. The third mechanism is the less intensive of them and is very broad.

All of them follow the Arrhenius law with the temperature as is shown in Figure 4.31 in all phases. In the isotropic phase the process has activation energy of 38 ± 2 kJ/mol and maintains the behavior in the columnar phase. As is shown in Fig 4.31 there is only a very small stepwise reduction of the relaxation times f_{R2} at the transition into the columnar

phase. Activation energies of 41 ± 3 kJ/mol and 56 ± 1 kJ/mol were calculated for f_{R1} and f_{R2} respectively in the columnar phase.

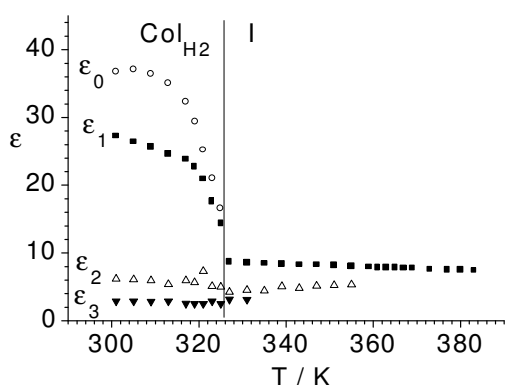


Figure 4.30 Limits of the dielectric permittivity versus the Temperature of 7.

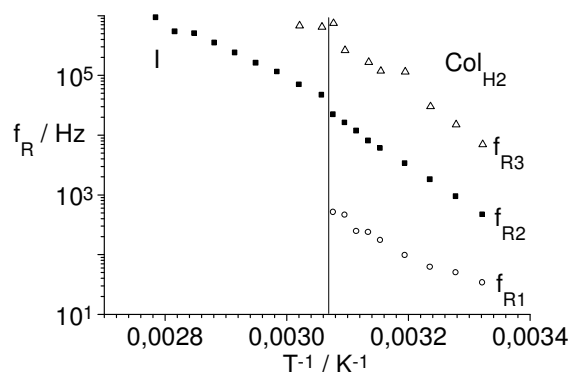


Figure 4.31 Relaxation frequencies versus inverse the Temperature of 7.

The compound 6 with two carbon chains has higher clearing temperatures. This is the reason why the relaxation in the isotropic phase could not be measured (Figure 4.32A). The description of the dielectric behavior in the columnar phase was possible with two mechanisms (Fig 4.32 B.) Both of them are Cole-Cole mechanisms with $\alpha_1 = 0$ and $\alpha_2 = 0,31$ at 328 K respectively. These processes reduce the dielectric permittivity from 21 (ϵ_0) to 17 (ϵ_1) at $1,8 \cdot 10^3$ Hz (f_{R1}) and from 17 to 3,8 (ϵ_3) at $3,5 \cdot 10^4$ Hz (f_{R3}).

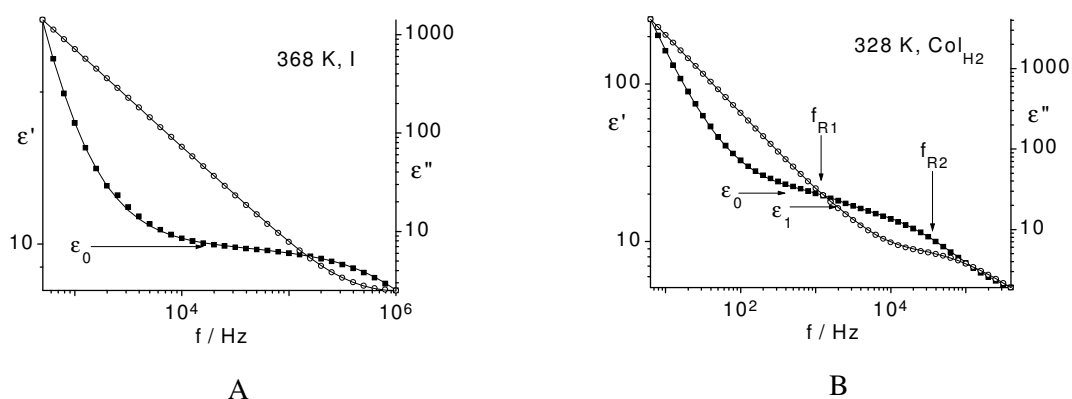


Figure 4.32 Complex dielectric permittivity of the compound 6 (A) in the isotropic phase at 368 K (B) in the columnar phase at 328 K.

At the phase transition into the columnar phase a stepwise increase of the dielectric permittivity is observed Fig 4.33 A. This behavior is due to the more parallel orientation of the columns in direction of the electrical measuring field as discuss before. Then the dielectric permittivity increases continuously with the decrease of the temperature

acquiring value of 25 before crystallization. In contradiction to the former substance **7** the broad absorption range at higher frequencies could be described as one relaxation process. The reason for it can be that the third relaxation process appears at so high frequencies where it influences not remarkable the common process, or the third processes shows practically the same relaxation frequency as the second one. The first and the second processes show an Arrhenius behavior within the columnar phase with activation energies of 45 ± 2 kJ/mol and 46 ± 2 kJ/mol for f_{R1} and f_{R2} respectively Figure 4.33 B.

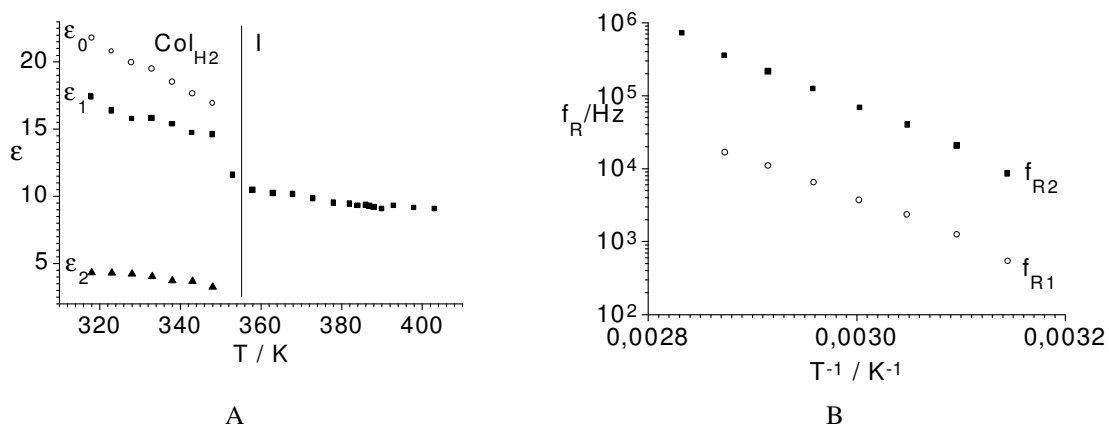
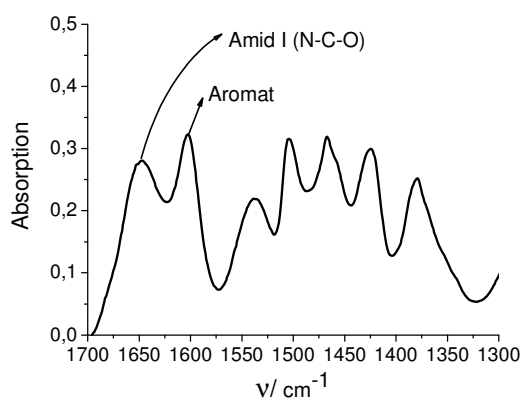


Figure 4.33 A) Limits of the dielectric permittivity versus the temperature of **6** B) Relaxation frequencies versus the temperature of **6**.

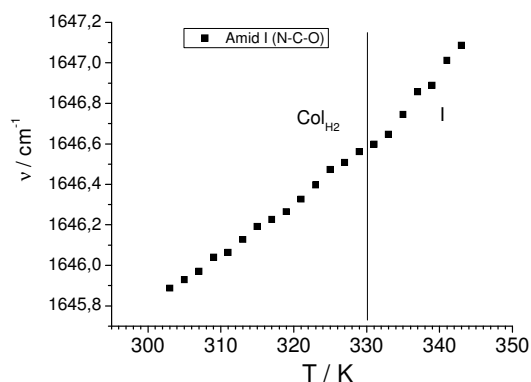
4.3.2.4 IR investigation at the isotropic/columnar phase transition

X-ray measurements of the compound **7** (the one with three alkyl chains) corroborate the presence of aggregates in the isotropic phase. Dielectric studies show that the relaxation time does not change at the phase transition isotropic/columnar. This implies that the intermolecular hydrogen bonds do not lead to any restriction of the rotational movements, and that hydrogen bonds already existed in the isotropic phase, before the columnar phase was formed. Hence, the question of which interactions are responsible for the formation of the columnar phase remains open. Infrared spectroscopy is a very useful tool to investigate these intermolecular interactions at atomic level, since the association of the molecules can influence the force constant of the bonds and thereby change the absorption frequency of the IR bands. To get insight of this phenomenon we study the compound **7** by means of IR spectroscopy at different temperatures (Figure 4.34 A). These measurements were favored

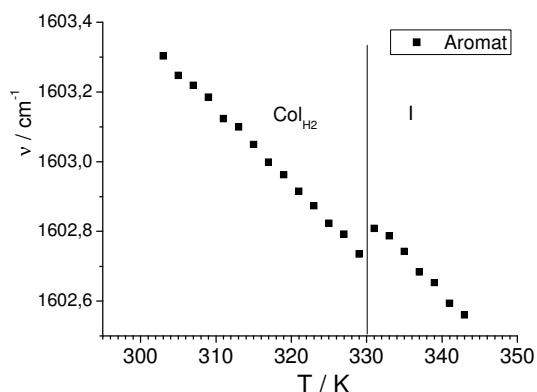
by the presence of a very low clearing temperature in the formation of the columnar phase. Figure 4.34B shows the behavior of the amide I band with the temperature. No change at the phase transition is seen, which agrees with the behavior of the relaxation times measured by dielectric spectroscopy. The wavenumber increases at lower temperatures as result of the strengthening of the hydrogen bonds. The band corresponding to the aromatic C=C stretching exhibit an increase of the wavenumber with the decrease of the temperature what suggests that the interactions between the aromatic rings are stronger with the decrease of the temperature. Here, a step at the phase transition is observed (Figure 4.34C). This indicates that the interaction between the aromatic rings is also responsible for the formation and stabilization of the columnar mesophase. X-ray investigations of disc-like molecules show that the intermolecular distances decreases at the transition into the isotropic state [62]. Probably this effect is also reflected in the IR spectra.



A



B



C

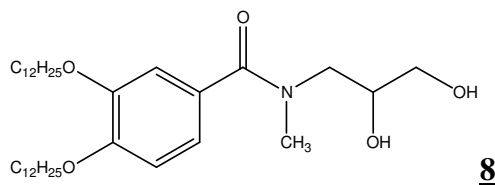
Fig 4.34 A) IR spectrum of the compound **7** at 343 K.

B) Wavenumber versus temperature of the Amide I Band. No changes are observed at the phase transition in the isotropic phase that means there is no changes in the restriction of the movement.

C) Wavenumber versus temperature of the aromatic C=C stretching band. At the phase transition in the Columnar phase the stepwise decrease of the wavenumber suggests that the interaction between the aromatics rings becomes stronger.

4.3.3. Study of the columnar mesophases of the methylated amide compound

An efficient synthetic approach to obtain this kind of diol molecules is to attach the diol to the aromatic ring by an amide group in classical liquid crystals molecules. The amide and the diol groups attached to the ring are responsible for the dielectric answer of the mesophase. The complex dielectric behavior of the amide compounds was already investigated and it was open to assign the different relaxation process of the dielectric spectrum, specially the low frequency process [89]. The question was what the influence of the intermolecular hydrogen bonds is and what that of the amide group on the dynamics is. To understand the dielectric answer of these compounds the NH group was replaced by NCH₃. This substitution reduces the number proton donors because the proton at the nitrogen atom cannot anymore take part in the network of hydrogen bonds. Furthermore, changes of the shape and the lateral interaction between the molecules with respect to the non-methylated compounds and other phase behavior can be expected because of the change in the shape ratio between the hydrophobic and hydrophilic part. The chemical structure of the substance used for this investigation is given below. The compound was synthesized by I. Grebenchtchikov [108].



Structure of N-(2,3-dihydroxypropyl)-N-methyl-3,4-didodecyloxybenzamide

Compound	Phase behavior and Temperatures (K)		
8	Cr	← 315 Col	← 361 I

Table 4.6 Mesophase behavior of N-(2,3-dihydroxypropyl)-N-methyl-3,4-didodecyloxybenzamide

4.3.3.1 X-Ray Measurements of the methylated amide compound

The methylated amide compound with 2 chains shows a columnar phase proved by two-dimensional X-ray patterns of an aligned sample represented in Figure 4.35A.

The hexagonal lattice parameter was determined from calibrated Guinier powder patterns and varies from $a=3.9$ nm at 358 K to 4.0 nm at 343 K on cooling. It should be noted that the small angle range of the 2D-Xray pattern of the isotropic liquid shows an intense scattering at values near that of the 10 reflection in the Col_H phase with full-width at half maximum of about 0.3° in theta as seen in Figure 4.35B. The inverse character of this phase indicated by the index 2 cannot be seen by x-ray measurements.

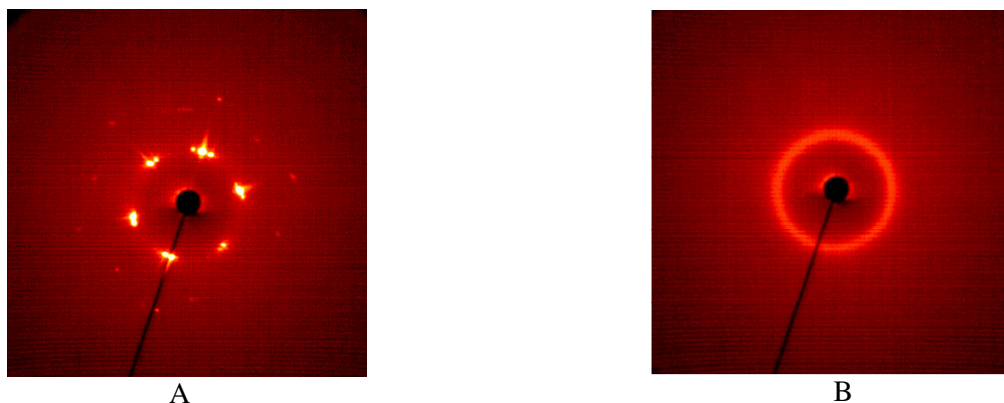


Figure 4.35 Small angle range of the X-Ray patterns A) for an aligned samples at 353 K on cooling B) for the isotropic liquid at 361 K just before the transition from the isotropic liquid phase to the columnar phase.

4.3.3.2 Dielectric Behavior of the methylated amide compound

Dielectric investigations on compound **8** could be performed in both, the low frequency and the high frequency range. The data obtained were plotted together whereby the limit for the low frequency equipment was taken by $f < 3$ MHz and that of the high frequency one at $f > 1$ MHz.

In this way the relaxation range in the isotropic phase at high frequencies could be separated (f_{R2} in Figure 4.36). The relaxation process in the isotropic phase occurs at high frequencies between 1.8×10^7 and 6.8×10^7 Hz, reduces the static dielectric permittivity from 5 to 3 and was fitted as a Cole-Cole_mechanism with $\alpha=0.3$.

For the fit experimental data at $f > 100$ MHz were excluded in order to reduce the influence of resonance effects observed at higher frequencies. This one increases the dielectric loss and reduces in a complex fit the high frequency limit of the static dielectric

permittivity. By chance, the relaxation ranges seen in both phases are well separated. Therefore, a more exact data analysis could be made separately for every equipment. In this way errors connected with the special equipments e.g. calibration and temperature measurements and especially that of orientation are reduced. Again, the dielectric spectrum of the diols is dominated at low frequencies by the contribution of the conductivity. The specific conductivity has an Arrhenius like behavior with activation energy 50 ± 3 kJ/mol in the isotropic state (see Figure 4.41). At the phase transition from the isotropic into the columnar phase the conductivity increases stepwise. This indicates a more parallel orientation of the columns to the electrical field at least for the low frequency measurement.

In the columnar phase of compound **8** another relaxation region at low frequency f_{R1} appears (Figure 4.37). This process is very difficult to separate from the conductivity and is only seen in the real part of the dielectric permittivity because the intense absorption of the conductivity in the imaginary part dominates the spectrum. At lower temperatures a third mechanism at high frequencies can be detected (Figure 4.38). This is an interesting dielectric answer of compound **8** because in the compounds investigated by us before this two processes were together in the same absorption peak and were separated only in the fit procedure. The first mechanism reduces the dielectric permittivity from 17 (ϵ_0) to 7 (ϵ_1) with a relaxation frequency of $f_{R1} = 4.9 \times 10^3$ Hz at 333 K and the second one f_{R2} at 2×10^6 Hz with $\alpha=0.37$ to $\epsilon_2 = 3.5$. The third mechanism is really very weak and difficult to fit because of the influence of resonance. He reduces again the dielectric permittivity to $\epsilon_3 = 1.8$ with $\alpha=0.3$ at 3.3×10^8 Hz. The value of ϵ_3 of about 0.5 units is too low and indicates the problems with the fit. Therefore the high frequency limit is not given in Figure 4.40. Nevertheless this absorption range exists. All of these processes were fitted with Cole-Cole model and follow the Arrhenius law (Figure 4.39, temperature dependence of the relaxation frequency) with activation energies of 88 ± 6 , 73 ± 2 and 13 ± 4 kJ/mol for f_1 , f_2 and f_3 respectively.

The dielectric constant increases at the phase transition I/Col_{H2}(Figure 4.40). The reorganization of the dipole moments due to the formation of the columns gives place to the positive correlation of the dipole moments what increase the dielectric constant at the phase transition. The first 2 mechanisms make the most important contributions to the

dielectric permittivity. The slope of the dielectric permittivity in the isotropic phase ($d\epsilon/dT$) amounts to -0.013 ($\epsilon = 6.0$). This value agrees well with that of chlorobenzene ($(d\epsilon/dT) = -0.0133$ ($\epsilon = 5.7$) [104]) and proves that it should be either related to non-associated molecules or to thermal very stable associates. We already now associates exist in the isotropic phase. In this case the value of the slope corroborates the existence of very stable associates.

At the phase transition the formation of the hydrogen bonds network like a wire in the middle of the columns take place. If the columns have an orientation preferably in direction of the electric field the conductivity increases. This is the behavior observed in Figure 4.41. The increase of the conductivity at the phase transition I/Col_{H_2} corroborates the formation of the columns.

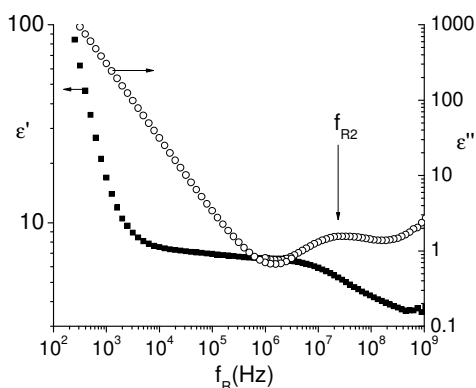


Figure 4.36 Complex dielectric function in the isotropic phase of compound **8**.

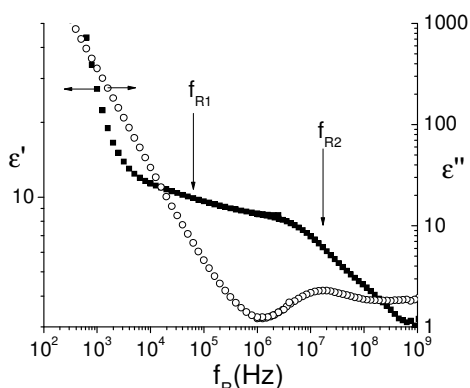


Figure 4.37 Complex dielectric function in the columnar phase at 358 K of compound **8**.

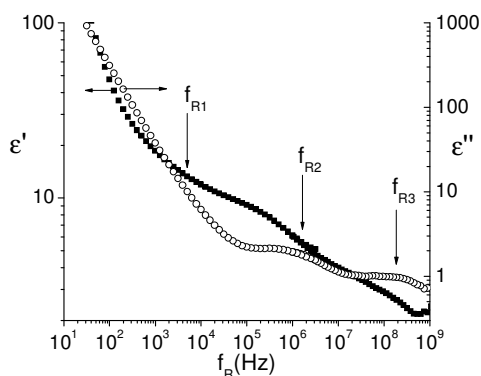


Figure 4.38 Complex dielectric function of compound **8** in the columnar phase at 333 K.

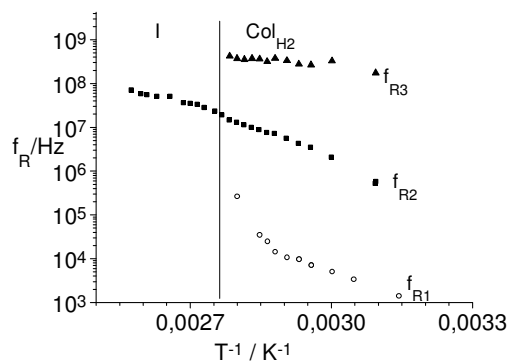


Figure 4.39 Relaxation frequencies of substance **8** calculated from the fit versus the inverse of the temperature.

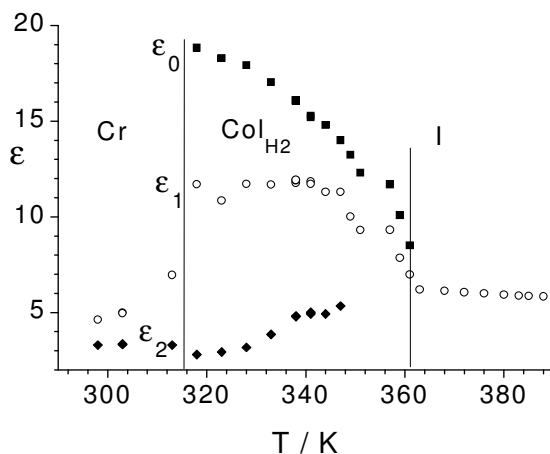


Figure 4.40 Limits of the dielectric permittivity of compound **8**. The high frequency limit is not given.

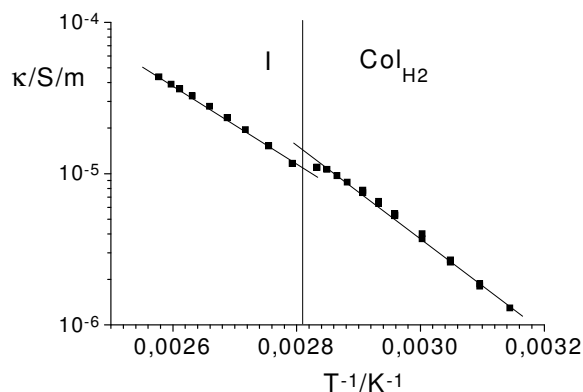
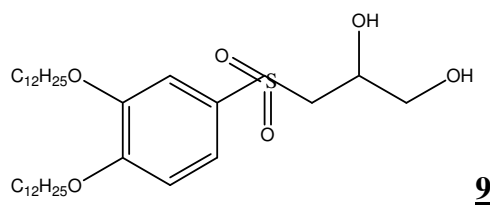


Figure 4.41 Conductivity versus reciprocal temperature of substance **8**.

4.3.4 Investigation of the sulfone compound

To understand the influence of the structure on dynamics of the columnar phase composed by diols an analogue compound with two alkyl chains attached to the ring and a polar group in the middle part of the molecule was synthesized. The $-\text{SO}_2-$ group is a polar group which can work as proton acceptor. The structure of this compound is:



Structure of 3-(3,4-Bis-dodecyloxy-benzenesulfonyl)-propane-1,2diol

Compound	Phase behavior and Temperatures (K)		
2	Cr	← 336	Col ← 381 I

Table 4.7 Mesophase behavior of 3-(3,4-Bis-dodecyloxy-benzenesulfonyl)-propane-1,2diol

4.3.4.1 X-Ray investigations of the sulfone compound

X-ray investigations of the compound prove the presence of the columnar hexagonal phase. Two dimensional small angle scattering show 3 reflections with d values in the ratio

of $1:1/\sqrt{3}:1/2$ and can also be assigned as Col_H with $a_{\text{hex}} = 4,0 \text{ nm}$ (Figure 4.42). The substitution of the middle part of the molecule does not change the phase behavior. Please note that the phase can be classified from X-ray investigations only as a columnar one (Col_H). The classification as inverse structure follows from the wedge-like shape of the molecule.

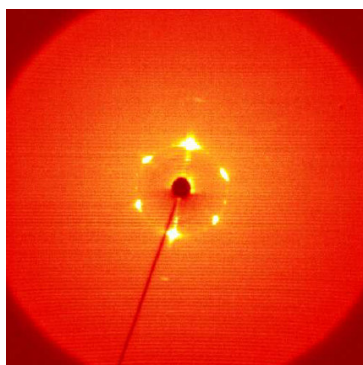


Figure 4.42 Small angle range of the X-Ray patterns for an aligned sample of compound **9** in the columnar phase at 383 K on cooling

For the analogue compounds **8**, **7** and **6** the presence of aggregates in the isotropic phase was proven by X-ray method. This compound shows intense reflexes in the isotropic phase with the same distance than that of the columnar one after the transition at 394 K (Figure 4.43B) and even at 455 K this reflection is seen but more diffuse (Figure 4.43C). That gives evidence of the presence of the aggregates even at very high temperatures as discussed in chapter 4.3.3.1.

For the analogue compounds the presence of aggregates in the isotropic phase was corroborated with X-ray. This compound shows intense reflexes in the isotropic phase with the same distance than that of the columnar one after the transition at 394 K (Figure 4.43 B) even at 455 K this reflection is seen but more diffuse (Figure 4.43 C). That corroborates the presence of the aggregates even at very high temperatures.

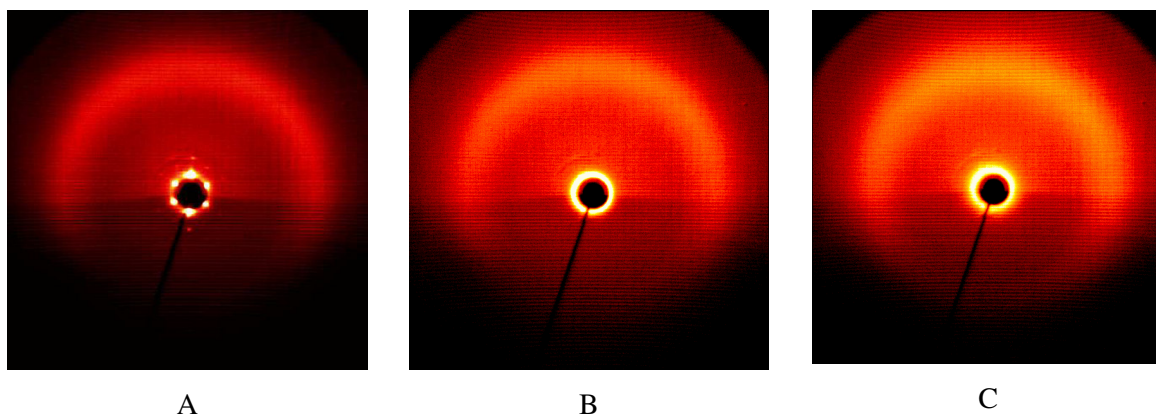


Figure 4.43 Wide angle range of the X-Ray pattern A) for an aligned sample of compound **9** in the columnar phase at 383 K on cooling B) for the isotropic liquid at 394 K just before the transition from the isotropic liquid phase to the columnar phase C) for the isotropic liquid at 455 K on heating.

4.3.4.2 Dielectric Investigations of the sulfone compound

The dielectric behavior of this compound is similar to the others that exhibit a columnar phase. In the isotropic phase only one relaxation mechanism at 10^8 Hz is observed (Figure 4.44). This process was fitted with the small Cole-Cole distribution of $\alpha = 0.03$. This relative intensive process reduces the dielectric permittivity from 7 to 2.76. The high frequency limit is low and indicates that one cannot expect a further relaxation mechanism in the GHz range. A relaxation frequency of 5×10^7 Hz was fitted at 385 K (Fig 4.44). The dielectric behavior changes at the phase transition and a second absorption range at about 10^4 Hz appears (Figure 4.45). This process is only seen in the real part of the dielectric permittivity like in the others columnar phases investigated before. The low frequency mechanism reduces the dielectric permittivity from 19 (ϵ_0) to 13.4 (ϵ_1) at 8×10^3 Hz with a Cole-Cole distribution parameter of $\alpha = 0.33$. At higher frequencies a process with the same nature as in the isotropic phase reduces again the dielectric permittivity to $\epsilon_2 = 2.76$ at 10^7 Hz with $\alpha = 0.03$.

In Fig 4.46 the behavior of the dielectric permittivity versus the temperature is represented in the whole temperature range. Again a big increase of the dielectric permittivity at the phase transition to the columnar phase is observed. Both, ϵ_0 and ϵ_1 , are higher than the low frequency value measured in the isotropic phase. Also in this case the network of hydrogen bonds is oriented parallel to the electrical field. The relaxation frequencies show an

Arrhenius behavior for all processes (Fig 4.47). Activation energies of 37 ± 2 and 35 ± 2 kJ/mol were calculated for f_{R1} and f_{R2} respectively.

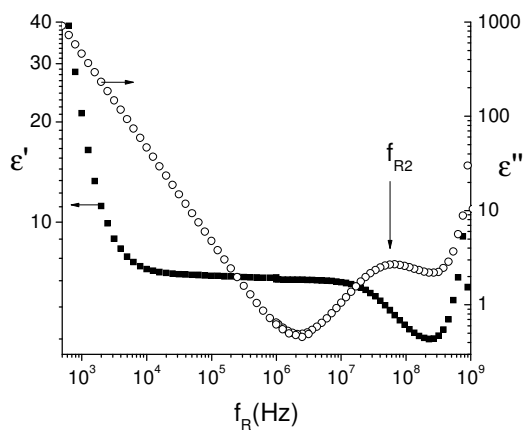


Figure 4.44 Complex dielectric permittivity of the isotropic phase at 385 K of compound **9**.

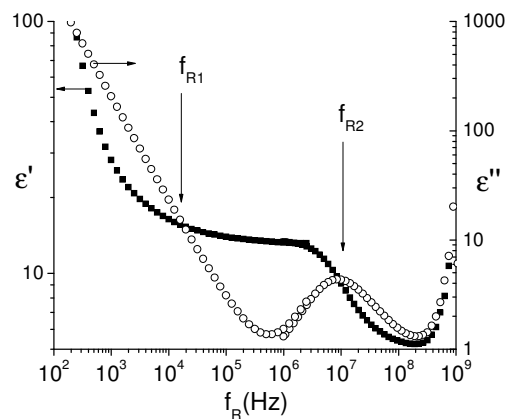


Figure 4.45 Complex dielectric permittivity of the columnar phase at 358 K of compound **9**.

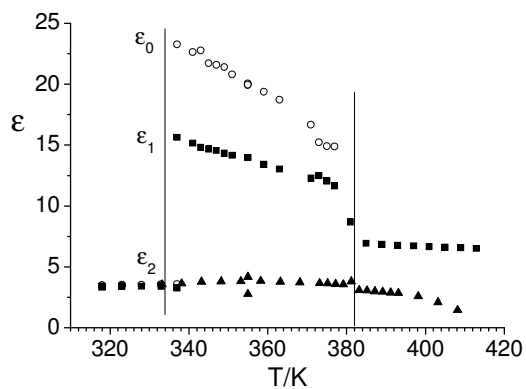


Figure 4.46 Limits of the dielectric permittivity versus temperature compound **9**.

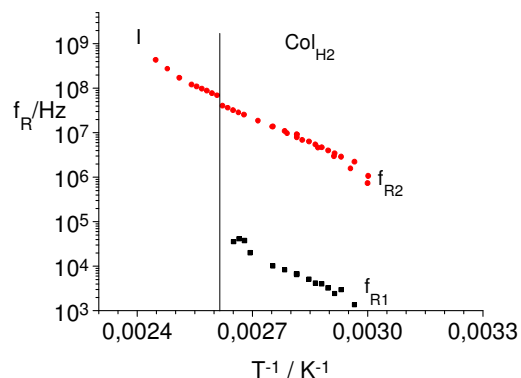


Figure 4.47 Relaxation frequency versus temperature compound **9**.

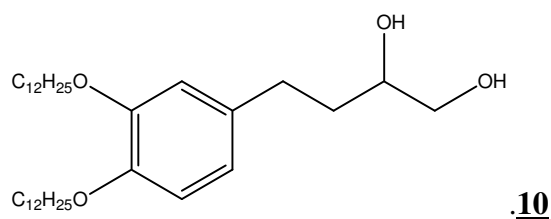
4.3.5 Investigation of a methylene compound

A substitution of the polar group in the middle part of the molecule by $-\text{CH}_2-$ reduces the dipole moment and the possibility to form hydrogen bridges. In order to demonstrate which

is the role of the polar group in the middle part of the molecule in the dielectric behavior it is very important the investigation of this molecule.

It is known that a polar group attached directly to the aromatic ring doesn't have any importance for the process of self organization [79]. The phase behavior doesn't change when this group is substituted by a polar group. Indeed the columnar H₂ phase is stabilized by the π -packing of the aromatic rings and the formation of the hydrogen bonds network formed by the diols. An alkyl chain in between the diol and the ring separate this two effects on the molecular level and facilitate the investigation of the dynamic of the different parts of the molecule by NMR. In that way the geometry of the different movements can be studied.

For this purpose compound **10** was synthesized:



Structure of 4-(3,4-Bis-dodecyloxy-phenyl)-butane-1,2-diol

Compound	Phase behavior and Temperatures (K)		
	10	Cr	Col

$\xleftrightarrow[313]{313}$ $\xleftrightarrow[343]{343}$

Table 4.8 Mesophase behavior of compound **10**

The substitution of the middle part of the molecule by a methylene group reduces the clearing temperatures of the columnar mesophases composed by two alkyl chains as aliphatic part to 343 K in that way the temperature range of the columnar phase of this compound result to be the smallest of all the homologues compounds (30 K).

4.3.5.1 X-ray investigations of the methylene substituted compound

The introduction of the methylene group in the middle part of the molecule doesn't change the phase behavior. The substance shows a columnar phase between 313 and 343 K on cooling. 2D-xray patterns prove the existence of the hexagonal columnar phase (Figure

4.48, 4.49). The 3 reflections have d values in the ratio of $1:1/\sqrt{3}:1/2$ corresponding to the reflections (1,0),(2,0) and (1,1) with 33.5, 16.75 and 19.5 nm respectively.

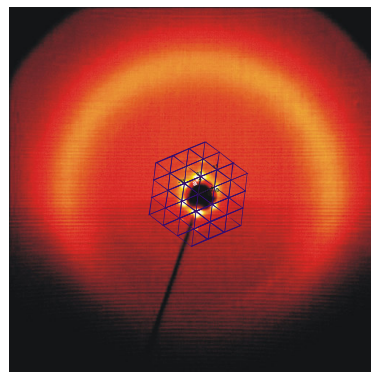
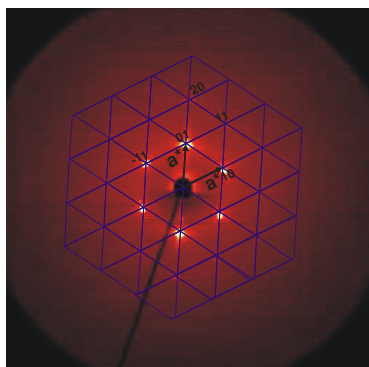


Figure 4.48 Small angle range of the X-Ray patterns for an aligned sample in the columnar phase of compound **10** at 338 K on cooling with the assignment of some reflections.

Figure 4.49 Wide angle range of the X-Ray patterns for an aligned sample in the columnar phase of compound **10** at 338 K on cooling.

4.3.5.2 Dielectric investigation of the methylene compound

The introduction of the non polar group in the middle part of the molecule make the compound generally more apolar and decreases so the dielectric permittivity to about 4 as seen on the data measured in the isotropic phase (Figure 4.50). In the isotropic phase just the begin of a relaxation range at frequencies of about 1GHz is visible in Figure 4.50. At low temperatures just before crystallization of the columnar phase a very weak relaxation process at 0.2×10^9 Hz is observed (Figure 4.51). This process is very difficult to fit because it is not really separated from the answer of the resonance of the cell. Only relaxation data at two temperatures could be analyzed. For this reason it doesn't make any sense to discuss the behavior of the dielectric permittivity versus the temperature for compound **10**. Another very weak process could be fitted at low frequencies. For the fitting procedure only the data obtained with the low frequency equipment were used. The results are shown in the Figures 4.52 and 4.53. This is relaxation process appears only in the columnar phase and reduces the dielectric permittivity from 7.8 to 5.3 at 318 K (Fig 4.52). The relaxation frequencies in the columnar phase were calculated to be between 513 to 807 Hz and scatter in a wide range (Fig 4.53). The existence of the low frequency relaxation

process even when the polar group is removed evidence that this process is a characteristic of the columnar phase and not related to a special polar structure of the molecule.

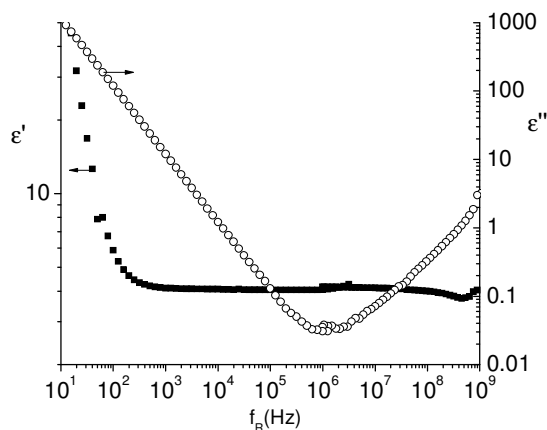


Figure 4.50 Complex dielectric permittivity of compound **10** in the isotropic phase at 346 K.

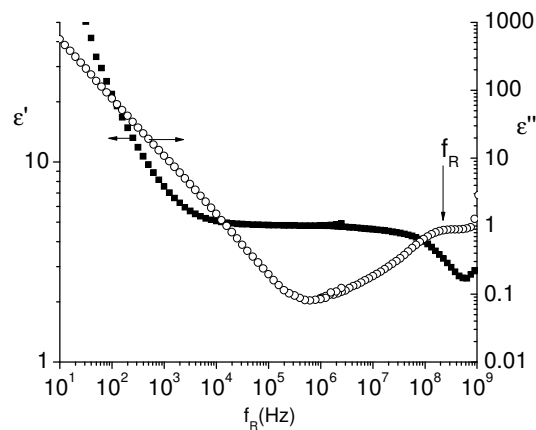


Figure 4.51 Complex dielectric permittivity of compound **10** in the columnar phase at 333 K.

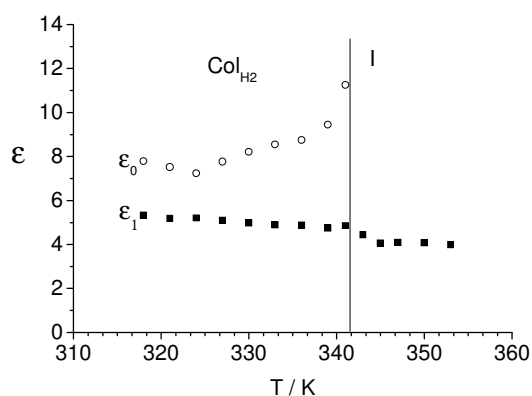


Figure 4.52 Dielectric permittivity versus the temperature of compound **10**.

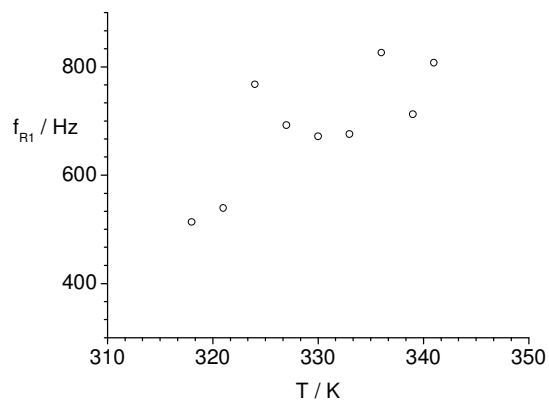


Figure 4.53 Relaxation frequency versus the temperature of compound **10**.

To understand the dynamics of this substance in the columnar phase another method should be applied. The Nuclear Magnetic Resonance method is a very powerful tool to understand the geometry of the movements on a molecular level. In this way the movements of the molecules inside of the columnar lattice could be better understood and the assignment of the different relaxation process could be done.

4.3.5.3 Nuclear Magnetic Resonance investigation of the methylene substituted compound

It is already known that discotic molecules that form hexagonal columnar phases can move in two ways. The molecules can rotate around the principal axis of the columns. This movement reduces the coupling constant in a half of the value with respect to the solid lattice. Another rotation around the principal axis of the molecule reduces more the coupling constant. In that way for discotic molecules the order parameter which is defined as a $S = D_{\text{sol}}/2D_{\text{LQ}}$ has values of about 0,8 what is a sign of librational movements in addition to the expected axial rotation in discotic molecules [58,60]. In the case of the simple diol molecules arranged in a hexagonal columnar lattice the molecules are supposed to form discs but there is no way to confirm this. The study of the dynamics in a molecular level can help to understand the structure of the molecules inside of the columnar lattice.

Qualitative Cross Polarization Magic Angle Spining (CP-MAS) measurements are carried out to now a little about the nature of the movements to support also the dielectric results. Thus dielectric answer at about 1 MHz was found in all other compounds. The elucidation of the different movements can help also to assign the dielectric absorption bands.

First the assignments of the signals were carried out with two dimensional experiments in liquid state see Appendix 1.

The spectrum of the substance is shown in the Fig 4.54. Like in solution state spectrum only one resonance is expected for every carbon in the structure. But the most part of the signals show different resonances. That means that the carbons are not equivalents in the solid lattice.

The intensity of selected signals versus transfer time during the cross polarization experiment is represented in the Fig 4.56 for different parts of the molecule. From this graphic the order parameter can be calculated. During this time the polarization of the H atoms is transferred to the C atoms modulated by the different coupling constants in dependence of the mobility of the different parts of the molecule. The coupling constant can not be calculated for those experiments but the time when the polarization acquire the

maxima intensity can be used like a reference for the preliminary calculation of the order parameter in the different parts of the molecule $S = \tau_{\text{sol}} X^2 / \tau_{\text{liq}}$.

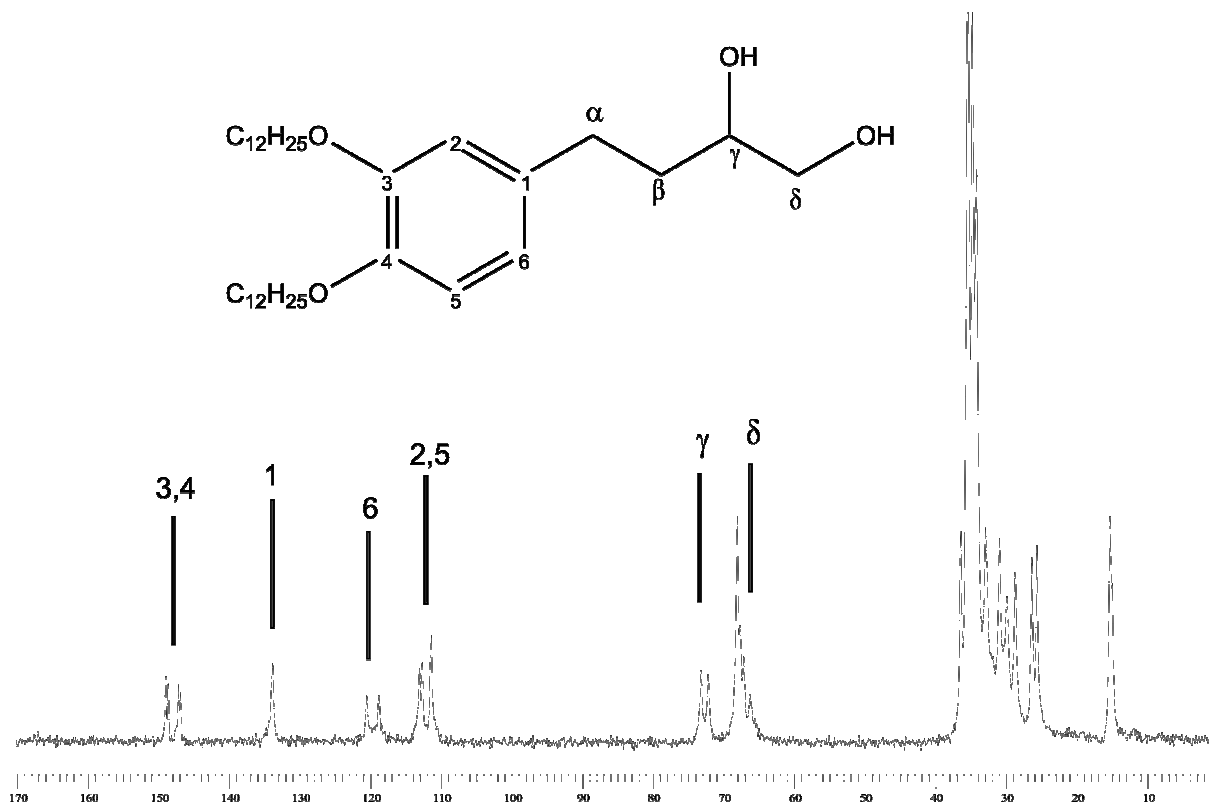


Fig 4.54 CP-MAS Spectrum of the Substance with the assignment of the signals at room temperature after recrystallization.

In that way for the signal of the aromatic rings at 115 ppm (Fig 4.56 A) and of the chain directly attached to the ring signal at 36 ppm (Figure 4.56 C) the order parameter is about 0.25 ($60 \times 2 / 500$). For the diol part the order parameter is 0.17 ($60 \times 2 / 700$) (signal at 73 ppm Fig 4.56 B). For discotic molecules order parameter of about 0.8 where calculated [58, 60]. To establish a relation between the order parameter and the movements several simulations have to be done like quantitative measurements of the coupling constant.

The diol part exhibits a higher mobility than the aromatic core with a smaller order parameter. It has to be pointed out that the dynamics of the nonpolar aromatic part cannot be detected by the dielectric method. From the values of the local order parameter it can be concluded that these compounds have a high mobility inside of the columnar arrangement in comparison with discotic molecules. Since the aromatic rings are not covalently attached to each other in the columnar arrangement a new movement has to be

considered for the interpretation of the reduction of the coupling constant, the rotation around the long axis of the molecule.

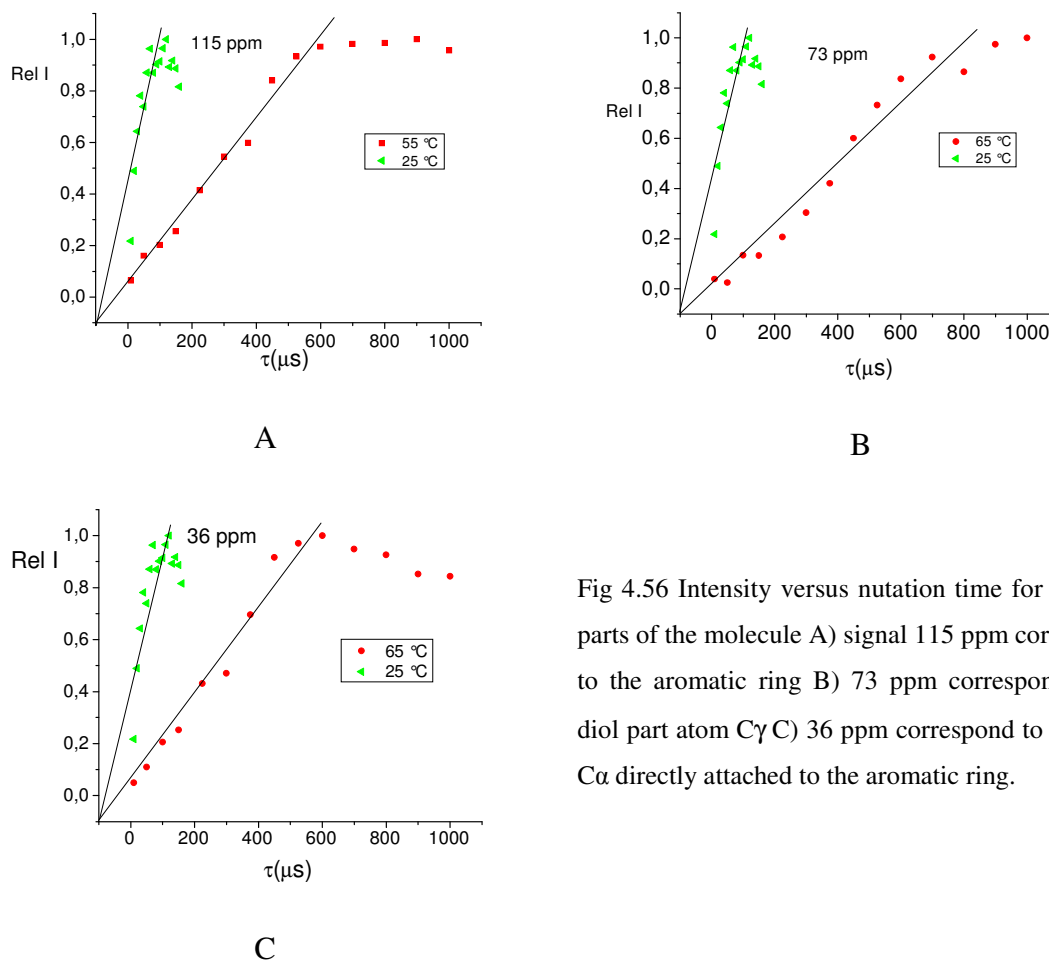


Fig 4.56 Intensity versus nutation time for different parts of the molecule A) signal 115 ppm corresponds to the aromatic ring B) 73 ppm correspond to the diol part atom $C\gamma$ C) 36 ppm correspond to the atom $C\alpha$ directly attached to the aromatic ring.

4.3.6 Assignment of the different relaxation processes in the columnar phase

The dielectric relaxation process is the consequence of the interaction of the dipole moments with the external electric field. The dipole moments can be produced by a special order as a collective movement, as dynamics of the whole molecule or as that of groups of molecules. In first approximation the relaxation frequencies increases in the order given. Furthermore one has to consider that the different types of dynamics are influenced in different way by phase transitions. Thus, collective processes are connected with a special structure. Taking this into account the low frequency relaxation has to be regarded as collective motion. The interaction of the different polar groups und its superposition in the dynamics makes it difficult to separate the molecular mechanisms. It has to be noted that

the relaxation ranges detected by dielectric measurements are marked by numbers with increasing frequency as usually. Therefore, identical numbers do not mean an identical mechanism!

The low frequency mechanism is observed only in the columnar phase and disappears in the isotropic state. It is also observed if the chemical structure of the middle part is changed or even in a mixture where the columnar phase is induced. The relaxation frequency varies for different molecules. Thus, the urea-compound **6** with two alkyloxy chains shows at 320 K a relaxation frequency of 2 kHz and substance **7** with three chains at the same temperature only 1 kHz. This may indicate that the columns in compound **6** are destabilized. A small hint for this statement is coming from the packing models given in the figures 4.23 and 4.24. In the following table the relaxation frequencies of the low frequency mechanism are summarized at 340 K. Only compounds with the same basic structure but with a variation in the middle part are considered.

Subst Nr	f_{R1}/kHz
<u>8</u>	10
<u>9</u>	2
<u>10</u>	0.8

Table 4.9 Relaxation frequencies of the low frequency mechanism at 340 K

Compound **10** with the non polar methylene group in the middle part shows the lowest relaxation frequency, whereas the methylated amino group in the middle part increases the relaxation frequency of more than one decade. This gives also a hint that the lateral methyl group of compound **8** destroys the stability of the packing to columns and therefore the collective reaction to the external electrical field becomes faster. May be that the low frequency mechanism is related to the nonsymmetrical packing of the molecules within the discs which produces a torque to the whole column in the electrical field.

For the analysis of the second and third relaxation range some data are summarized in Table 4.10.

Subst. Nr	f_{R2}/MHz 333 K	f_{R3}/MHz 333 K	$\epsilon_1(\text{Col})$ 320 K	$\epsilon(\text{Iso})$ 360 K
0,6 (mixture)	0,2(13)	1(6)	27*	9
<u>6</u>	0,1(12)	-	16,5	10
<u>7</u>	0,1(20*)	2(4*)	27*	9
<u>8</u>	2(8)	100(2)	12	6
<u>9</u>	2(13)	-	17	7,5
<u>10</u>	200(2)	-	5,2	4

Table 4.10 Characteristic data of the second and third relaxation range. The homologous compounds of substance 8 without the methyl group at the nitrogen atom exhibit according to Schmalfuss [109] at 333K a relaxation frequency of 1 MHz and a dielectric strength ϵ_1 - ϵ_2 of 3.2. The compound shows a high conductivity disturbing calculations at lower frequencies. The relaxation strength is given in brackets after the related relaxation frequency. * Only in this case the data are given at T = 310 K. Note that $\epsilon_1(\text{Col})$ does not contain the first relaxation process.

The results on compound 10 are the basis for the discussion. This sample does not contain any polar group in the middle part of the molecule. Therefore the dielectric relaxation effect seen must be related to the dynamics of the alkyloxy groups and that of the network of hydrogen bonds. The relaxation frequency is with 0.2 GHz the highest which was measured. That is in agreement with the NMR data which suggest as fastest motion from the investigated one the dynamics of the hydrogen bonds. The dielectric strength of about 2 for this motion is very low, even if we consider that it is difficult to compare this data due to the unknown orientation of the sample. But we have to consider that also the dielectric permittivity in the isotropic phase of about 4 is low and this one does not depend on the orientation. Furthermore the measurements were carried out with two different equipments in different laboratories. Thus, we can exclude errors from calibration.

Possible movements of the whole molecule are sketched in Figure 4.57. Thus, the molecules can in principle rotate about the short (3) and long axis (2) as shown in the figure. The rotation about the short axis is restricted due to the intermolecular interactions of the net of hydrogen bonds. Like in classical amphiphilic substances the molecules are fixed on one side. The rotation about the long axis need not too much place and should be the main process observed. Of course, this rotation can be splitted in the dynamics of different polar groups, like the dipoles in the middle part of the molecule between the diol

groups and the substituted phenyle, that of the diole and of alkyl oxy groups. The last two are expected to be faster. Furthermore, a bent of the whole molecule up and down of the plain of the discs (1) can be expected. The last motion should show a very small dielectric response because the change of dipole moment is small.

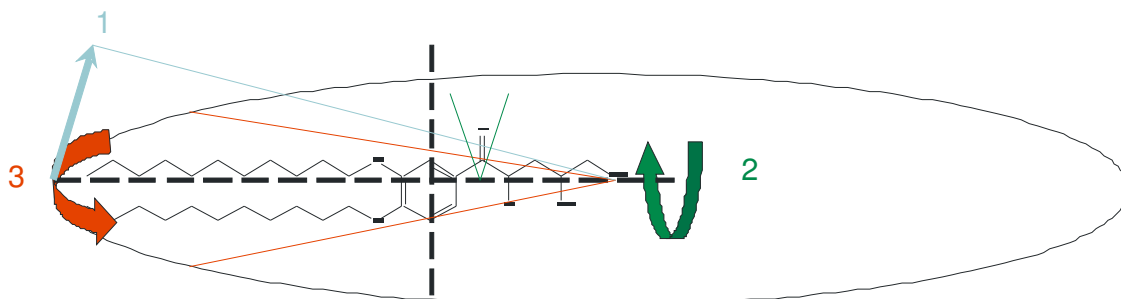


Figure 4.57 Possible movements of the molecule inside of the columnar arrangement.

The problem is now that not all mechanisms could be separated in single relaxation ranges. A model, based on the idea that the different dipolar groups are rigidly attached in the molecule should make different contributions to the dielectric relaxation strength can help us. This idea is useful to assign the absorption bands of the dielectric spectrum in first approximation. But we have to consider that dipoles in the middle part of the molecules can interact with the network of hydrogen bonds. Thus, we can expect that the dipole moments in the middle part of the molecule are not anymore statistically distributed. This effect will increase the dielectric strength of the related relaxation mechanism.

Compound **8** with the methylated amino group in the middle part of the molecule shows the high frequency absorption at 0.2 GHz and additionally a second one at about 2 MHz. The dielectric strength of the process at 2 MHz $\epsilon_1 - \epsilon_2$ of about 8 must result from the middle group of the molecule. For the sulfonyl compound **9** the absorption at about 0.2 GHz could not be isolated because of the dominating influence of the resonance effect. The high frequency limit of the intensive absorption at 2 MHz $\epsilon_2 = 3.7$ (see fig 4.46) makes additional high frequency absorption at about 0.2 GHz possible. The relaxation frequency of the second mechanism increases of a factor 2 at the phase transition into the isotropic state. This may indicate that the short range order changes not so strongly, or in other words, the columnar order still exists in the isotropic phase. This statement is supported by no change in the amide I vibration in Figure 4.34. On the other hand the lines of the

aromatic part indicate a weakening in the packing at the transition in the isotropic phase which may indicate a better rotation of the benzene molecules.

For the mixture and compound **7** in Table 4.10 a splitting of the mechanism in the MHz range is observed. All of the compounds exhibit a -NH- group in the middle part which is able to form hydrogen bridges with the diol groups. This effect may be responsible for the slower dynamics of a part of the molecule and will be discussed later.

Both, the mixture 0.6 and the nonmethylated compound **8** show the same relaxation frequency of 1 MHz at 333 K. This indicates that the mixture of molecules with one and three dodecyloxy chains is equivalent to the compound with two dodecyloxy chains with respect to forming a columnar phase and the dynamics.

In the isotropic phase the dielectric permittivity of some compounds show an unusual behavior: it increases partially or decreases very slightly with the increase of the temperature. That gives evidence of the existence of cybotactic groups in the isotropic phase which was confirmed by X-ray investigations.

The discussion is summarized in Fig 4.58 where the real part of the dielectric permittivity is given for all measurements with an extended frequency range. Here the curve of the compound with the -CH₂- group in the middle part of the molecule don't show any clear absorption band in the frequency range where the other compounds show an intensive absorption band. The overlapping of the relaxation ranges caused by the dynamics in the middle part and that of the faster -OR and -OH groups is also demonstrated. Furthermore the existence of low frequency absorption at about 10³ Hz is also clearly seen for the last compound shown. Generally three absorption ranges are discussed were the collective motion and the high frequency absorption are present in all samples showing the columnar phase.

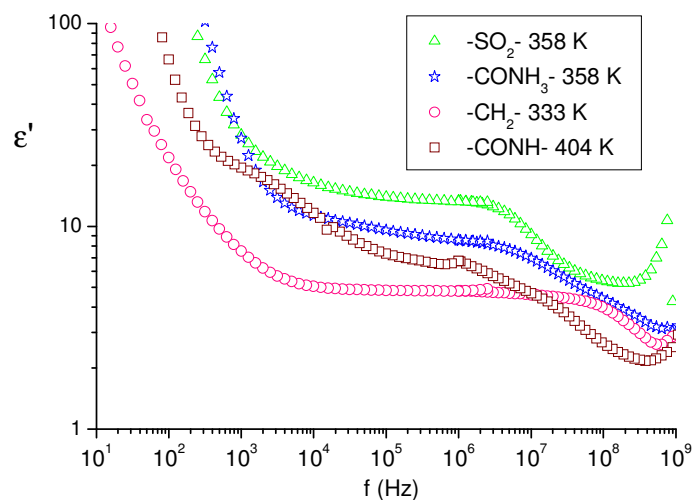


Figure 4.58 Comparison between the curves of the real part of the dielectric permittivity of compounds with different groups in the middle part of the molecule in the columnar phase. Comparison between compounds **2** (-CONH-), **8** (-CONH₃-), **9** (-SO₂-) and **10** (-CH₂-) at different temperatures. Note that the columnar phase appears at different range of temperature.

The dependence of the relaxation times can also help to the assign of the bands. Therefore relaxation frequencies of the second mechanism of different compounds are represented in Figure 4.59. The urea compound **6** and the compound with the -NH- group **2** in the middle part show lower relaxation frequencies than those of compounds **8** and **9** (Figure 4.59 red arrow). This is an indication that the dipole moments of the -NH- group in the middle part of the molecules are restricted in the movement due to the network of hydrogen bonds.

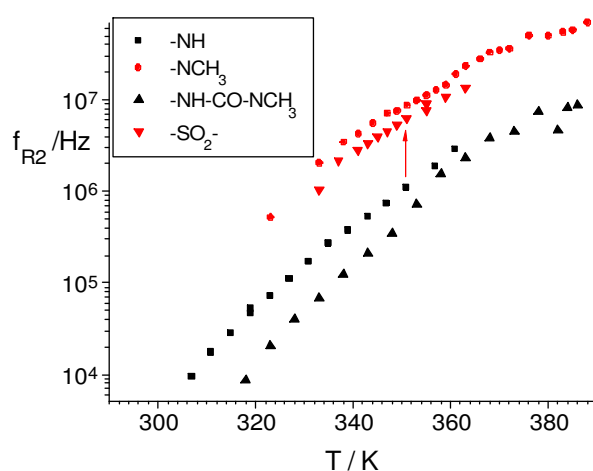


Fig 4.59 Influence of the H-bonds in the relaxation frequencies of the high frequency process f_{R2} . Comparison between compounds with two alkyl chains as hydrophobic group that exhibit columnar mesophase, **2** (-NH), **6** (-NH-CO-NH₃), **8** (-NCH₃), **9** (-SO₂-).

4.4 Investigation of the Cubic phase

4.4.1 The formation of the micellar cubic phase

In the cubic phase the orientation effects do not play any role because there is not preferable orientation of the molecules inside of the lattice. The molecules in the cubic phase are organized in micelles where the dipole moments in the longitudinal direction of the molecules are compensated and the hydrogen bonds are localized in the middle of the micelles. The network of hydrogen bonds is isolated and forms a point-like structure. The micelles are organized again in a super structure, a cubic lattice (Figure 4.61).

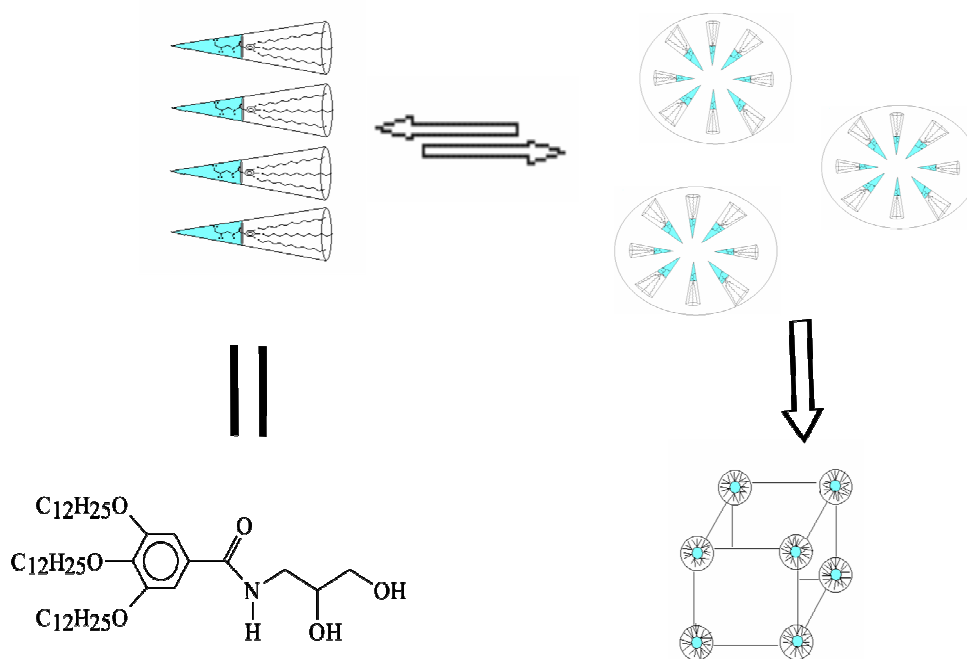


Fig 4.61 Schema of the formation of the cubic phase from the micelles in equilibrium with the monomers.

4.4.2 Dielectric investigations

The conductivity dominates the spectrum in the low frequency range for all of these mesophases. The real part represented by squares in the curve of Figure 4.62 is constant below frequencies of 0.1 MHz. The structure of localized and isolated hydrogen bonds network of the cubic phase reduces the conductivity, which is seen by the small contribution of the conductivity in the imaginary part of the curve. Also in the small values

of the imaginary part in comparison with those of the smectic phase the isolated character of the hydrogen bonds is seen. That is a result of compensation of dipole moments inside of the micells (negative correlation of dipole moments) and of the cubic order.

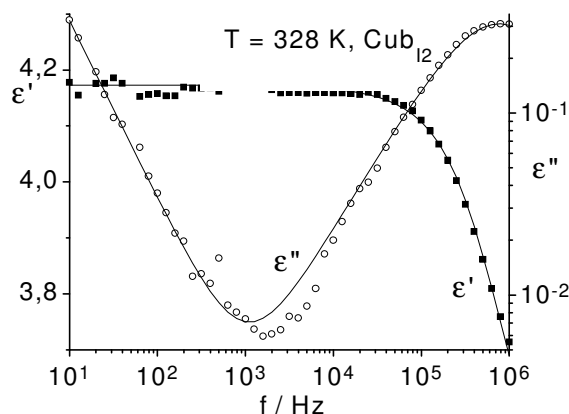


Figure 4.62 The complex dielectric function of compound **3** in the Cub_{12} phase.

In contradiction to the results of compound **1** the static dielectric permittivity ϵ_0 of compound **3** decreases at the phase transition I/Cub_{12} (Fig 4.63, $\Delta\epsilon_{\text{ph}}$). This is a consequence of the formation of the cubic lattice where the dipole moments are partially compensated. In the isotropic phase the dielectric permittivity increases with the increasing temperature. This is an unusual effect, as the normal behavior is the decrease of the dielectric permittivity with the temperature. The increase of permittivity with the increase of the temperature must be related to an increase of dipole moment per unit volume. This effect can be only explained by the presence of equilibrium between micelles and single molecules. The destruction of the micelles with a compensation of the longitudinal dipole moments and the formation of single molecules increases the dipole moment per unit volume and increases so the dielectric permittivity. This equilibrium is shifted at higher temperatures in direction of the formation of single molecules. That gives evidence of the presence of micelles at the isotropic phase as sketched in Figure 4.61.

The change in the order is also seen in the stepwise decrease of the specific conductivity at the phase transition I/Cub_{12} to 20% of the value of the isotropic phase (Figure 4.64). That reflects clearly the stepwise formation of the isolated system of hydrogen bonds because the cubic phase has no preferred axes and no orientation effects have to be considered.

Similar results were obtained for the mixture with $x_3 = 0.9$ which forms also the Cub_{12} phase.

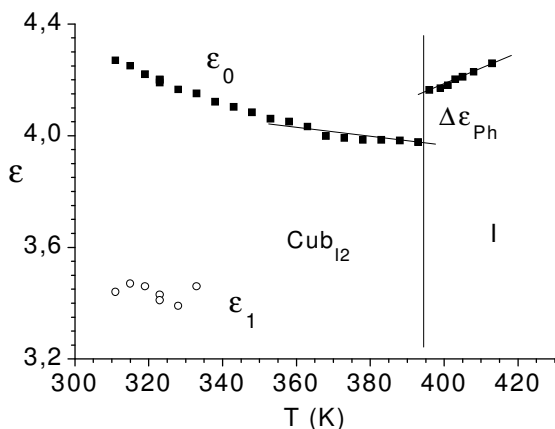


Figure 4.63 Static dielectric constants vs Temperature (K) of compound **3**.

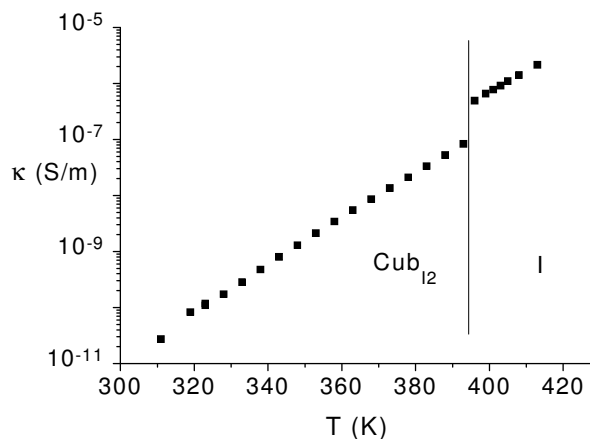


Figure 4.64 Specific conductivity vs Temperature (K) of compound **3**.

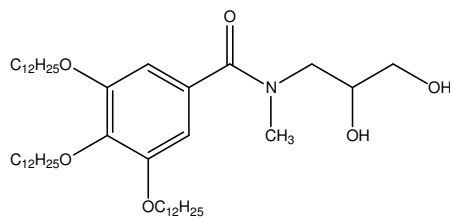
4.4.3 Specific behavior of the micellar cubic phase

The micellar cubic phase is typical for compounds with a very big difference between the volume of the hydrophobic and hydrophilic part of the molecule. The cubic lattice is formed by aggregates where the polar part is isolated in the middle part of the micelles. That gives this mesophase dielectric property like those only seen by unpolar compounds. They exhibit a very low dielectric permittivity because of the negative correlation of the dipole moments and also low values of the conductivity since the hydrogen bonds are isolated avoiding the flow of charge inside the cubic lattice. The phase transition into the cubic phase is characterized by a decrease of conductivity and dielectric permittivity. A low frequency dielectric absorption like in the columnar phase could not be detected down to a frequency of 10 Hz (see Figure 4.62).

4.5. Study of the cubic/columnar phase transition of the methyl-amide compound with three alkyl chains

Compounds with more than one mesophase give us the chance to compare the mesophase behavior of the different phases without the influence of the special chemical structure.

Thus, the compound with three chains exhibits a polymorphism cubic/columnar with a phase behavior I 327 Cub 307 Col 285 Cr.



11

For the transition I/Cub of this substance the phase transition could not be detected by DSC traces. This might be due to supercooling/overheating effects of this phase transition. The peaks could be smeared out over a broad temperature range.

4.5.1 X-Ray investigations

The Guinier-film pattern of the columnar phase show 3 reflections with d values in the ratio of $1:1/\sqrt{3}:1/2$ and can also be assigned as Col_{H2} with $a_{\text{hex}} = 4.0$ nm at 303 K. 2D X-ray experiments were done but the results are not shown because the columnar phase could not be well oriented by cooling from the cubic phase. The optically isotropic high-temperature phase causes Bragg reflections in the small angle range suffering from strong splitting according to orientation effects, which is typical for a cubic phase.

4.5.2 Dielectric investigations

The dielectric permittivity can be a powerful tool to investigate changes between structures with differences in the organization of the dipole moments. Thus, a stepwise increase of the dielectric permittivity is observed at the phase transition Cub/Col (Figure 4.65). In the cubic phase the molecules are organized in micelles where the dipole moments are compensated so that the resulting dipole moment is lower than that of the isotropic state. This again results in a decrease of the dielectric permittivity at the phase transition I/Cub as demonstrated in the inserted part of Figure 4.66. In contradiction to the DSC measurements a much lower cooling rate was used by the dielectric investigations. Therefore the transition was observed at a characteristic temperature. Furthermore, by the dielectric method the permittivity is measured directly whereas the DSC measures the heat flow

which is smaller if the cooling rate decreases. Figure 4.66 also shows that for substance **11** the dielectric permittivity increases in the isotropic phase by heating.

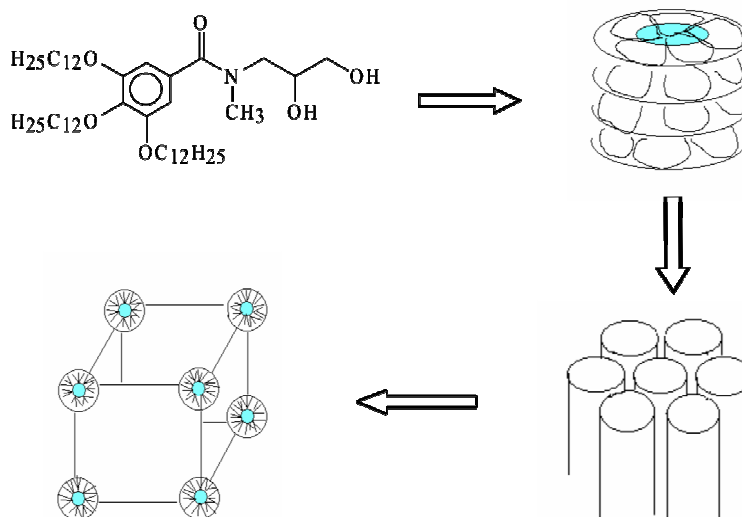


Figure 4.65 Schema of the columnar/cubic phase transition.

As already shown the segregation of the polar part in the middle of the micelles like a point reduces the conductivity in the cubic phase. In contrast to it the hydrogen bonds in columnar phase are organized like a wire in the middle of the columns favorable for the conductivity of the charge. Thus, an interesting change of the conductivity is observed at this phase transition (Figure 4.67).

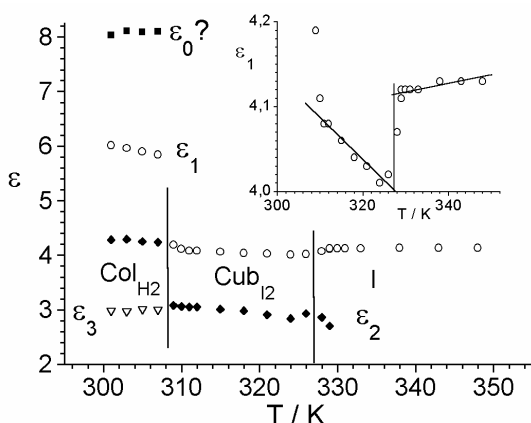


Figure 4.66 Limits of the dielectric permittivity versus temperature.

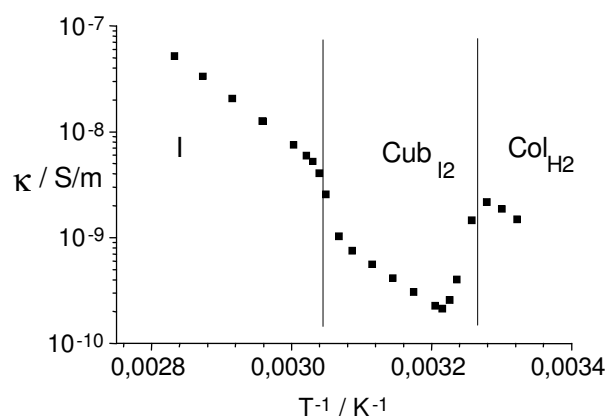


Figure 4.67 Specific Conductivity versus the reciprocal temperature.

The dielectric behavior of compound **11** in the columnar phase is dominated by the contribution of an asymmetrical mechanism at high frequencies (Fig 4.68). This relaxation process was splitted into two Cole-Cole processes by a fit. Activation energies of 43 ± 5 kJmol^{-1} (Col_{H_2}) and 38 ± 3 kJmol^{-1} (Cub_{I_2}) have been calculated for the high frequency mechanism 2 indicated by open circles (Figure 4.69). It is to note that also for the other methyl substituted amide compound **8** with two alkyloxy chains two different processes in the MHz range could be separated (Figure 4.68). For this reason it is not an error to think that this asymmetrical absorption band is the result of the superposition of two different rotation modes. The high frequency limit of the dielectric permittivity of about 3 in the columnar and cubic phase (Figure 4.66) makes the existence of a less intensive relaxation range at about 1 GHz possible which could be related to the dynamics of hydrogen bonds. The existence of low frequency absorption at about 2 Hz in the columnar phase could not be not undoubtedly proven.

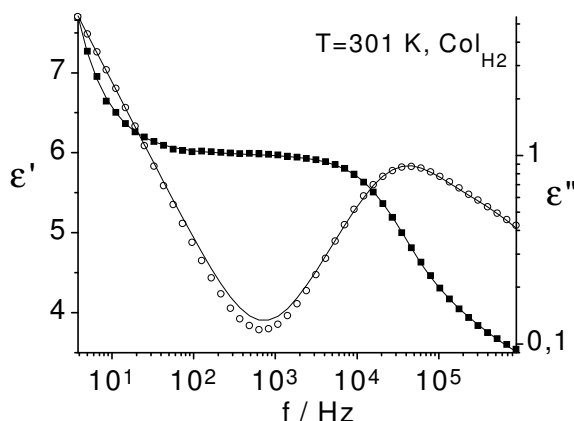


Figure 4.68 Complex dielectric function of the compound in the columnar phase.

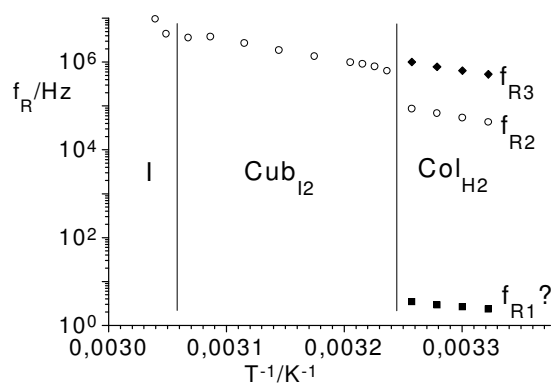


Figure 4.69 Relaxation frequencies versus temperature.

4.5.3. Study of the columnar/cubic phase transition by Infrared Spectroscopy

The columnar/cubic phase transition was also studied by IR spectroscopy. The spectra of the methylated compound **11** (shown in red) and the amide compound **3** (black) are shown in Figure 4.70, with the bands relevant for this IR study (i.e. Amide I and the aromatic C=C bond stretching) assigned on it. The phase transition Cub/Col could be studied by following the variations of these two bands with the temperature. The vibration frequency of the Amide I band displays a prompt shift to higher frequencies when the molecules form the cubic phase (Figure 4.71A). That evidences an increase of the force constant of the

C=O bonds in the cubic phase. This might indicate that in the cubic phase the CO groups are less involved in the hydrogen bonds networks. On the other hand, the aromatic C=C stretching band does not show a discontinuous change at the Cub/Col phase transition (Fig 4.71 B).

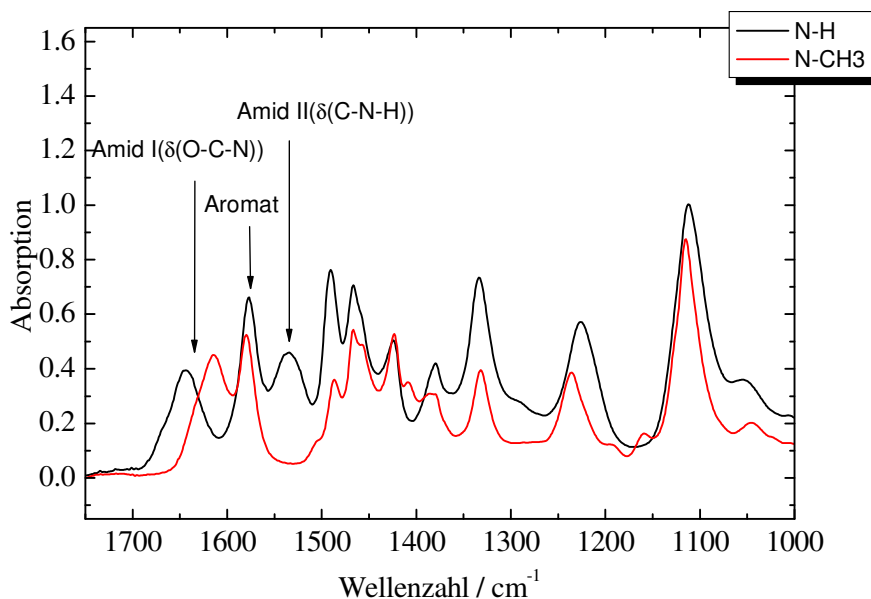


Figure 4.70 IR-Spectrum of the amide compound **3** and amide substituted compound **11**.

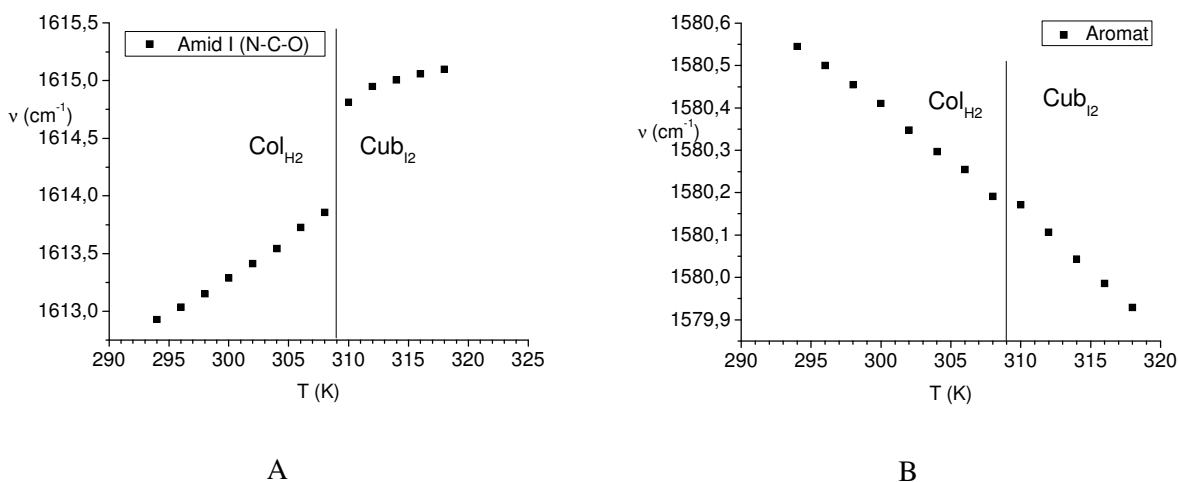


Figure 4.71 A) Wavenumber versus temperature of the amide I mode of the compound **11** B) Wavenumber versus temperature of the aromatic mode of the compound **11**.

5. Discussion of the results on the binary system

As demonstrated, the dielectric results give insight in the process of self assembling. This was discussed for both components and partially for the mixtures before. In order to see special effects in the middle concentration range the data have to be summarized. Figures 5.1 and 5.2 show the limits of the dielectric permittivities of the different mesophases at 363 K and the steps of the dielectric permittivities at the phase transition $\Delta\epsilon_{\text{PhI}} = \epsilon_{\text{LC}} - \epsilon_{\text{I}}$ estimated from linear extrapolation of the data. Thereby the data near to the phase transition were excluded in order to avoid the influence of the two phase range. Open symbols were taken for a second run at the same concentration. Especially in the SmA phase they show big differences to the first measurements (closed symbols) in the ϵ data but not in the relaxation frequencies. This effect is related to different orientations in the SmA and columnar phases. The dielectric permittivity increases with the increase of the content of the compound **1** (Figure 5.1). In the SmA and Cub_{12} phases only one relaxation process with a relaxation frequency of about 1MHz at 343 K was detected, which is also seen in the $\text{Col}_{\text{H}2}$ state. This process we have to relate to the dynamics within the middle part of the molecules which is influenced by hydrogen bonded system. The additional low frequency process seen only in the $\text{Col}_{\text{H}2}$ phase must be related to the structure of the columns as discussed before.

The steps in the dielectric permittivity at the phase transition LC/I $\Delta\epsilon_{\text{Ph}} = \epsilon_{\text{LC}} - \epsilon_{\text{I}}$ (Figure 5.2) show big changes due to the formation of the columnar or SmA phases (\blacksquare, \square). Taking into account additionally the small linear decrease of the dielectric permittivity in the isotropic phase we assume that this step contains both contributions, a part of the organization of the molecules to columns and that of columns to a hexagonal phase. In the columnar phase two steps are seen whereby the squares are related to the low frequency limit of the dielectric permittivity (\blacksquare, \square). A change of sign related to strong changes of orientation is seen only in the SmA phase.

The relaxation frequencies versus the molar fraction are summarized in the Figure 5.3. Only in the columnar phase two relaxation processes are observed (f_{R1} and f_{R2} at 20 kHz and 1 MHz respectively). The second relaxation process f_{R2} is observed in all liquid crystalline phases. The faster dynamics in the cubic phase may be related to changes in the

interaction between the network of hydrogen bonds and the middle part of the molecules. This effect is also reflected in the line shift of the IR-spectrum at the ColH₂/CubI₂ transition in Figure 4.71A.

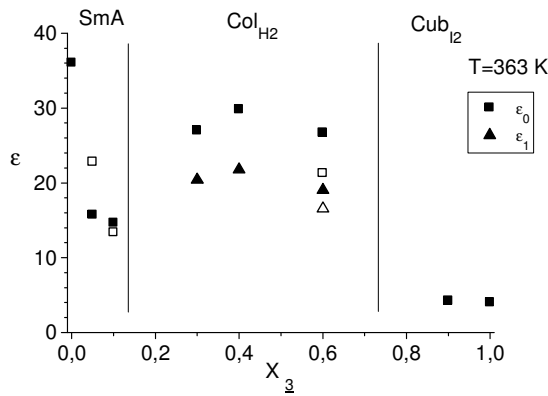


Figure 5.1 Dielectric permittivity at 363 K versus molar fraction.

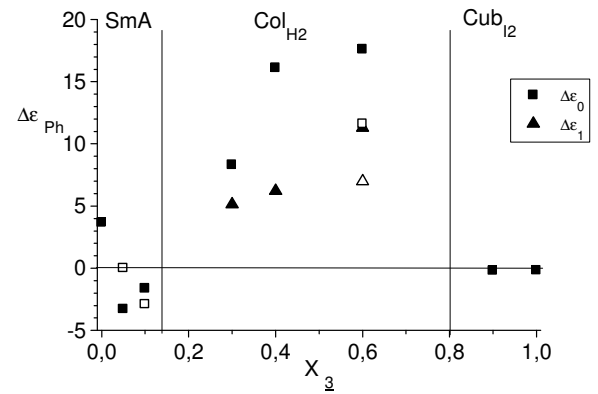


Figure 5.2 The step of the dielectric permittivity at the clearing temperature.

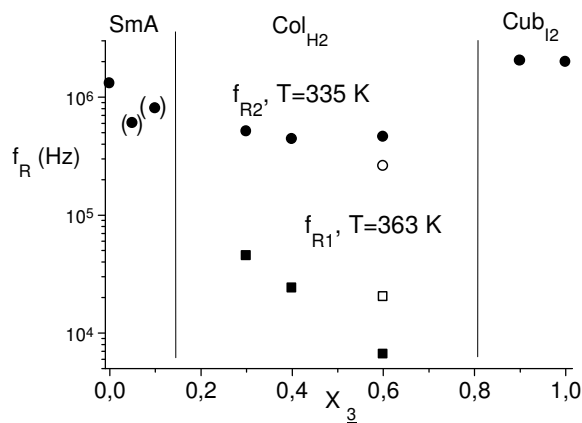


Figure 5.3 Relaxation frequencies versus molar fraction. (■) f_{R1} measured at 363 K, (●) f_{R2} measured at 335 K. The open symbols (□○) represent data obtained by repetition of the measurements for the $x_3=0,6$. Data in brackets were obtained from extrapolation.

Summarizing the results of the binary system and comparing with that obtained before one can say that the structure of the phase is dominating the dielectric behavior. Therefore the investigation of further substances with the same general structure will not give in principle new results.

6. Summary

This work is focused on the study of the structure and the dynamics of diol molecules forming different kind of liquid crystalline mesophases, with the aim to understand the process of self-organization, the dynamics within the liquid crystalline mesophases and their physical properties. The basic idea was to change the geometry of the hydrogen bonds network from a plane via a line to a point. For that purpose, several diols molecules that form smectic, columnar and cubic phases were synthesized. In order to understand the variation of the physical properties of the mesophases with the change in the superstructure, a binary mixture of compounds with very different structure was investigated. Microscopic, calorimetric, DSC, IR and X-ray studies were used to characterize phase transitions and the structure of the mesophases. Dynamical investigations were done by means of dielectric and NMR spectroscopy.

Generally, it was found that every phase shows a particular physical behavior. The variation of the chemical structure resulted only in modifications of these “finger prints”. Thus, the dielectric permittivity shows differences because of the different arrangement of the hydrogen bonds inside of the structure. In that way, substances exhibiting the cubic phase displayed low dielectric permittivities of about 4, characteristic for nonpolar compounds. This is caused by the spherical shape and the point-like not extended network of hydrogen bonds inside of the micelles. The columnar phases with a hydrogen bond network like a wire along the columns has higher dielectric permittivity at about of 25 and SmA phases with a 2D hydrogen bond network can reach dielectric permittivities of about 40. The samples could not be oriented, but the change of electrical conductivity at the clearing point gives an idea about the general orientation of the network of hydrogen bonds in the smectic A and columnar phases. Dielectric investigations in a binary mixture also show the same results.

To get inside in the relation between dynamics and structure, investigations of molecules with different dimensions of the hydrogen bonded network were carried out. The SmA phase and the cubic phase exhibit a dielectric spectrum dominated by the orientation of the polar central group at frequencies of about 1MHz. The columnar phase features a complex dynamical behavior with contributions of at least three different processes. One of them appears at low frequencies of about 1 kHz. This process is related to the dynamics of the

columnar arrangement and was detected for all compounds. Such a low frequency process is also observed in other columnar mesophases with helical arrangement forced by chiral disc-like molecules. It may be that the helical order is not necessary for appearing of this relaxation range. A net dipole moment as result of an asymmetrical packing may be sufficient enough for the reaction of the external electrical field with the elastic column. The other relaxation processes occurs between 1 MHz and 10 MHz. It is related to the dynamics of the dipoles in the middle part of the molecules. If some atoms in the middle part of the molecule are able to interact with the net of hydrogen bridges, an increase of the dielectric permittivity as well as a splitting off of this relaxation range is observed. The third process, not investigated for all substances, is the very fast dynamic within the network of hydrogen bonds in the GHz range. For comparison purposes, NMR spectroscopy was used. A qualitative investigation reveals that the mobility of the molecules inside of the columnar lattice is higher than the mobility of disc-like molecules exhibiting also columnar hexagonal arrangement.

The process of self organization of these compounds is driven by the shape of the molecules and the phase separation. In all cases the formation of a hydrogen bonds network takes place. In the columnar and cubic phase a two-fold self-assembling process takes place, namely the formation of columns and micells which again are organized to a columnar or cubic mesophase. Such an organization of the molecules can be destroyed at the clearing point in two ways: the collapse of the columns and micells as basic units or only the destruction of the liquid crystalline order. Our investigations did prove the existence of cybotactic groups in the isotropic phase by X-ray investigations and dielectric spectroscopy. Dielectric measurements show indirectly the destruction of the micells by further heating of the isotropic phase. IR investigations demonstrate that the interaction between the aromatic rings in the isotropic phase becomes weaker after the clearing process of the columnar mesophases. The restriction of the movements caused by the association by hydrogen bonds does not change at the phase transition. Thus, we can conclude that the formation of the liquid crystalline arrangement is accompanied by an increase of the local short range order and the aggregation of the basic units, columns and micells, within the isotropic phase. These units are in equilibrium with single molecules. At the transition into the mesophase the formation of the liquid crystalline order did also stabilize the basic units.

The methylated amide with three alkyloxy chains **11** shows the very interesting phase sequence Cr-Col-Cub-I. Therefore it was used to investigate this phase transition in more detail. The cubic/columnar phase transition is accompanied with a drastic change in the dielectric permittivity. This phase transition needs time for the reorganization of the basic units and shows a hysteresis. Within the cubic phase both, the electrical conductivity and dielectric permittivity are much lower than those of the isotropic and columnar phases. This behavior again demonstrates that the phase and not the chemical structure dominate mainly the physical behavior of the investigated compounds.

7. References

- [1] (a) F. Reinitzer, *Monatsch. Chem.* **1888**, 9, 421-441. (b) O. Lehmann, *Z. Phys. Chem.* **1889**, 4, 462-472.
- [2] P. J. Collings, M. Hird, *Introduction to Liquid Crystals – Chemistry and Physics*, Taylor and Francis, London, **1997**.
- [3] Westphal S., Diele S., Mädicke A., Kuschel F., Schem U., Rühlmann K., Hisgen B., Ringsdorf H., *Makromol Chem Rapid Commun* **1988**, 9, 489
- [4] Kresse H., Lindau J., Diele, S., Salfetnikova J., Hauser, A., Hempel, E, *Colloid Polymer Sci* **2005**, 284, 160-166.
- [5] Tschierske C., *J. Mater. Chem.*, **1998**, 8, 1485-1508
- [6] D. Demus, *Mol. Cryst. Liq. Cryst.* **1988**, 165, 45-84.
- [7] (a) J. W. Goodby, *Curr. Opin. Solid State Mater. Sci.* **1999**, 4, 361-368. (b) Themenheft *J. Mater. Chem.* **2001**, 11, 2631 – 2886. (c) T. Kato, N. Mizoshita, K. Kishimoto, *Angew. Chem. Int. Ed.* **2006**, 45, 38-68.
- [8] W. Kast, *Ann. Phys.* **1927** 83, 418.
- [9] P.W. Glamann, K. Herrmann, and A. Krummacher, *Z. Kristallogr.* **1930** 74, 73.
- [10] A. M. Levelut and M. Lambert, *C. R. Hebd. Seances Acad. Sci.* **1971**, 272, 1018.
- [11] S. Diele, P. Brand, and H. Sackmann, *Mol. Cryst. Liq. Cryst.* **1972**, 16, 105.
- [12] I. G. Cristyakov and W. M. Chaikovsky, *Mol. Cryst. Liq. Cryst.* **1969**, 7, 269.
- [13] A. De Vriess, *Mol. Cryst. Liq. Cryst.* **1970**, 10, 219
- [14] S. Diele, D. Demus and H. Sackmann, *Mol. Cryst. Liq. Cryst. Lett.* **1980**, 56, 217.
- [15] A. J. Leadbetter, J. P. Gaughan, B. Kelley, G. W. Gray and J. W. Goodby, *J. Phys.* **1979**, 40, C3
- [16] A. De Vries and D. L. Fishel, *Mol. Cryst. Liq. Cryst* **1972**, 16, 311
- [17] J. Doucet, A. M. Levelut, and M. Lambert, *Phys. Rev. Lett*, **1974**, 32, 301.
- [18] S. Diele, H. Hartung, P. Ebeling, D. Vettters, H. Krüger and D. Demus, *Adv. Lyq. Cryst. Res. Appl., Proc. Liq. Cryst. Conf. Soc. Countries, 3rd*, 1979, **1981** Vol. 1, p. 39.
- [19] S. Diele, *Phys. Status Solidi*, **1974**, A 25, K 183.
- [20] Vorländer, *Z. Phys. Chem.* **1923**, 105, 211-254.
- [21] S. Chandrasekhar, B. K. Sadashiva, K. A. Suresh, *Pramana* **1977**, 9, 471-480
- [22] Daniel Guillon, *Columnar Order in thermotropic mesophases, Structure and Bonding, Liquid Crystals II*, **1999**, 42-78

- [23] R.J. Bushby, O.R. Lozman, *Curr. Opin. Colloid and Interface Science* **2002**, 7, 343-354
- [24] W. Weissflog, P. Möckel, H. Kresse and D. Demus *Z. Chem.* **1979**, 19, 291.
- [25] R. Wolff, W. Weissflog, H. Kresse, D. Demus, H. Zschke, *Z. Chem.* **1981**, 21, 34
- [26] W. Weissflog, H. Kresse, and A. Kolbe, *Z. Chem.* **1980**, 20, 259
- [27] H. Kresse, J. Pietscher, H.J.Deutscher, D. Demus and W. Weisflog , *Z. Phys. Chem.* (Leipzig) **1978**, 259, 779.
- [28] W. Weissflog, P. Möckel, H. Kresse, Sh. Tschimeg and D. Demus, *J. Prakt. Chem.* **1981**, 16, 1439.
- [29] L. Benguigui, *Phys. Lett. A.* **1978**, 66A, 383.
- [30] M.I. Barnick, S. W. Beljajev, W.G. Rjumzev, W.A. Zwetkov, and N.M. Shtykov, **1978**, Forschung über Flüssigkristalle p. 84. Wissenschaft. Beitr. MLU Halle, GDR.
- [31] H. Kresse, A. Wiegeleben and D. Demus, *Krist Tech*, **1980**, 15, 341.
- [32] C. Druon and J. M. Wacrenier. *J. Phys* (Orsay France) **1977**, 38, 47.
- [33] G. Pelzl, H.J. Deutscher and D. Demus *Cryst. Res. Technol.* **1981**,16, 603.
- [34] W. Meier and G. Meier, *Z. Naturforsch. A*, **1961**, 16 A, 1200.
- [35] X. P. Nguyen, S. Urban, S. Wroble and H. Kresse, *Acta. Phys. Pol A*, **1978**, A 54, 617.
- [36] G. Pelzl, H.J. Deutscher and D. Demus, *Cryst. Tech* **1980**, 15, 1345.
- [37] B. Gajewska, H. Kresse, W. Weissflog, *Cryst. Res. Technol.*, **1982**, 17, 897
- [38] H. Kresse, and B. Gajewska, *Phys. Status Solidi*, **1981**, A67, K21
- [39] H. Kresse, Dielectric behavior of liquid Crystals, *Advances in liquid Crystals*, **1983**, 6, 109-167
- [40] H. Kresse, C. Sebmann, D. Demus, A. Buka and L. Bata, *Cryst. Res. Technol.* **1981**, 16, 1439.
- [41] A. Buka, L. Bata and H. Kresse, *Rep. Hung. Acad. Sci.* **1980**. KFKI-1980-04
- [42] Handbook of Liquid Crystals; Demus D. , Goodby J., Gray G. W. , Spiess H. W., Vill, V., Eds.; Wiley-VCH.: Weinheim, Germany, 1998.
- [43] Pisula W., Menon A., Stepputat M., Lieberwirth I., Kolb U., Tracz A. Siringhaus H., Pakuta T., Müllen K., *Adv. Mater.* **2005**, 17, 684-689.
- [44] an de Craats A. M., Warman J. M., Fechtenkötter A., Brand J. D., Harbison M.A., Müllen K. *Adv. Mater.* **1999**, 11, 1469-1472.
- [45] Iino H., Hanna J., Haarer D., *Physical Review* **2005**, B 72, 193203.

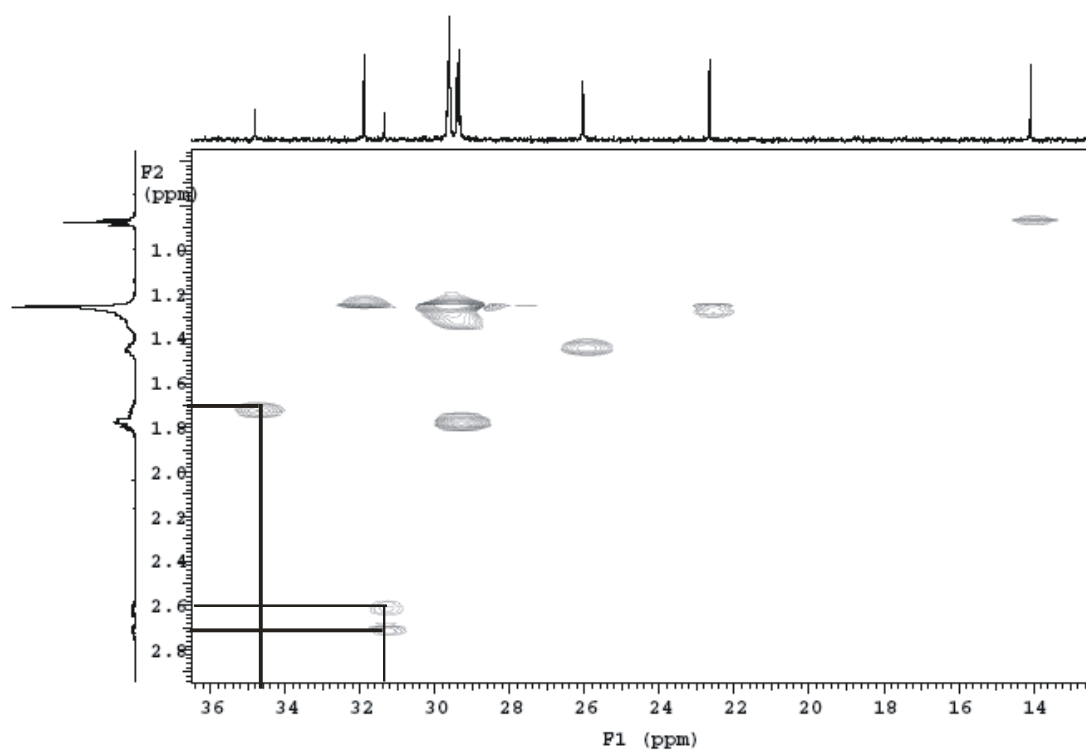
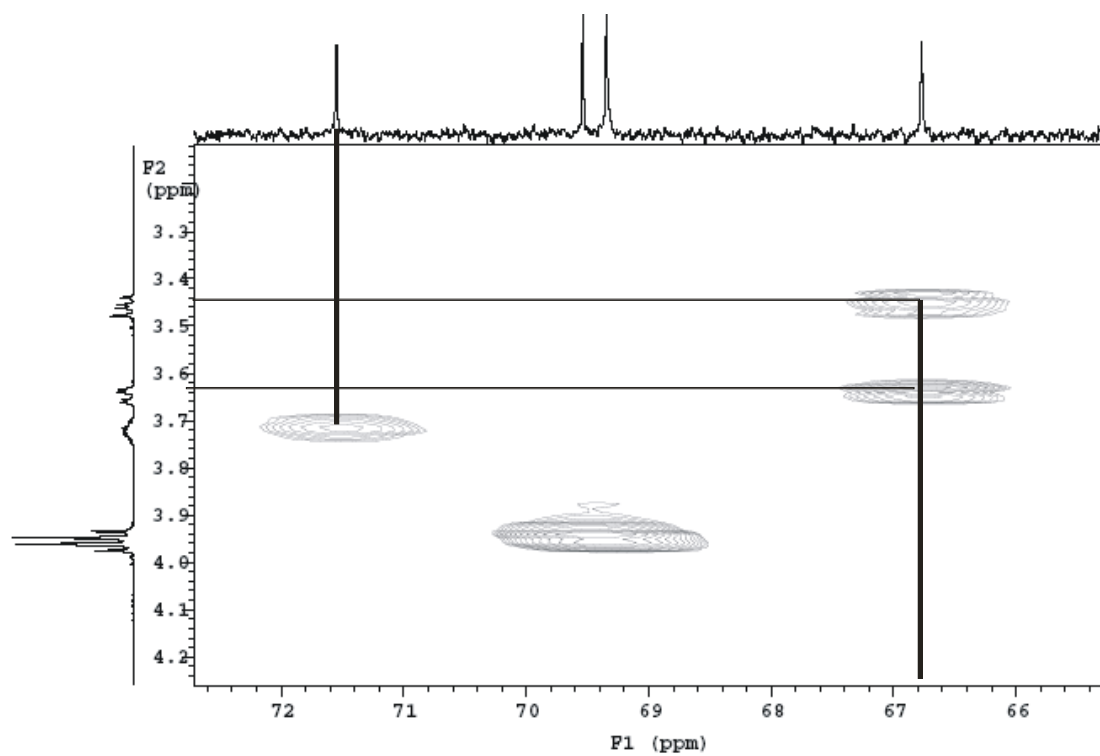
- [46] Schouten PG, Wamann J.M., de Hass M.P. van Nostrum C.F., gelink G.H. Nol R.J., Copyn M.J., Zwickker L.W., Engel M.K., Hanack M., Chang Y.H., Ford W.T., *J. A. Chem. Soc.*, **1994**, *116*, 6880.
- [47] A.M. van de Craats, J.M. Warmann, K. Müllen, Y. Geerts and J.D. Brand, *Adv.Mater.* **1998**, *10*, 36
- [48] U.Rohr, P. Schlichting, A. Böhm, M. Gross, K. Meerholz, C. Bräuchle and K. Müllen, *Angew. Int. Ed.*, **1998**, *37*, 1434.
- [49] Herwig P. Kayser C.W. Müllen K., Spiess H.W., *Adv. Mater*, **1996**, *8*, 510.
- [50] A. Fechtenkötter, K. Saalwächter, M.A. Harbison, K. Müllen, and H.W. Spiess, *Angew. Chem., Int. Ed.*, **1999**, *38*, 3039.
- [51] S.Ito, P.T. Herwig, T. Böhme, J.P. Rabe, W. rettig, and K. Müllen, *J. Am.Chem. Soc.*, **2000**, *122*, 7698.
- [52] P. Schlichting, U. Rohr and K. Müllen, *J. Mater. Chem.* **1998**, *8*, 2651
- [53] R. A. Cornier and B.A. Gregg, *Chem. Mater*, **1998**, *10*, 1309
- [54] F. Würthner, C. Thalaker, S. Diele, and T. Tschierske, *Chem. Eur. J*, **2001**, *7*, 2245.
- [55] S. Benning, H.S. Kitzerow, H. Bock and M.F. Achard, *Liq. Cryst.*, **2000**, *27*, 901.
- [56] S. Kumar, D.S.S. Rao and S.K.Prasad. *J.Mater. Chem.*, **1999**, *9*, 2751.
- [57] B. Mohr, G. Wegner and K. Ohta, *Chem. Commun.* **1995**, 995.
- [58] Elmahdy M. M., Dou X., Mondeshki M., Floudas G., Butt H. J., Spiess H.W., Müllen K., *J. Am. Chem. Soc.* **2008**, *130*, 5311-5319.
- [59] Groothues H., Kremer F., Collar D., Lillya C., *Liq. Cryst.* **1995**, *18*, 117-121.
- [60] Elmahdy M. M., Floudas G., Mondeshki M., Spiess H.W., Dou X., Müllen K., *Phys. Rev. Lett.* **2008**, *100*, 107801.
- [61] Vallerien S.U., Werth M., Kremer F., Spiess H.W., *Liq. Cryst.* **1990**, *8*, 889-893.
- [62] Möller M., Wendorff J.H., Werth M., Spiess H.W., *J. of Non Cryst. Sol.* **1994**, *170*, 295-299.
- [63] Glüsen B., Kettner A. Kopitzke J., Wendorff J.H., *J. of Non Cryst. Sol.* **1998**, *241*, 113-120.
- [64] Werth M., Vallerien S.U., Spiess H.W., *Liq. Cryst.* **1991**, *10*, 759-770.
- [65] Möller M., Wendorff J.H., Werth M., Spiess H.W., Bengs H., Karthaus O., Ringsdorf H., *Liq. Cryst.* **1994**, *17*, 381-395.
- [66] Kruglova O., Mendes E., Yildirim Z., Wübbenhost M., Mulder F.M., Stride J.A., Picken S.J., Kearley G.J., *Chem. Phys. Chem.*, **2007**, *8*, 1338-1344.

- [67] Fimmen W., Glüssen B., Kettner A., Witenberg M., Wennendorff, J.H., *Liq. Cryst.* **1997**, *23*, 569-573.
- [68] (a) Barberá J., Iglesias R., Serrano J. L., Sierra T., De la Fuente M.R., Palacios B., Perez-Jubindo M.A., *J. Am. Chem. Soc.* **1998**, *120*, 2908. (b) Palacios B., De la Fuente M.R., Perez-Jubindo M.A., Iglesias R., Serrano J. L., Sierra T., *Liq. Cryst.* **1998**, *5*, 481-485.
- [69] (a) J. Lagerwall et al, *Liq. Cryst.*, **2002**, *29*, 163. (b) J.P.F. Lagerwall, *Phys. Rev. E*, **2005**, *71*, 051703.
- [70] Heppke G., Moro D., Müller M., Sawade H., *Poster Presentation at the European Conference on Liquid Crystals*, Zakopane, Poland, March 3-8, **1997**.
- [71] Skoulios A., Guillon D., *Mol. Cryst. Liq. Cryst.* **1988**, *165*, 317-332.
- [72] Tschierske C., *J. Mater. Chem.* **1998**, *8*, 1485-1508.
- [73] Chen W., Wunderlich B., *Macromol. Chem. Phys.* **1999**, *200*, 283-311.
- [74] Tschierske C., *J. Mater. Chem.* **2001**, *11*, 2647-2671.
- [75] Tschierske C., *Prog. Polym. Sci.* **1996**, *21*, 775-852.
- [76] Blunk D., Präfcke K., Vill V.: Amphotropic Liquid in Demus D., Goodby J., Gray G.W., Spiess H.W., Vill V. (Hrsg), *Handbook of Liquid Crystals, Bd. 3*, Wiley-VCH, Weinheim, **1998**, Kap VI 305-340.
- [77] Tschierske C., *Curr. Opin. Colloid and Interface Science* **2002**, *7*, 69-80.
- [78] Tschierske C., *J. Mater. Chem.*, **1998**, *8*, 1485-1508.
- [79] Tschierske C., Hentrich F., Joachimi D., Agert O., Zschke H., *Liq. Cryst.* **1991**, *9*, 571-582
- [80] Borisch K., Diele S., Göring P., Tschierske C., *Chem. Commun.* **1996**, 237.
- [81] Borisch K., Diele S., Göring P., Müller C, Tschierske C., *Liq. Cryst.* **1997**, *22*, 427.
- [82] Borisch K., Diele S., Göring P., Kresse H., Tschierske C., *Angew. Chem* **1997**, *109*, 2188: *Angew. Chem. Int. Ed. Engl.* **1997**, *36*, 2087.
- [83] Borisch K., Diele S., Göring P., Kresse H., Tschierske C., *J. Mater. Chem.* **1998**, *8*, 529.
- [84] Borisch K., Tschierske C., Göring P., Diele S., *Chem. Commun.* **1998**, 2711.
- [85] Borisch K., Tschierske C., Göring P., Diele S., *Langmuir* **2000**, *16*, 6701.
- [86] Fuchs P., Tschierske C., Raith K., Das K., Diele S., *Angew. Chem. Int. Ed.* **2002**, *41*, 628-631.
- [87] Gestblom B., Kresse H., Tschierske C., Urban S., Wroble S., *Liq. Cryst.* **1993**, *15*, 409-415.

- [88] Gestblom B., Kresse H., Tschierske C., Urban S., Wroble S., *Liq. Cryst.* **1997**, 22, 459-462.
- [89] Kresse H., Schmalfuss H., Gestblom B., Borisch K., Tschierske C., *Liq. Cryst.* **1997**, 23, 891-896.
- [90] Grebenchtchikov I., Chen B., Tschierske C., Kresse H., *Proc. 32th. Arbeitstagung Flüssigkristalle*, Halle **2004**, P24.
- [91] Smyth C. P. “*Dielectric Behavior and Structure*”, pp 80, 343. Mc Graw-Hill, New York **1955**
- [92] Debye P. “*Polare Molekeln*” Hirzel Verlag, Leipzig **1929**.
- [93] Böttcher C.J.F. and Bordewijk P. “*Theory of Electric Polarization*” Vol II Elsevier, Amsterdam, **1978**.
- [94] D.R. Link, G. Natale, R. Shao, J.E. McLennan., N.A. Clark, E. Körblova, and D.M. Walba, *Science* **1997**, 278, 1924-1927.
- [95] (a) Onsager L., *J. Am. Chem. Soc.* **1936**, 58, 1486. (b) Kirkwood J. G., *J. Chem. Phys.* **1939**, 7, 911.
- [96] Shönhals A., Kremer F., **2003**, “*Analysis of dielectric spectra*” in “*Broadband Dielectric Spectroscopy*”, ed. Kremer F. and Shönhals A., Springer, Berlin, p.60ff.
- [97] N.E.Hill, V.E.Vanghan, A.H. Price, and Davis M. “*Dielectric Properties und Molecular Behavior.*” Van Nostrand-Reinhold, Princeton, New Jersey, **1969**.
- [98] Meier W. and Saupe A., *Z. Naturforschung* **1958**, A 13A, 564.
- [99] H. Kresse, Contribution in “*Relaxation Phenomena*” Haase W., Wróbel S., *Springer-Verlag Berlin Heidelberg* **2003**, 400-422.
- [100] Keith C., Amaranatha R.R., Prehm M., Baumeister U., Kresse H., Lorenzo Chao J., Hahn H., Lang H., Tschierske C., *Chem. Eur. J.* **2007**, 13, 2556-2577.
- [101] Vakhovskaya Z., Lorenzo Chao J., Baumeister U., Pelz K., Schröder M.W., Weissflog W., Kresse H., *Phase Transitions* **2009**, 82, 470-484.
- [102] Laws D.D., Bitter H.L., Jerschow A., *Angew. Chem. Int. Ed.* **2002**, 41, 3096-3129.
- [103] Brown S.P., Schnell I., Brand J.D., Müllen K., Spiess H.W., *J. Am Chem. Soc.* **1999**, 121, 6712-6718.
- [104] C.D. Hodgman, R.C. Weast, R.S. Shankland, S.M. Selby. *Handbook of Chemistry and Physics*, 2611, The Chemical Rubber Publ.Co. Cleveland, Ohio, **1962**.
- [105] I. Grebenchtchikov, unpublished results.
- [106] Immirzi A., Perini B., *Acta Cryst. Sect. A* **1977**, 33, 216-218.
- [107] Kitaigorodski A. I., “*Molekülkristalle*”, *Akademie-Verlag Berlin*, **1979**.

- [108] J. Lorenzo Chao, I Grebenchtchikov, R. Kieffer, Z. Vakhoskaya, U. Baumeister, C. Tschierske, H. Kresse, *Liq. Cryst.* **2006**, Vol 33, N° 10, 1095-1102.
- [109] H. Schmalfuss, Dissertation, Halle 1999

Appendix 1. NMR-HSQC measurements of compound **10** in the liquid state



Acknowledgements

I would like to thank everybody who helped me to complete this work. The collection of the data was only possible thanks to:

First of all to my doctor father and advisor Prof. Dr. H. Kresse who offered me this project and introduced me in the dielectric spectroscopy.

The understanding of the structure and self-organization of the liquid crystals was very important to fulfill this thesis. Therefore I would like to thank Dr. Ute Baumeister for her excellent introduction to the X-ray crystallography, as well as Dr. K. Pelz, Dr. M. W. Schröder, Dr. R. A. Reddy and Dr. Marko Prehm for very productive discussions.

The organic synthetic is the basis for the work with liquid crystals. First of all I want to thank Ilia Grebentchikov, who synthesized several of the molecules that were used in this work. I am also very thankful to Dr. Ralph Kluge for his outstanding support in the synthetic work and for his friendship. I also want to thank Prof. Dr. Carsten Tschierske for allowing me to work at his laboratory, for very good advice and for productive discussions. I appreciated a lot the work with two members of his group, Diplom. Chem. Constance Nürnberger and Diplom Chem. Sarah Hein. Last but not least I want to thank Dr. Daniel Garcia, Diplom Chem. Fredy Diaz Leon and Diplom Chem. Orlando Pando for their valuable help in practical aspects of the organic synthesis.

Other methods were used to understand the process of self assembly and the dynamics of the liquid crystalline mesophases at molecular level. In this point the help of Prof. Kay Saalwächter and his solid state NMR group was very good. He also contributed with helpful discussions about dynamics. Dr. Dieter Strohl and the members of the NMR department of the Faculty of Chemistry are thanked for the NMR measurements. For the IR measurement the collaboration with members of the group of Prof. Alfred Blume was determinant. Specifically discussions with Dr. Andreas Kerth and the help of Dr. Martin Schieweck and Dr. Cristian Schwieger were very important, and in general the work in the Institute of Physical Chemistry very pleasant. I want to thank all the members of the Physical Chemistry Department for the excellent atmosphere.

I also thank Dr. Zina Vakhosvskaya and Dr. Diana Ster for their excellent collaborations and for providing an excellent work atmosphere.

Prof. Angel Alegria of the “Universidad del Pais Vasco” and the Donostia International Physics Center (<http://dipc.ehu.es>) are acknowledged for providing access to high frequency dielectric spectroscopy measurements and for financial support.

The Graduiertenkolleg 894 is acknowledged for financial support.

The member of the “Centro de Documentacion de La UNESCO” in Havanna are thanked for helping during the time I was writing at home, and Dr. Leslie Perez Fernandez for language corrections.

Last but no least I want to thank my family for their great support.

To all the people who help me in some way, thank you very much.

Publications

1. **Jessie Lorenzo Chao** , Zinaida Vakhovskaya, Ilja Grebenchtchikov, Carsten Tschierske and Horst Kresse, **Dielectric Investigation of a binary system of self-organized diols**, *Liq. Cryst.* **2005**, 32(10), 1295-1300.
2. **Jessie Lorenzo Chao**, Ilja Grebenchtchikov, Robert Kieffer, Zinaida Vakhovskaya, Ute Baumeister, Carsten Tschierske and Horst Kresse, **Self-assembled diols: synthesis, structure and dielectric studies.**, *Liq. Cryst.*, **2006**, 33(10), 1095-1102.
3. Christina Keith, Ramaiahgari Amaratha Reddy, Marko Prehm, Ute Baumaister, Horst Kresse, **Jessie Lorenzo Chao**, Harald Hahn, Heinrich Lang and Carsten Tschierske, **Layer Frustration, Polar Order and Chirality in Liquid Crystalline Phases of Silyl-Terminated Achiral Bent Core Molecules** *Chem. Eur. J.*, **2007**, 13, 2556-2577.
4. D. Ster, U. Baumeister, J. Lorenzo Chao, C. Tschierske, G. Israel, **Synthesis and mesophase behaviour of ionic liquid crystals**, *J. Mater. Chem.*, **2007**, 32,3393-3400.
5. Z. Vakhovskaya, J. Lorenzo Chao, U. Baumeister, K. Pelz, M. W. Schröder, W. Weissflog, H. Kresse, **A new type of five-ring banana-shaped mesogens with strong dielectric response**, *Phase Transitions* 2009, 82(6), 470-484.

Curriculum Vitae

Surname	Lorenzo Chao
Name	Jessie
Date of birth	16.06.1977
Place of birth	Havana, Cuba

Studies

Since 2004	PhD Student at the Martin Luther University (Halle Saale), Institute of Physical Chemistry
2003(Jan-Jun)	Practicum at the Institute of Organic Chemistry at the MLU, Halle
2001-2003	Practicum at the Institute of Bio-Physical Chemistry, University of Frankfurt am Main
1995-2000	Chemistry Studies at the University of Havana, Diploma in Chemistry
1983-1992	High School, Havana, Cuba

Halle/Saale, im März 2010

Eidstattliche Erklärung

Hiermit erkläre ich, dass die vorliegende Arbeit von mir selbständig und nur unter Verwendung der angegebenen Hilfsmittel angefertigt wurde. Ich versichere weiterhin, dass alle wörtlich oder inhaltlich entnommenen Stellen als solch gekennzeichnet sind.

Diese Arbeit wurde bisher an keine andere Universität vorgelegt.

Halle/Saale, im März 2010